Characterization of Dihydrodipicolinate Synthase and Dihydrodipicolinate Reductase from *Chlamydomonas reinhardtii, Cyanidioschyzon merolae, Selaginella moellendorffii, Ostreococcus tauri* and *Ostreococcus lucimarinus*

A thesis submitted in partial fulfilment of the requirements for the Degree

of Master of Science in Biochemistry

in the University of Canterbury

by Longyuan Hu

University of Canterbury

2016

Table of Contents

List of Figures

List of Tables

Acknowledgements

I wish to express sincere appreciation to my supervisor Dr. Grant Pearce for his patience in helping me carry out experiments and giving me advice on thesis writing. I also wish to thank Mrs Jackie Healy for her support in coordinating the equipments and material in the lab.

Abstract

Lysine is an important amino acid for life [1]. The first two committed reactions in the lysine biosynthesis pathway are catalyzed by dihydrodipicolinate synthase (DHDPS) and dihydrodipicolinate reductase (DHDPR) [1]. These enzymes are find in bacteria and plants but not in humans, thus they can be good targets of antibiotics and herbicides [1]. In previous research on DHDPS and DHDPR, it was found that plant DHDPS and DHDPR are different from bacteria ones in both structure and activity [2]. In order to further study the difference of plant and bacteria DHDPS and DHDPR in behavior and evolution, five species in the evolutionary tree between bacteria and plants are chosen and their DHDPS and DHDPR are characterized in kinetics, structure, and stability. It is found only the SMO DHDPS and DHDPR behave like plant DHDPS and DHDPR while other enzymes all behave like the bacteria ones.

Glossary

DHDPS	Dihydrodipicolinate synthase
DHDPR	Dihydrodipicolinate reductase
ASA	(S)-aspartate-semi-aldehyde
°C	Degrees Celsius
Da	Daltons
kDa	kilo Daltons
RFU	Relative fluorescence units
dRFU/dt	Change in fluorescence (relative fluorescence units) with respect to time
HEPES	N-2-hydroxyethylpiperazine-N-2-ethane sulphonic acid
HTPA	(2S,4S)-4-hydroxy-2,3,4,5-tetrahydrodipicolinic acid
K_{cat}	Turnover number
K_m	Michaelis-Menten constant
K_m ASA	Michaelis-Menten constant with respect to ASA
K_m pyruvate	Michaelis-Menten constant with respect to pyruvate
mg	Milligrams
ml	Milliliters
µl	Microliters
M	Molar
mM	Millimolar
µM	Micromolar
NADPH	Nicotinamide adenine dinucleotide phosphate
NADH	Nicotinamide adenine dinucleotide
r.m.s.d.	Root mean square deviation

Characterization of Dihydrodipicolinate Synthase and Dihydrodipicolinate Reductase from *Chlamydomonas reinhardtii, Cyanidioschyzon merolae, Selaginella moellendorffii, Ostreococcus tauri* and *Ostreococcus lucimarinus*

Introduction

Lysine is an essential amino acid for life [1]. In bacteria and plants, dihydrodipicolinate synthase (DHDPS) and dihydrodipicolinate reductase (DHDPR) catalyze the first two committed reactions of the lysine biosynthesis pathway: the condensation of pyruvate and (S)-aspartate-β-semialdehyde ((S)-ASA) to form (2S,4S)-4-hydroxy-2,3,4,5-tetrahydrodipicolinic acid (HTPA) and the reduction of HTPA to form tetrahydrodipicolinate (THDP) [2].

These enzymes are found in bacteria and plants but not in humans, thus DHDPS and DHDPR have been well studied as potent targets of antibiotics and herbicides that do not affect humans [1]. In addition, by studying how to increase the catalytic power of these enzymes in order to make more lysine, the nutrition level of many crops can be raised because lysine is a limiting amino acid [1].The next section is a summary of the research done on DHDPS and DHDPR from different plant and bacteria species. The studies done on the structure of DHDPS from different species will be discussed first.

DHDPS Structure:

Bacteria DHDPS structure:

Many wild type bacteria DHDPS crystal structures have been solved until now. Some examples of the crystallized DHDPS are summarized in Table 1. The *E. coli* DHDPS will be discussed here as an example here.

Crystal Structure	PDB code	Resolution (angstrom)
Escherichia coli DHDPS [3]	1DHP	2.30
Staphylococcus aureus DHDPS [4]	3DI0	2.38
Pseudomonas aeruginosa DHDPS [5]	3PUO	2.65
Bacteroides thetaiotaomicron DHDPS [6]	4XKY	2.10

Table 1 PDB code and resolution of some crystallized DHDPS structures

In 1995, the *E. coli* DHDPS crystal structure was solved at 2.5 angstroms resolution [3]. The enzyme was found to be a homotetramer with a "dimer of dimer" quaternary structure arrangement with a big cleft in the middle as shown in Figure 1 below[3].

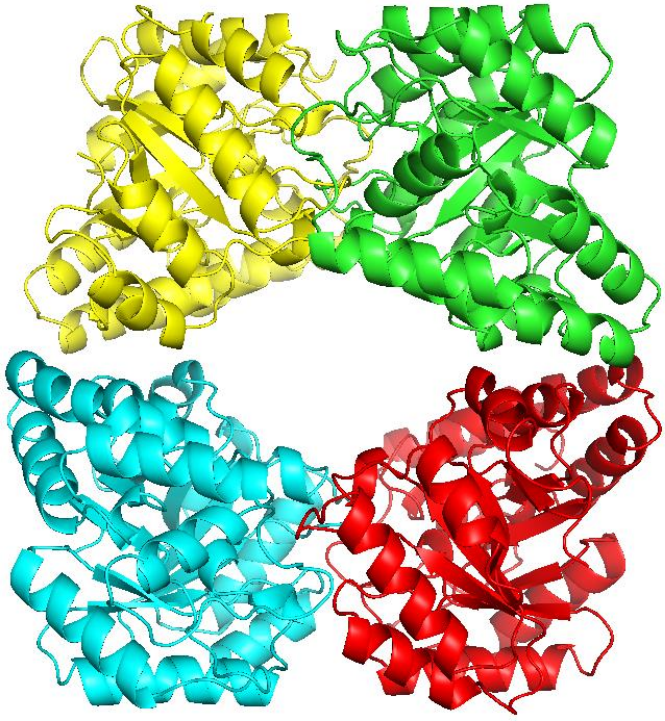

Figure 1Crystal structure of the *E. coli* DHDPS homotetramer, the four monomers are shown in different colors. PDB code: 1DHP

Each *E. coli* DHDPS monomer contains two domains: the N-terminal domain, consisting of amino acid 1 to 224, forming the TIM barrel-like structure and the C-terminal domain is made up of three alpha helices fixed around the barrel structure by hydrogen bonds and ionic interactions as shown in Figure 2 [3].

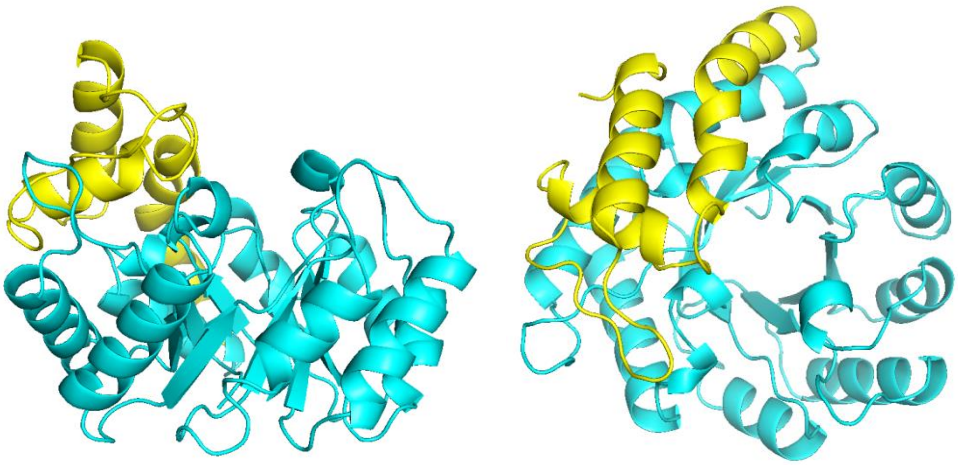

Figure 2a Figure 2b

Figure 2 Crystal structure of the *E. coli* DHDPS monomer. The N-terminal barrel domain is in cyan and the C-terminal domain is in yellow. Figure 2a is the view from one side of the barrel and Figure 2b is the view from above. PDB code: 1DHP

The characterized bacteria DHDPS have similar overall shape and fold as the Cα atoms in the crystal structures of DHDPS from *Rhodopseudomonas palustris, Mycobacterium tuberculosis, Streptococcus pneumoniae, Campylobacter jejuni, B. thetaiotaomicron and E. coli* were aligned and the root mean square deviation (r.m.s.d.) value only ranged between 1.8 to 2.2 angstrom [6]. However, the characterized plant DHDPS have a different arrangement of their quaternary structures.

Plant DHDPS structure:

Compared to bacteria, fewer plant DHDPS crystal structures have been solved. The *Nicotiana sylvestris* DHDPS crystal structure was solved at 2.8 angstrom in 1997 [7], the *Arabidopsis*

thaliana DHDPS crystal structure was solved at 2.0 angstrom in 2012 [2] and the *Vitis vinifera* DHDPS crystal structure was solved at 2.4 angstrom in 2013 [8,9]. The three plant DHDPS structures are similar to each other but different from the bacteria DHDPS [2].
When comparing the *N. sylvestris* DHDPS and *E. coli* DHDPS, their dimer-dimer interface was on the opposite side of the dimer [7]. The buried surface area of the dimer-dimer interface was 810 angstrom^2 in *N. sylvestris* DHDPS and 650 angstrom^2 in *E. coli* DHDPS [7]. The number of residues interacting at the dimer-dimer interface to hold the quaternary structure together was 16 in *N. sylvestris* DHDPS and 3 in *E. coli* DHDPS [7].

Figure 3 below shows the crystal structure of the quaternary structure arrangement of a plant DHDPS from *A. thaliana*.

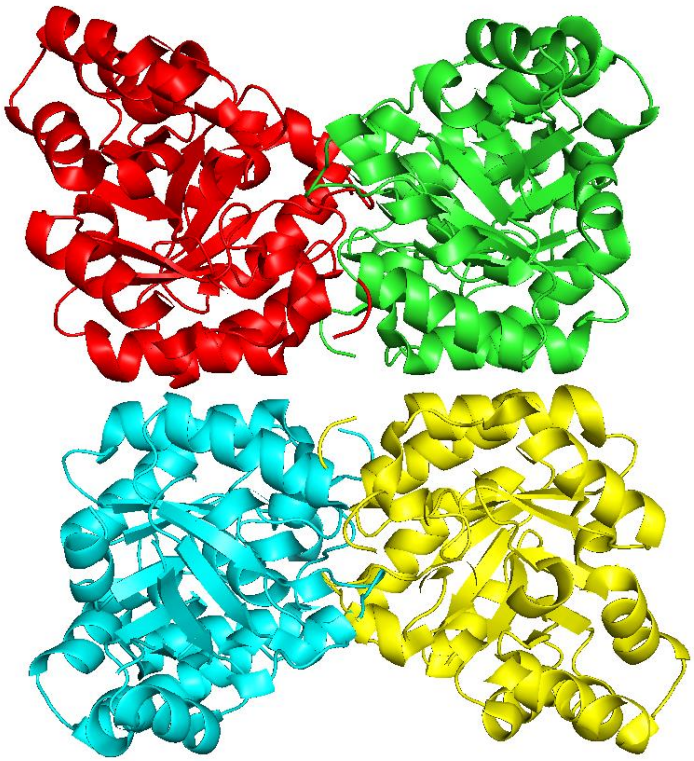

Figure 3 The crystal structure of *A. thaliana* DHDPS. Different monomers are shown in different colors. PDB code: 4DPP

This observation of significant structural difference between plant and bacteria DHDPS led to a hypothesis that the ancestral DHDPS was a dimer, and evolved differently in bacteria and plant species to form the different tetramers seen today [2]. Besides the overall shape and structure of DHDPS, the residues that are important for enzyme functioning are further studied in details, such as the residues at the substrate binding site [10-12] and inhibitor binding site [9,13] of DHDPS.

DHDPS mechanism:

In 1997, a 3 step reaction mechanism of *E. coli* DHDPS was proposed by x-ray crystallography and NMR studies [10]. The first step was Lys161 attacking pyruvate, formation of the tetrahedral transition state with the help of Tyr133 hydrogen bonding to the keto oxygen, and the loss of a water molecule to form the schiff base imine [10]. The second step was the addition of ASA through its aldehyde group to the enamine form of the schiff base after its tautomerization, resulting in the formation of a new C-C bond and the loss of another water molecule [10]. And the final step was the amino group of ASA attacking the central carbon of the tetrahedral transition state, formation of the HTPA ring and then release from Lys161 [10].

This mechanism was also testified by isothermal titration calorimetry experiment in which the result showed that ASA did not bind to the *E coli* DHDPS when there was no Schiff base formed by pyruvate, but ASA did bind to the enzyme when there was a Schiff base mimic [11]. This supported the idea that formation of the Schiff base drives the binding of ASA [11].

Based on the DHDPS mechanism, three residues (Tyr133, Thr44 and Tyr107) around the active site in *E. coli* DHDPS were hypothesized to form a catalytic triad and transfer protons to and from the transition state during catalysis [12].In order to test this hypothesis, three site-directed mutagenesis (Y133F, T44V and Y107F) experiments were carried out [12]. Replacing tyrosine by phenylalanine and threonine by valine removed their proton transfer function by taking the hydroxide groups away but kept their benzene rings and side chain carbons unchanged to minimize the effect of size and shape on the enzyme [12]. All three mutant enzymes lost most of their activity compared to the wild type: only 0.3% of the DHDPS activity remained in the

mutant Y133F, 0.1% activity remained in T44V and 10% activity remained in Y107F [12].These results strongly supported the hypothesis that the proton shuttle catalytic triad residues aid the catalytic process of DHDPS [12].Besides catalysis, the inhibition of DHDPS and the residues at the inhibitor binding sites are also well studied.

Lysine inhibition:

It was found that the activity of DHDPS was allosterically regulated by the feedback inhibition of (S)-lysine which was the final product of the lysine biosynthesis pathway [13].In 2005, the crystal structure of *E. coli* DHDPS with lysine bound was solved at 2.0 angstrom and was compared with the native *E. coli* DHDPS solved at 1.9 angstrom [13]. The lysine binding site was found at the tight dimer interface, and was connected to the active site through a water channel [13]. Figure 4 below shows the position of lysine binding site and active site residues in a *E. coli* DHDPS dimer [13].

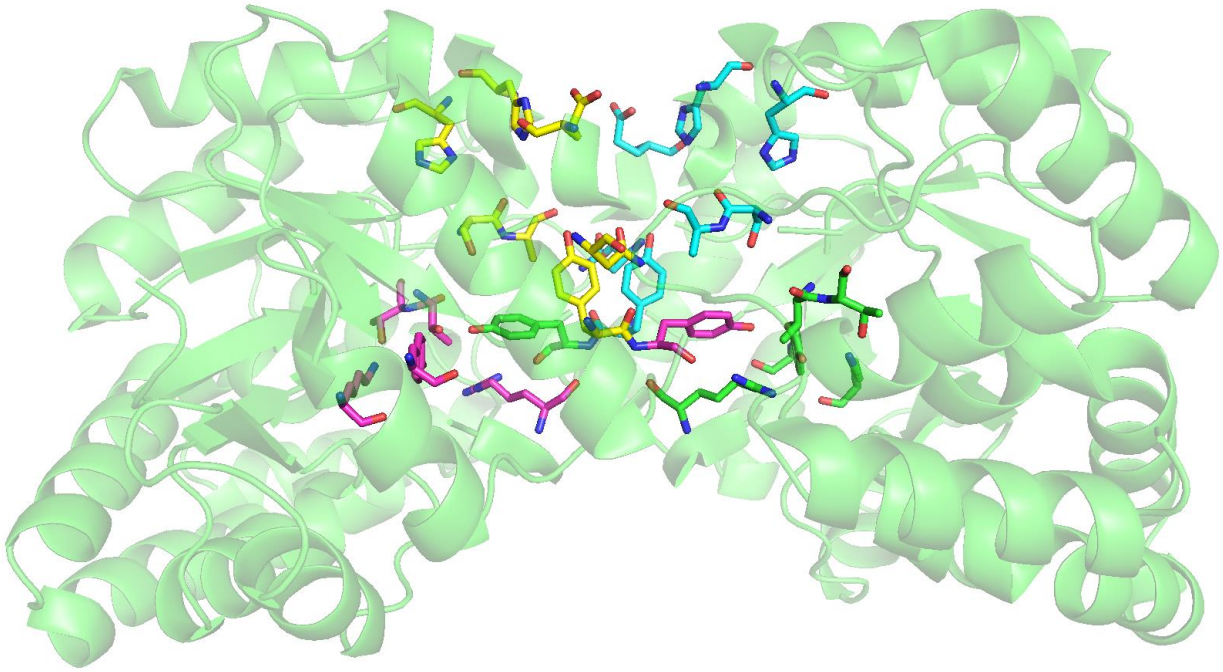

Figure 4 Positioning of residues at *E. coli* DHDPS substrate binding site and the inhibitor (S)- lysine binding site in an *E. coli* DHDPS dimer. The substrate binding sites residues from the monomer on the left are shown in purple, the substrate binding sites residues from the monomer on the right are shown in green. The lysine binding sites

residues from the monomer on the left are shown in yellow and the lysine binding sites residues from the monomer on the right are shown in cyan. PDB code: 1YXC

The positioning of lysine binding site residues were slightly altered when lysine binds to the enzyme as shown in Figure 5 below [13].However, there was no significant structural difference between the lysine bound and unbound enzymes, the r.m.s.d. for the overlay of those two structures was 0.17 angstrom [13].

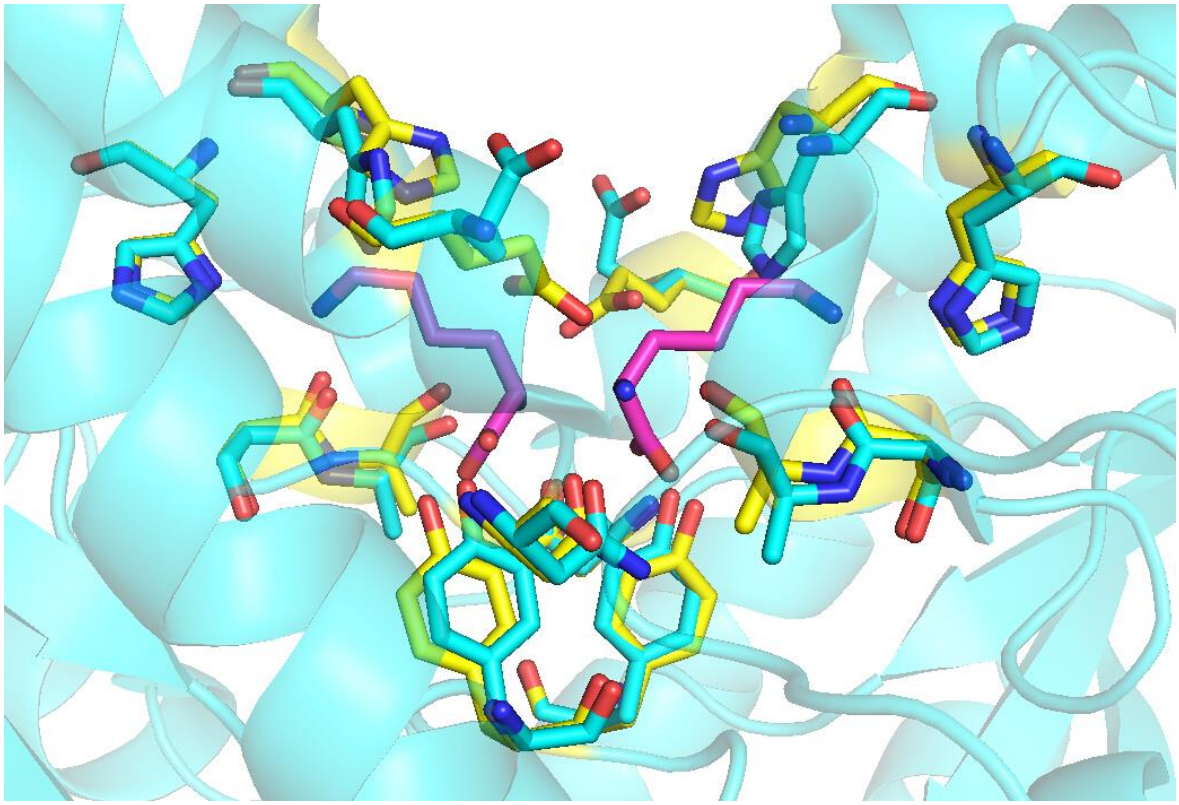

Figure 5 Overlay of the lysine binding site residues with and without lysine bound. Binding site residues with lysine bound were shown in yellow, those without lysine bound were shown in cyan, and the two lysines bound are shown in purple. PDB code: 1YXC (structure without lysine bound) and 1YXD (structure with lysine bound)

In 2013, another lysine inhibition study proposed a structural mechanism of lysine inhibition on DHDPS from the common grapevine *V. vinifera.* When comparing the lysine bound and unbound *V. vinifera* DHDPS crystal structures, their overall structural difference was also very small, with

the r.m.s.d. value of 0.34 angstrom [9]. However, different from the *E. coli* DHDPS lysine binding site residues, Trp78 which is sitting beside the lysine binding cleft moved significantly towards the lysine binding site, acting as a cap to prevent solvent into the allosteric site once lysine bound to the enzyme [9].

The positions of Trp78 with lysine bound and unbound are shown in Figure 6 below[9].

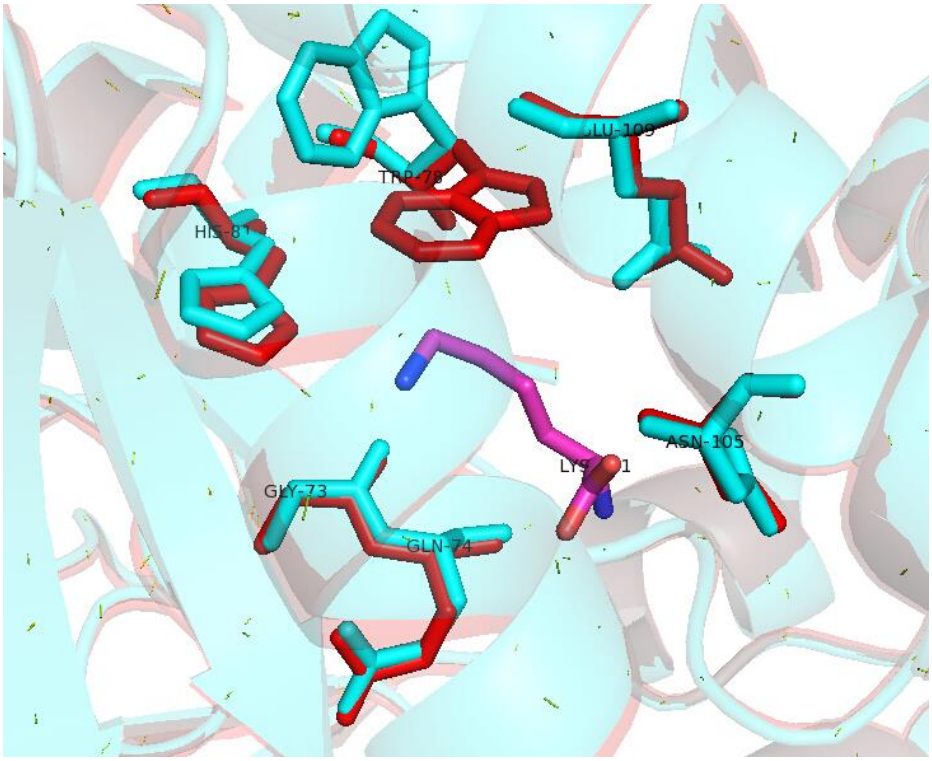

Figure 6 Overlay of the lysine binding site residues of lysine bound and unbound *V. vinifera* DHDPS. Lysine binding site residues with lysine bound are shown in red, residues without lysine bound are shown in cyan. The bound inhibitor lysine is shown in purple. PDB code: 3TUU (structure without lysine bound) and 4HNN (structure with lysine bound)

Another residue Tyr131 formed a hydrophobic stack with one of the catalytic triad residue, Tyr132 in the lysine unbound form of *V. vinifera* DHDPS [9]. Once lysine bound to the allosteric site, Tyr131 was attracted to the carboxyl group of lysine by 0.69 angstrom and its interaction with Tyr132 was disrupted, which displaced the -OH group of Tyr132 by 0.56 angstrom [9]. This

process disrupted the proton transferring function of the catalytic triad in catalysis, and it was proposed to be a potential mechanism of lysine inhibiting the *V. vinifera* DHDPS enzyme function [9].

In the lysine inhibition studies described above, lysine binding has little effect on the large scale DHDPS monomer conformation, however in a research on *C. jejuni* DHDPS, lysine binding significantly moved one of its domain [14]. The fixed domain was composed of both C-terminal and N-terminal of the monomer, residues 1-80 and 188-298, and the moving domain was in between, from residue104 to 184 [14].

Moving of that domain broke some hydrogen bonds and hydrophobic interactions between the weak dimer interface, and decreased the volume of both the active site and allosteric site [14]. This is another potential mechanism of lysine inhibiting the enzyme activity [14]. In the center of the moving domain, there were 2 tyrosine residues Tyr110 and Tyr111 which were considered possible link between the lysine binding site and the active site because Tyr110 was hydrogen bonded to the carboxyl group of the inhibitor lysine and Tyr111 was one of the catalytic triad (Y137, T47 and Y111) in *C. jejuni* DHDPS [14]. This Tyr110 was mutated into a phenylalanine to remove the hydrogen bond by taking away the hydroxide group and keep its size and shape by the unchanged benzene ring [14]. The kinetic data of the Y110F enzyme was similar to the wild type, only the K_{cat} value was reduced by a little bit, thus the removal of the -OH group on Tyr110 did not have a significant effect on the catalytic power of the enzyme [14]. However, the IC_{50} of lysine was significantly increased after mutating the Tyr110 [14]. While comparing the crystal structure of the mutant and wild type enzyme, the hydrogen bond between Tyr110 and the lysine's carboxyl group was broken, the other hydrogen bonds formed between lysine and the enzyme were not affected, thus the Tyr110-lysine hydrogen bond played an important role in the inhibition signal transduction [14].

DHDPS Kinetics

Besides the structure of DHDPS, the catalytic power of this enzyme is also well studied. The kinetic parameters of DHDPS from various plant and bacteria species have been measured. As

DHDPS has two substrates, the pyruvate and ASA, two K_m values can be measured for each DHDPS. In addition, as DHDPS is feedback inhibited by lysine, the $K_{0.5}$ lysine of DHDPS of multiple plant and bacteria species have also been measured. The DHDPS kinetics was usually measured by a DHDPS-DHDPR coupled assay [1]. By adding excess DHDPR into the DHDPS reaction system and measure the consumption rate of NADPH at 340nm absorbance, we can indirectly measure the rate of DHDPS catalyzed reaction [1]. Table 2 summarizes the kinetic parameters of some of the previously characterized bacteria DHDPS and Table 3 summarizes the kinetic parameters of previously characterized plant DHDPS. If not specifically mentioned, the reaction condition of the kinetic data described below will be in 100mM HEPES buffer at 30°C and pH 8.0.

Bacteria species	K_m pyruvate (mM)	K_m ASA (mM)	K_{cat} (s^{-1})
E. coli [20]	0.26	0.11	124
S. aureus [18]	0.22	0.11	70
N. meningitidis [15]	0.5	0.052	47
B. anthracis[16]	0.43	0.18	76
M. tuberculosis[21]	0.17	0.43	138
C. glutamicum[22]	0.32	0.63	213

Table 2 K_m and K_{cat} values of some of the characterized bacteria DHDPS

Plant species	K_m pyruvate (mM)	K_m ASA (mM)	K_{cat} (s^{-1})
Pisum sativum [23]	1.7	0.4	ND
Zea mays [25]	2.1	0.6	ND
Triticum aestivum[24]	11.7	0.8	ND
A. thaliana [2]	1	0.09	93
V. vinifera[8]	1	0.18	45

Table 3 K_m and K_{cat} values from characterized plant DHDPS. ND indicates not determined.

The *P. sativum* and *T. aestivum* DHDPS kinetics were measured by the ABA method that the reaction takes place in 100 mM Tris buffer with 1 mg ABA added [23,24], which may account for the significant differences between these values and values for other plant species determined using the coupled assay.

From Table 2 and 3 we can see in general the plant DHDPS have higher K_m pyruvate values than bacteria DHDPS [5]. As for the K_m ASA values, in general bacteria DHDPS have lower K_m ASA values than plant species. However the plant DHDPS can have very low K_m ASA like the *A. thaliana* K_m ASA of 0.09 mM [2] and the bacteria DHDPS can have high K_m ASA like the *C. glutamicum* K_m ASA of 0.63 mM [22] and the *M. tuberculosis* K_m ASA of 0.43 mM [21]. Thus K_m ASA cannot be used as a kinetic parameter to distinguish between plant and bacteria DHDPS. As for the K_{cat} values, not much difference was found between plant and bacteria DHDPS. So the K_{cat} value cannot be used as a kinetic parameter to distinguish between plant and bacteria DHDPS as well.

DHDPS thermal stability

The ability to tolerate high temperature of DHDPS has also drawn scientists' attention because the thermal stability of an enzyme can relate to the temperature of natural environment that the organism lives in. The melting temperature (the temperature that the enzyme starts unfolding and lose activity) of various DHDPS have been measured by different methods like Differential Scanning Fluorimetry (DSF) , Circular Dichroism (CD) Spectroscopy and thermal inactivation assay.

The melting temperatures of those DHDPS alone are summarized in Table 4 below:

Species	Melting temperature (°C)	Method
E. coli[15]	59.5	DSF
N. meningitidis [15]	50.5	DSF
B. anthracis [26]	50-60	CD
T. aestivum [24]	Lower than 60	Heating at 60°C

B. megaterium [27]	50-60	Thermal inactivation assay
P. aeruginosa [5]	65	CD
B. licheniformis [28]	50-80	Thermal inactivation assay
T. maritima [29, 56]	117	DSF
M. tuberculosis [57]	82	Thermal inactivation assay
T. tengcongensis [30]	Higher than 80	Activity measurement at elevated temperature
Aquifex aeolicus [31]	90-120	Molecular dynamics simulation

Table 4 melting temperature of characterized plant and bacteria DHDPS

The heat stability of *T. aestivum* DHDPS was measured by heating the enzyme for 1, 3 and 5 minutes [24]. The enzyme lost half of its activity after 1min and became completely inactive after 5min [24]. This result shows that 60°C is higher than the melting point of *T. aestivum* DHDPS.

The thermal stability of *T. tengcongensis* DHDPS is acquired by measuring the activity of the enzyme at different temperatures from 30°C to 90°C [30]. The enzyme reaches its maximum activity at 80°C, and the activity starts decreasing when the temperature goes over 80°C [30].

The *A. aeolicus* DHDPS thermal stability was measured by molecular dynamics simulation at 25°C, 90°C and 120°C[31]. The backbone structure of the enzyme did not change when the temperature was raised from 25°C to 90°C, but significant change of the r.m.s.d. value of the backbone structure was observed when the temperature was further raised up to 120°C[31]. This suggests that the protein starts unfolding at a temperature between 90°C and 120°C[31]
.
When pyruvate was added, the melting temperatures of *E. coli* DHDPS [32], *B. anthracis*[26], *B. megaterium* [27] and *B. licheniformis* [28] are significantly increased, which means these DHDPS are stabilized by their substrate pyruvate.

From Table 3 we can see that except for the thermophilic species (*T. maritima*, *T. tengcongensis* and *A. aeolicus*) the previously characterized bacteria DHDPS all have high melting temperatures at around 60°C [5, 15,26-28]. *N. meningitidis* DHDPS has the lowest melting temperature among all the mesophilic bacteria species described above, and it has been found living in human brain [33], thus the enzymes in this species do not need to tolerate the temperature too much higher than normal human body temperature. On the other hand the *T. maritima* has the highest melting temperature in Table 4, and it was usually found in environments with very high temperature like thermal vents and hot springs [34], so DHDPS from *T. maritima* has to have a very high melting temperature up to 117°C in order to survive the harsh environments [56].

DHDPR structure:

As the enzyme catalyzing the 2nd committed reaction in lysine biosynthesis pathway right after DHDPS and an important enzyme to aid the kinetic assay of DHDPS in the commonly used DHDPS-DHDPR coupled assay [1], DHDPR has been studied by scientists as well. And again, the structure of characterized DHDPR from plant and bacteria species are found significantly different from each other [2].

Bacteria DHDPR structure

Few bacteria DHDPR have been crystallized, including *E. coli* DHDPR [35,36], *M. tuberculosis* DHDPR [37,38] , *S. aureus* DHDPR [40] and *Burkholderia thailandensis* DHDPR [40]. They all have similar overall structures [38], and again the *E. coli* DHDPR will be discussed herein details as an example.

In 1995, the *E. coli* DHDPR, complexed with its cofactor NADPH, was solved at 2.2 angstrom resolution [35]. The enzyme was found to be a tetramer in solution, also with the "dimer of dimer" symmetry arrangement found in DHDPS [35]. The crystal structure of *E. coli* DHDPR homotetramer is shown in Figure 7 below:

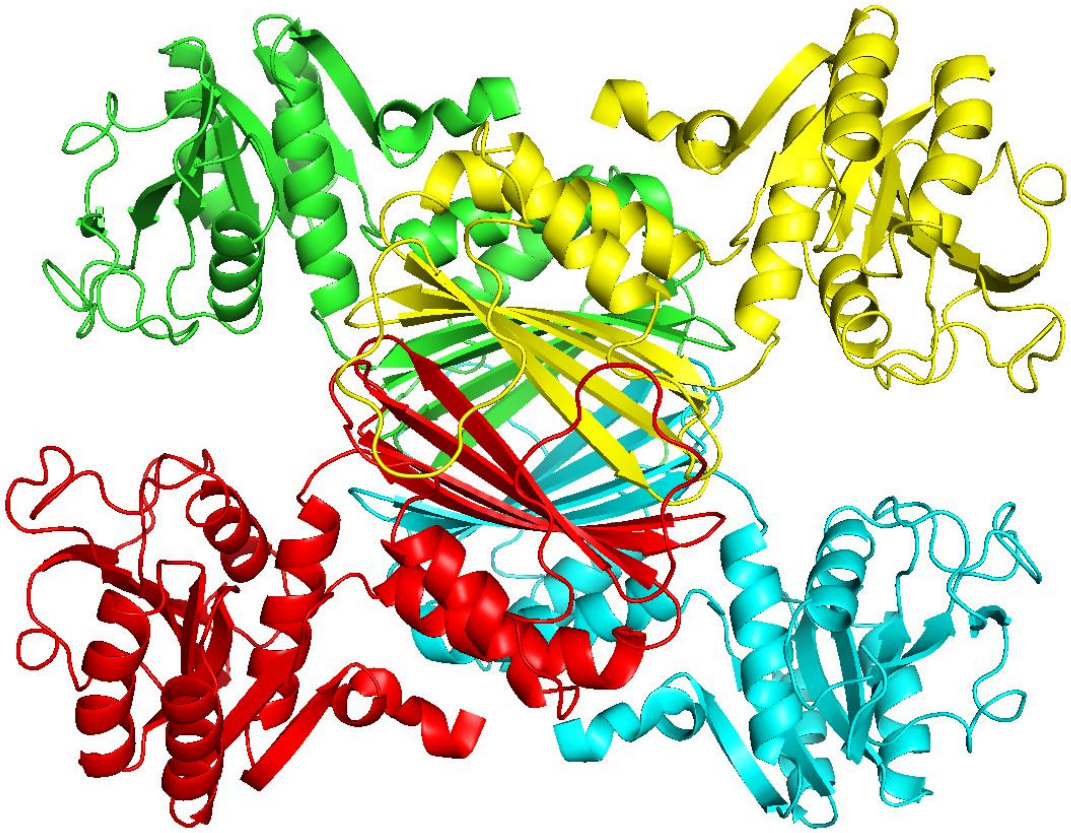

Figure 7 X-ray crystal structure of *E. coli* DHDPR homotetramer. Different monomers of the enzyme are shown in different colors. PDB code: 1DIH

Like the *E. coli* DHDPS, *E. coli* DHDPR monomer also contains two domains [35].A close look at these two domains of the *E. coli* DHDPR monomer structure is shown in Figure 8 below. The first domain was N-terminal domain at the bottom left part of the monomer shown in cyan in Figure 8 [35]. This domain had 4 alpha helices and 7 beta strands (A1 A2 A3 A6 and B1 B2 B3 B4 B5 B6 B11) which formed the dinucleotide binding fold or the Rossmann fold found in many dehydrogenases [35]. NADPH was found to be binding at the C-terminal end of the beta strain B1 in this domain [35]. The C-terminal domain at the top right part of the monomer shown in red in Figure 8 was the HTPA binding domain [35]. This domain had 2 alpha helices and 4 beta strands (A4 A5 and B7 B8 B9 B10). The two domains were linked by 2 loops, one connecting alpha helix A4 and beta strand B6, and the other connecting A6 and B10 [35]. In solution, the HTPA binding domain of four *E. coli* DHDPR monomers interacted in a circle to form a homotetramer [35].

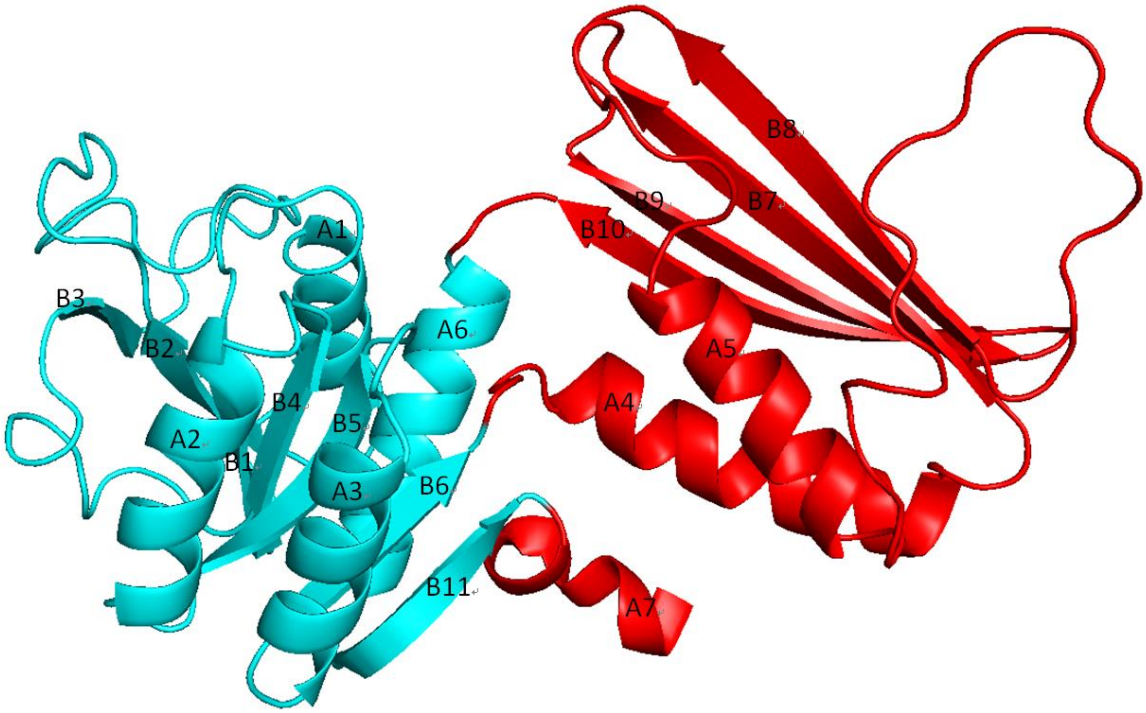

Figure 8 Crystal structure of *E. coli* DHDPR with NADPH bound. The N-terminal domain is shown in cyan, and the C-terminal domain is shown in red. The seven alpha helices are labeled A1 to A7 and the eleven beta strands are labeled B1 to B11. PDB code: 1DIH

The detailed secondary structure arrangement and interactions between the HTPA binding domains from the four monomers is shown in Figure 9 below:

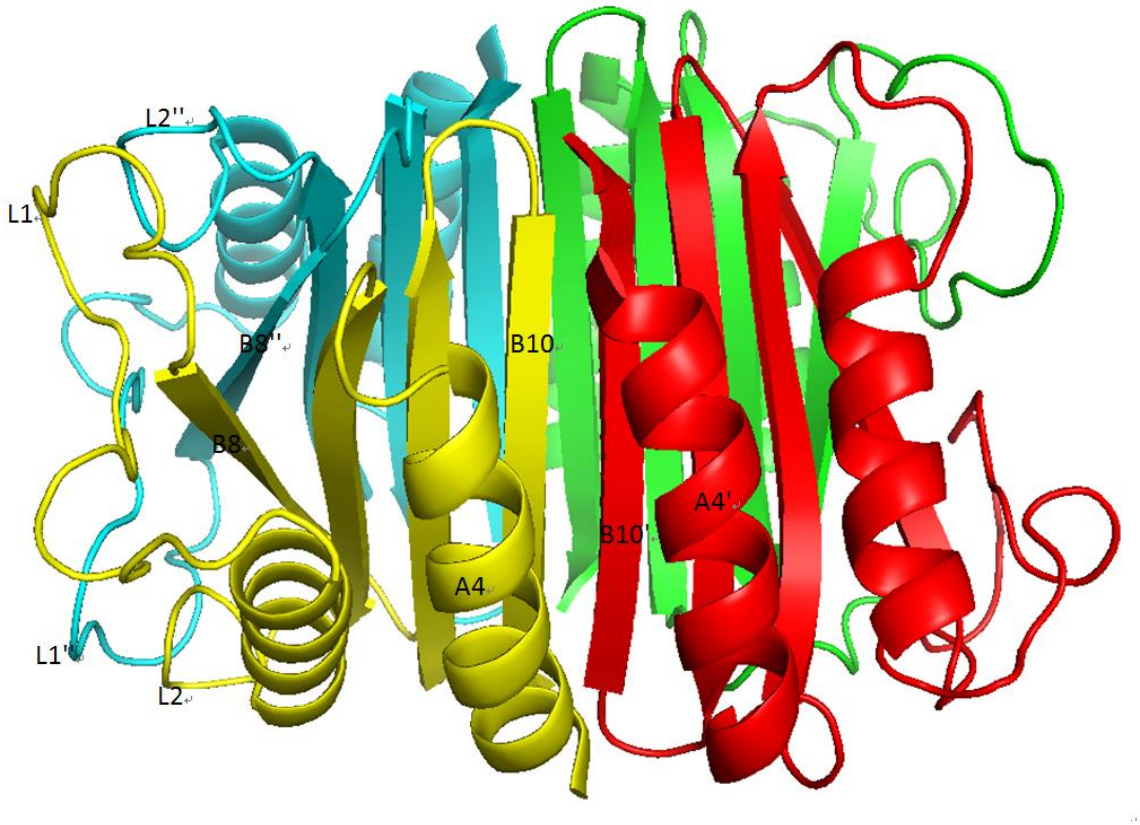

Figure 9 Crystal structure of the central beta barrel of *E. coli* DHDPR. the substrate binding domain from different DHDPR monomers are shown in different colors. The same secondary structure from different monomers are labeled with ' marks like A4 and A4', B8 and B8". PDB code: 1DIH

The four beta strands in the substrate binding domain of each monomer are aligned to form a 16 beta strand barrel in the center [35]. Hydrogen bonds are formed between beta strand B10 from the yellow monomer and B10' from the red monomer [35]. There is also a helix-helix interaction between A4 from the yellow monomer and A4' from the red monomer outside the beta strand cluster[35]. The cyan and green monomers at the opposite end interact in the same pattern because of the symmetry of the quaternary structure [35]. The yellow and cyan monomer are linked by the interactions of the beta strand B8 from the yellow monomer and B8" from the cyan monomer. The loop L1 - L2" and L2 - L1" interaction also aid the formation of the beta barrel structure. The red monomer and green monomer again interact in the same pattern [35].

In 1998, the *E. coli* DHDPR was crystallized with NADH and the inhibitor 2,6-Pyridinedicarboxylate (2,6-PDC) bound to three of the monomers in the enzyme tetramer [36]. It was found that the 222 symmetry previously reported was disrupted because of the movement of one monomer with no ligands bound to it [36]. The monomer without ligands was described as in its open conformation and the other three with NADH and inhibitor bound in their closed form [36]. The movement between open and closed form is shown below in Figure 10together with the bound NADH and 2,6-PDC.

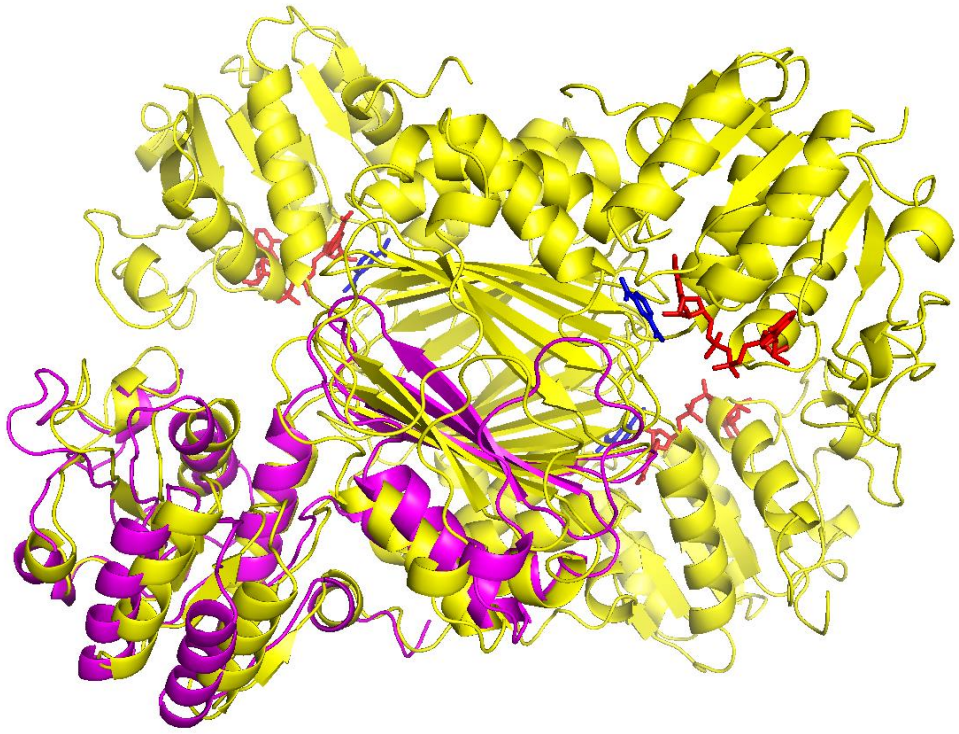

Figure 10 Overlay of open and closed form of *E. coli* DHDPR monomer crystal structures. The closed form monomers are shown in yellow, and the open form monomer is shown in purple. The NADH is shown in red and 2,6-PDC is shown in blue. PDB code: 1ARZ

The monomer in open form was compared to the monomers in closed form by both overlay of their structures and calculating their r.m.s.d. A 16 degree rotation of the monomer between the open and closed form is measured [36].

Plant DHDPR structure:

Not many plant DHDPR structures are studied like the bacteria ones. Until now, no plant DHDPR crystal structure has been solved. *A. thaliana* DHDPR was studied by scattering and analytical ultracentrifugation in 2012 [2]. The main peak of size-exclusion chromatography was calculated to be a dimer with 67.5 kDa, a very small tetramer peak was also observed as well [2]. In the sedimentation velocity experiments, the major peak of *A. thaliana* DHDPR which was considered the dimer peak had a sedimentation coefficient of around 4S, and the minor peak which was considered the tetramer peak had a sedimentation coefficient of around 6.5S [2]. Small angle X-ray scattering was used to study the shape and structure of the *A. thaliana* DHDPR, and it was found its scattering profile was different from the bacteria DHDPR [2]. Instead of the spheroidal structure of the bacteria DHDPR, *A. thaliana* DHDPR had a negatively skewed scattering curve representing an elongated shape in solution [2].

The SWISS-MODEL was used to generate a structural homology model of *A. thaliana* DHDPR using the *E. coli* DHDPR as a template [2]. In the model, most of the secondary structures were conserved, but differences were observed in some loop regions [2]. In 1983, the maize DHDPR was also reported to be a dimer [41]. Thus the degree of polymerization can be a characteristic used to distinguish between plant and bacteria DHDPR. Plant DHDPR exist as dimers and bacteria DHDPR exist as homotetramers.

DHDPR mechanism

A catalytic mechanism of the *E. coli* DHDPR is proposed based on the binding pattern of the inhibitor 2,6-PDC and previous studies [36].The first step was a rapid hydride transfer from the C4(R) position to the unsaturated C4 of the dihydrodipicolinate [36]. The second step was the proton transferred to the unsaturated C3 of dihydrodipicolinate on its *re* face [36].

The substrate binding site residues Lys163, His159 and Lys160 are all conserved among all the characterized DHDPR enzymes, site directed mutagenesis experiments were carried out to find out their roles in the catalytic process [36]. Replacing His159 or Lys163 by uncharged residues

raise the inhibition constant (K_i) by about 10 fold [36]. Replacing His159 by alanine or glutamine sharply lowered the maximum velocity by 200 fold, indicating they cannot activate the proton donor water molecule as histidine does in the catalytic process [36]. Replacing Lys163 by alanine, glutamine or cysteine even more greatly decreased the V_{max} by 600 to 800 fold, which tells that these residues cannot stabilize the catalytic intermediate like lysine does [36]. This supported the proposed mechanism in which His159 and Lys163 aided the catalytic process [36].

DHDPR kinetics

As the substrate of DHDPR is not stable in solution, it needs to be synthesized by DHDPS right before measuring the DHDPR kinetic parameters in a coupled assay similar to the one mentioned before which was used to measure DHDPS kinetic parameters [1]. The reaction rate is still acquired by measuring the consumption rate of NADPH at 340 nm absorbance, however the setup of the assay is different from the DHDPS coupled assay [1]. In the DHDPR coupled assay, pyruvate, ASA, NADPH and excess DHDPS is added to the reaction system first, the system is mixed well and placed in the water bath with optimal temperature for DHDPS to let the DHDPS catalyzed reaction take place for about one minute [1]. Then DHDPR is added to convert the HTPA synthesized by DHDPS in that one minute into THDP, consuming NADPH as well [1]. Some DHDPR can utilize both NADH and NADPH as the cofactor, thus sometimes 3 K_m values (K_m HTPA, K_m NADH and K_m NADPH) can be measured while characterizing a DHDPR [1]. As the DHDPS consumes one pyruvate and one ASA per HTPA produced, the amount of HTPA can be controlled by the amount of pyruvate added into the reaction system [1].

The kinetic parameters of DHDPR from fewer species have been measured compared to DHDPS. The kinetic parameters of bacteria and plant DHDPR are summarized in Table 5 below:

Species	K_m NADPH (μM)	K_m NADH (μM)	K_m HTPA (μM)	K_{cat} NADPH (s^{-1})	K_{cat} NADH (s^{-1})	K_{cat} HTPA (s^{-1})
bacteria						
E. coli[43]	5.6	1.6	ND	ND	ND	ND

M. tuberculosis[37]	11.8	3.2	ND	ND	ND	ND
Bacillus cereus[44]	8	ND	62	ND	ND	ND
B.megaterium[44]	13	ND	59	ND	ND	ND
*T.maritima*30°C [45]	0.6	2.5	7.6	2.6	0.093	8.1
*T.maritima*45°C [45]	2.1	1.8	13	17	0.49	19
S. aureus[42]	12	26	28 (NADPH) 39(NADH)	ND	20	20
Plant						
Z. mays[41]	46	ND	430	ND	ND	ND
A. thaliana[2]	35	ND	57	ND	ND	ND

Table 5 kinetic parameters of previously characterized bacteria and plant DHDPR. ND indicates not determined.

Little difference is found between plant and bacteria DHDPR kinetic parameters in Table 5. Thus the kinetic parameters of DHDPR cannot be used to distinguish between plant and bacteria DHDPR.

DHDPR cofactor preference

From Table 4 we can see that some DHDPR have higher K_m NADPH than K_m NADH values while some have higher K_m NADH than K_m NADPH. The K_{cat} values of DHDPR when NADPH is used as the cofactor are also different from the K_{cat} values of DHDPR when NADH is used. Thus some DHDPR prefer NADPH and some prefer NADH as their cofactor. The cofactor preference and the nucleotide binding site residues have been well studied in DHDPR from *E. coli*[46], *M. tuberculosis*[37], *T. maritima*[45]and *S. aureus*[39].

A close look at the NADH/NADPH binding site of the E. coli crystal structure is shown in Figure 11 below. The NADH had hydrophobic interactions with the Arg39, Gly84, His88, Glu38, Arg81 and the conserved ^{12}GXXGXXG^{18} dinucleotide binding motif [36].

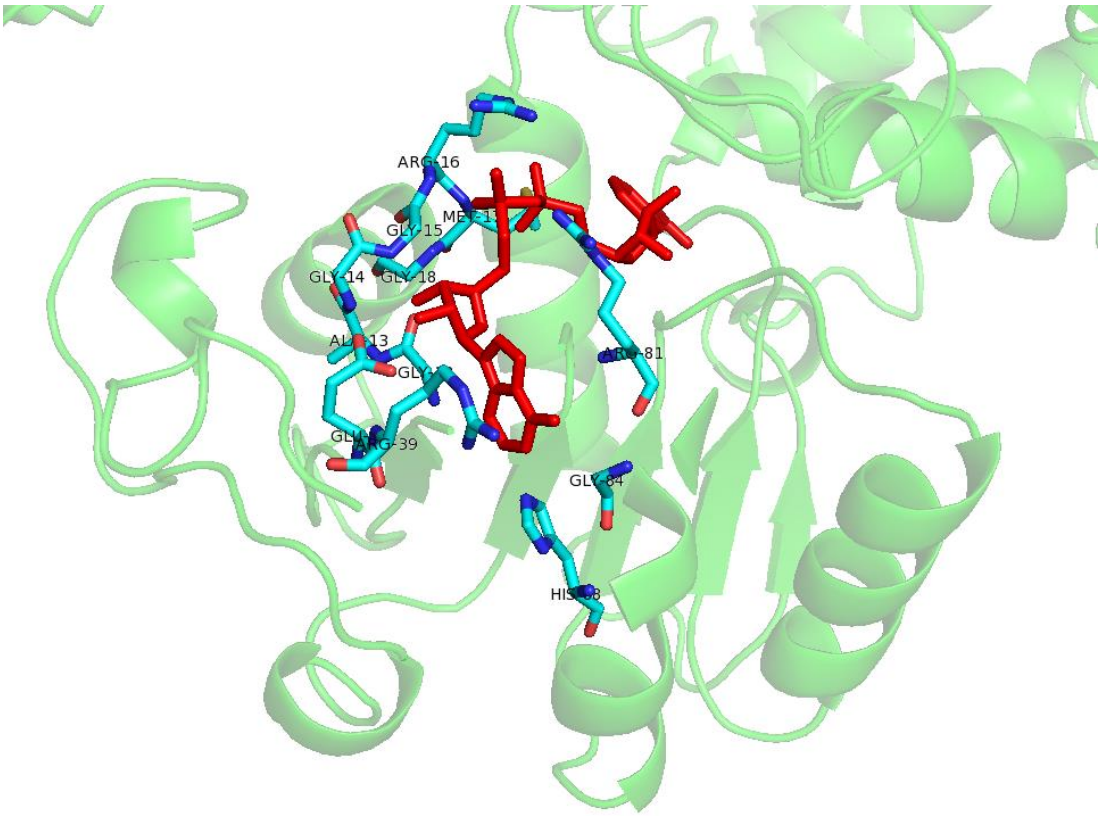

Figure 11 Structure of *E.coli* DHDPR cofactor binding site. The binding site residues are shown in cyan and the NADH bound is shown in red. PDB code: 1ARZ

The nucleotide binding site residues may be different in DHDPR from different species but has the same role. For example Glu38 in *E. coli* DHDPR and Asp33 in *M. tuberculosis* DHDPR are found to act as an acidic residue to interact with the hydroxyl group on carbon 3 of the cofactor. [40]. Residues like the Arg39 in *E. coli* DHDPR, the Lys9 and Lys11 in M. tuberculosis DHDPR and Lys35 in *S. aureus* DHDPR are all found important interacting with NADPH [39].

The affinity for NADH or NADPH is measured by Isothermal Titration Calorimetry (ITC), and it is found *E. coli* and *M. tuberculosis* DHDPR have lower K_d NADH than K_d NADPH, which means they have stronger interactions to NADH than NADPH [37, 46]. The *S. aureus* and *T. maritima* DHDPR have lower K_d NADPH and they prefer NADPH as their cofactor [39, 45].

DHDPR thermal stability

Like DHDPS, the thermal stability of DHDPR from several species, Table 6 below summarizes the four characterized DHDPR melting temperatures.

Species	Melting temperature (°C)	Method
E. coli [45]	70	DSF
S. aureus [47]	65	CD
T. maritima [45]	96	DSF
Z. mays [41]	45	Thermal inactivation assay

Table 6 Melting temperatures of previously characterized DHDPR

The bacteria DHDPR all have high melting temperatures, especially the *T. maritima* DHDPR which can still be stable over ninety degrees [46]. The maize DHDPR on the other hand has a relatively low melting temperature because maize does not live in very hot environments [42].

From the characterized enzymes discussed above, we can find that bacteria DHDPS and DHDPR are different from plant DHDPS and DHDPR in both structure and activity. In order to test the hypothesis that plant and bacteria DHDPS evolved differently from the same ancestral form, and further study the evolution and differences between plant and bacteria DHDPS and DHDPR, some algae and moss species between plant and bacteria in the evolutionary tree are chosen and the DHDPS and DHDPR from these species are studied in their thermal stability, structure and activity. The chosen species are: the green algae *Chlamydomonas reinhardtii* (CRE), *Ostreococcus tauri* (OTA), *Ostreococcus lucimarinus* (OLU), the red algae *Cyanidioschyzon merolae* (CME) and the moss *Selaginella moellendorffii* (SMO).

Material and methods

DHDPS and DHDPR genes

The CRE CME SMO and OTA DHDPS and DHDPR genes are acquired by looking for similar genes to the previously characterized DHDPS and DHDPR in their genome. The gene code from NCBI and the protein FASTA sequences are shown below. The chloroplast transit peptide sequence predicted by the ChloroP website [58] is shown in green. The chloroplast transit sequence is chopped off in the vector.

Gene code:

DHDPS				DHDPR		
CRE	CME	OTA	SMO	CRE	OLU	SMO
CHLREDRAFT_126518	CYME_CME179C	Ot05g01340	SELMODRAFT_179125	CHLREDRAFT_205760	OSTLU_40454	SELMODRAFT_75294

Table 7 Gene code of the chosen DHDPS and DHDPR from algae and moss species.

FASTA sequence:

CRE DHDPS:

MSLFSRTRAPTCPGARRARPSAVRVQATLLPLPASETRSTVDRLKKLRLITAIKTPYLANGKFDLPAYDA
LVSHQIENGVEGLIVGGTTGEGHLMSWDEHVMLIAHTVNAFGDKTAVIGNTGSNSTREALHATEQGFAVG
MHASLQINPYYGKTSKAGLLNHFNAVLNEGPAVVYNVPGRTGQDIPDDVVMEICQHSNFLGMKECTGNSR
IKNYTSKGVNCWSGNDDESHDARHSNGAVGVISVTSNVIPGLMHKLMHGSPDPQLNADLKELMAWMFCEP
NPISLNTALAMCGLARPVFRLPYVPLSRAQREKGAVLLNKVQEHIPGCKSVRVMEDHEFILVGRH

CRE DHDPR:

MVNSCTGKMGHAAAEALVDAGVKLVPHTFTGMSAGVAVKNIGVRGVATQLVGAEKRQAALDLIKAEYPGM

MIVDYTLAHCVEDHVRLYADNGLPFVMGTMGGDRDRMRAYVEEKGVYAVLPSAAGEQAMNLFALLTSLGA
PLPPHFDTYTWETVGRGDALALDLLNPQDAGEIVATLRAMGIQADDGQIYRMRASLQSRVGLNLEREPQG
ALHALQGRGSSRTCRITAPGAVPRLFLRHYGLSRAAFAAGAVEALRFLAARVAEGADQRVYDMVDVLRAY
QGEQDKLHAVRASQQFSSNVVVAGSSVTATAATSA

CME DHDPS:

MAFLSSCPGGSCLTRDHHKHRLAIRSRLQRSLCCTTARTEQQVQAQEVERPKHFFGRVITALVTPFKLTG
VEVDYGVAESLAAHLAENGSDAIIVAGTTGESATLTWSEEYELFRVVKSAVAGTKCRVIAGAGSNSTEEA
IEATKKSAKLGLDGTLQVVPYYNKPPQQGIMAHFRAIANAAPDLPMMLYNIPGRTGINMTAETSIKLAEM
CPNIVALKEASGNLEQFARIRRATSPDFALYSGDDALTLPLLSLGGNGVVSVASHFIGPEIQRMIEHFVD
LGNPEEAFRIHCRYMDLFEALFVMANPIPAKAALRLLGWPVGPTRLPLTDITASAEQQLRQAMIAAGLLS
NGSG

OTA DHDPS:

MFSKHKPFDAASLTTPRSIVSAAGDWGCPEQGCPVDVLRTKRLITAIKTPYLTSGKVDLYAYDALVEAQI
EGGVEGLIVGGTTGEGQLMSWDEHVMLIAHTAQKYGDRVLVIGNTGSNSTREAVHATSQGFAVGMDASLQ
INPYYGKTSRRGLIEHFGAVMDLGPAIVYNVPARTSQDIAPEVMFELAKHKNFAGVKECEGNVRIKGYTD
KGVTCWTGNDDEVHEARYEAGAVGVISVTSNLVPELMRELLFDGPNPELRDRLLPLMGWLFREPNPIGVN
TATAMLGVAKPVFRLPYVPYAADLRAEGAALLRDVGVANAQPLADDDFTLLREW

OLU DHDPR:

MRARGRAIVATRASADGATTRVMVNGVSGKMGHATACGVVKRAGFELVPYALTKRATAATTDVLGTEVRG
VDVGEEDAGETLERAKREYPGFIVVDYTQPDSVNSNAALYVKHGVPFVMGTTGGDRERMLREVKESGNYA
VIAPQMGKQVVAFQAAMKLMAEQFPGAFEGYTLTVTESHQSSKKDTSGTAKAIVASFNDLGCGFDLNDIE
LVRDVESQTGKMGVPEEHLLGHAFHTYRLTSADGTVSFEFQHNVCGRSIYAEGTVDAVGFLKRKVDAKDP
KTLYDMIDVLKEGAMGEWVK

SMO DHDPS:

MPEIRTQECRALASSALCGTLGRAPRSAARCGSRRACLQIRAAVMQSTPLPMRSNELKNSTPVEEMKKLR
LISAIKTPYLPDGRFDLEAYDSLVRTQVDHGVEGLIVGGTTGEGHLMNWDEHIMLIAHTVNCFGDKIKVI
GNTGSNSTREAIHATEQGFAAGMHAALHINPYYGKTSMDGLLLHFKSVLAMGPTVIYNVPGRTGQDIPPS
VIEKIASSPNFLGVKECMGNERVKHYTEQGIAVWSGNDDQCHDSRWDFGARGVISVVSNLVPKLMHELMF
SGKNQERNEKLMPLINWLFVEPNPIGLNTALSQLGLIRPVFRLPYAPLNVEKRQEFVKIVEGIGRENFPG
CTEVRLLKDDDFLLVERY

SMO DHDPR:

MVCCSLGLEWKARPGVLISASTAQGAKSSSSNIKVGSFHFPFSLVSRFLAQVIVSGACKDIGKAAIAAIS
KSRGMEVAGAIDTIRVGEDVGEVAGLEALEVPVSNNLVTVLGSLSQSRPTGVVVDFSEASEVLENVRQAT
AFGMRSVVAVPGVDLDVVSQLITFCEKASMGCVIAPTLSIGAVLLQEAAIAASFHYSHVDIVESQQSAKN
VYPSSEALRVAKSMTGMGRVYNDSDFSKEHPARGELVDDGIRIHSMVSPGFISSLAVSLSGPGEVFSLRH
DITDVKALMPGLLVAIRRVIRLQSLVYGLEKIL

The DHDPS and DHDPR genes, the polyhistidine tag and the Kanamycin and Chloramphenicol resistant genes are ligated into the pET151/D-TOPO vector and then used to transform the BL21(DE3) *E. coli* cell [49].

To get a brief overview of the relationship between the chosen enzymes and the previously characterized ones, the chosen DHDPS sequences are aligned in the Clustal Omega website [59] with 3 plant and 3 bacteria DHDPS, and same for the chosen DHDPR. The result is shown below:

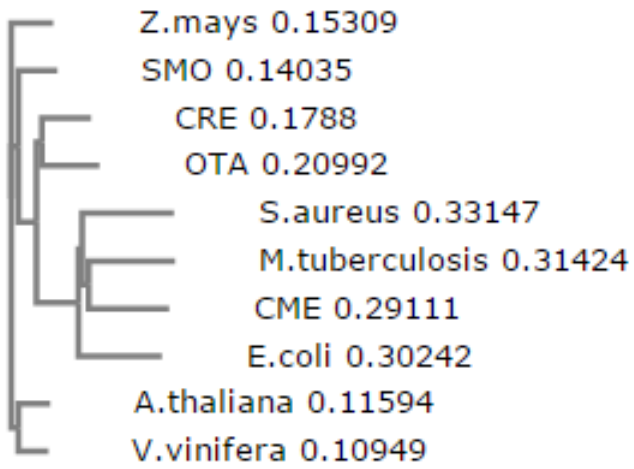

Figure 12 Phylogenetic tree of the sequence alignment of CRE, CME, OTA, SMO and some previously characterized DHDPS generated by Clustal Omega [59]. The numbers represent the tree branch length.

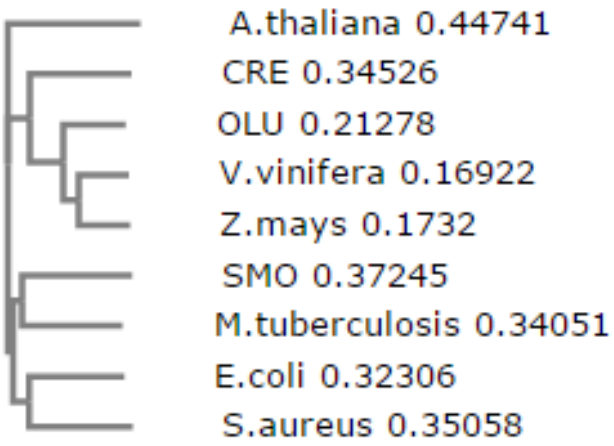

Figure 13 Phylogenetic tree of the sequence alignment of CRE, OLU, SMO and some previously characterized DHDPR generated by Clustal Omega [59]. The numbers represent the tree branch length.

From Figure 12 we can see the CME DHDPS is very closely related to bacteria DHDPS, especially the *M. tuberculosis* DHDPS. DHDPS from the two green algae species, the CRE and OTA are also closer to the bacteria DHDPS than plant ones in the phylogenetic tree, but not as close as the CME DHDPS. The SMO DHDPS is close to the maize DHDPS but far from DHDPS from the other two plant species, the *A. thaliana* and *V. vinifera*.

Looking at Figure 13, the CRE and OLU DHDPR are close to the plant DHDPR while SMO DHDPR is close to the bacteria ones, which is not consistent with the information from Figure 12 of the DHDPS alignment. The structure, activity and stability properties of the chosen DHDPS and DHDPR will be studied and compared to the previously characterized enzymes.

Culturing the bacteria

The media used to culture the transformed *E. coli* cells is the M9ZB Media [49]:

NH_4Cl	1g/L
KH_2PO_4	3g/L

Na_2HPO_4	6g/L
Bacto-tryptone	10g/L
NaCl	5g/L
Yeast extract	5g/L

Table 8 Contents of the M9ZB media

Antibiotics:

Antibiotics	Solvent	Concentration
Kanamycin	Distilled water	30 mg/ml
Chloramphenicol	100% ethanol	30 mg/ml

Table 9 Solvent and concentration of the antibiotics used in the bacteria culture to select the transformed bacteria

10µl of the freezer stock of transformed bacteria is inoculated in 10ml M9ZB media with 10µl of each of the two antibiotics added and then cultured in the 37 °C shaking incubator at 180 rpm overnight.

400µl of the two antibiotics, 0.4ml of 1M $MgSO_4$,4mlof 40% glucose and 3ml of the 10ml bacteria culture solution which has been cultured overnight are added into 0.4 L M9ZB media and incubated in the 37°C room on the shaker at 180 rpm for 4 hours [49]. Then 0.4 ml 100mg/ml IPTG was added into the culture to switch on the enzyme expression and the culture is then incubated in the 25 °C room on the shaker at 180 rpm overnight [49].

Centrifuge and Sonication

Affinity chromatography buffers [49]:

Buffer A:

Na_2HPO_4	20 mM
NaCl	500 mM
Imidazole	30 mM

Buffer B:

Na_2HPO_4	20 mM
NaCl	500 mM
Imidazole	300 mM

Table 10 Contents and concentration of the affinity chromatography buffer A and buffer B.

Cells were harvested by pelleting in a centrifuge for 10 min at 8000 rpm and 4 °C [49]. The supernatant is discarded and the pellet is resuspended on ice with 15 ml buffer A and then lysed by sonication at 0.5 cycle, 70% amplitude on ice for 20 min [49]. Soluble proteins were separated from cell debris by centrifugation at 12000 rpm for 20 min at 4 °C. The insoluble pellet is discarded and the supernatant is collected and affinity chromatography was used to purify the enzymes [49].

Affinity Chromatography

The supernatant containing the crude extract is loaded onto a GE Healthcare Histrap FF Crude 5 ml column pre-equilibrated with Buffer A [49]. Following loading, the column is washed with Buffer A until no more protein come off the column before subsequent elution of the enzyme bound to the column with Buffer B [49]. The UV detector is used to indicate the location of fractions containing the eluted enzyme [49].

Dialysis:

As the high concentration imidazole in buffer B will interfere the kinetic assay of DHDPS and DHDPR, the purified enzymes need to be dialysed to remove the imidazole in 20 mM Tris 150 mM NaCl pH 8.0 buffer overnight in the 4 °C room [49].

Purified Enzyme Concentration:

The concentration of the purified enzyme is measured by Nanodrop at 280 nm absorbance using the extinction coefficient of the chosen DHDPS and DHDPR determined by PROT PARAM [60] shown in Table 11.

Enzyme	Extinction Coefficient
CRE DHDPS	0.776
CME DHDPS	0.650
OTA DHDPS	0.939
SMO DHDPS	1.302
CRE DHDPR	0.614
OLU DHDPR	0.615
SMO DHDPR	0.240

Table 11 Extinction Coefficient of the enzymes studied.

Purity test

The purity of the enzymes purified is tested by SDS-PAGE.

Sample preparation [50]:
1μl enzyme solution
1μl LDS sample buffer
8μl distilled water

Load the marker and samples and run the gel in 1*MES buffer at 165V for 35 min [50].

Gel staining [50]:
Rinse the gel with distilled water
Microwave the gel with water for 1 min, shake 5 min
Remove water, microwave the gel with dye for 30 s, and shake overnight

Kinetic Assay

DHDPS Kinetic Assay:

The DHDPS-DHDPR coupled assay is used [1]:

Prepare 100 mM pH 8.0 HEPES buffer, 3.24 mM NADPH, and 40 mM pyruvate. The ASA powder is not pure thus its concentration can only be back calculated from the consumption of NADPH in the assay. Add NADPH, pyruvate, ASA, excess DHDPR and the HEPES buffer into the cuvette and initiate the assay by adding the target DHDPS at 25°C. The reaction rate equals the consumption rate of NADPH (the decrease rate of absorbance at 340 nm). Alter the volume of pyruvate or ASA added into the reaction system to measure the initial rate of DHDPS at different pyruvate or ASA concentrations. The pyruvate concentration is always 2 mM in each cuvette when then concentration of ASA is altered. The volume of ASA added is always 50μl in each cuvette when pyruvate concentration is altered. The NADPH concentration is always 0.162 mM in each cuvette. The volume of HEPES buffer is altered in each assay to make the total volume of the reaction system 1ml.*V.vinifera* DHDPR is used to measure the CRE, OTA and SMO DHDPS kinetics. *E. coli* DHDPR is used to measure the CME DHDPS kinetics.

The crude DHDPS concentration and volume of enzyme solution used in each assay is shown below in Table 12:

	crude DHDPS concentration	dilution	diluted DHDPS used
CRE DHDPS	6.0mg/ml	100 times	10μl
CME DHDPS	5.6mg/ml	10 times	5μl
OTA DHDPS	5.8mg/ml	10 times	5μl
SMO DHDPS	2.9mg/ml	10 times	5μl

Table 12 crude concentration, times of dilution and volume of each DHDPS used in their kinetic assays

DHDPR Kinetic Assay:

The DHDPS-DHDPR coupled assay is used [1]:

Prepare 100 mM pH 8.0 HEPES buffer, 3.24 mM NADPH and NADH, and 40 mM pyruvate. Add NADPH/NADH, pyruvate, ASA, excess DHDPS and the HEPES buffer into the cuvette and incubate at 25°C to let the DHDPS catalyzed reaction take place to accumulate HTPA for 1 min. Add target DHDPR to initiate the assay. The reaction rate equals the consumption rate of NADPH/NADH (the decrease rate of absorbance at 340 nm). Alter the volume of NADPH/NADH or pyruvate added into the reaction system to measure the initial rate of DHDPR at different NADPH/NADH or HTPA concentrations. The volume of ASA added to each cuvette is always 50μl. The pyruvate concentration is always 2 mM in each cuvette when the NADPH/NADH concentration is altered. The NADPH/NADH concentration is always 0.162 mM in each cuvette when the HTPA concentration is altered. CME DHDPS is used when measuring CRE DHDPR kinetics. SMO DHDPS is used when measuring SMO and OLU DHDPR kinetics.

The crude DHDPR concentration and volume of enzyme solution used in each assay is shown below in Table 13:

	crude DHDPR concentration	dilution	diluted DHDPS used
CRE DHDPR	4.2mg/ml	10 times	3µl
SMO DHDPR	17.7mg/ml	100 times	5µl
OLU DHDPR	3.2mg/ml	10 times	5µl

Table 13 crude concentration, times of dilution and volume of each DHDPR used in their kinetic assays

Kinetic Data Analysis:

The initial rate of each assay is plotted by Origin Pro 8.5. The DHDPS rate vs pyruvate concentration, DHDPS rate vs ASA concentration and DHDPR rate vs NAD(P)H concentration data is fitted with the hyperbl equation of $y=P_1x/(P_2+x)$ from Origin Pro 8.5 in which x represents the substrate concentration, y represents the initial rate, P_1represents V_{max} and P_2represents K_m. The lysine inhibition data and DHDPR rate vs HTPA concentration data except the SMO DHDPR vs HTPA concentration with NADPH used as a cofactor is fitted with the equation $v=V_{max}/(1+[I]/K_i)+V_{rem}$ in which v represents the initial rate, V_{max} represents the maximum velocity, [I] represents the inhibitor concentration, K_i represents the inhibition constant and V_{rem} represents the remaining rate when higher inhibitor concentration cannot reduce the rate any further [45]. The SMO DHDPR vs HTPA concentration with NADPH used as a cofactor data is fitted with the equation $v=V_{max}[S]/ (K_m+[S] +[S]^2/K_{iS})$ in which v represents the initial rate, [S] represents the substrate concentration, and K_{iS} represents the substrate inhibition constant.

Differential Scanning Fluorimetry

DSF is performed on CRE, CME, OTA, SMO DHDPS and CRE, SMO DHDPR using the Bio-Radi Cycler iQ5 Multi color Real-Time PCR Detection System. Temperature is stepped from 20°C to 95°C in increments of 0.5°C and each temperature is held for 20 seconds. Fluorescence changes in wells are monitored simultaneously with a charge-coupled device camera. Excitation

and emission wavelengths are 490 and 575 nm, respectively. All measurements were carried out in triplicate. [51]

Sample Preparation:

Prepare 20 mM Tris, 150 mM NaCl, pH 8.0 buffer and 100 times diluted sypro-orange dye.

For DHDPS, each group contains 10µl purified enzyme solution, 20µl diluted sypro-orange dye, and 70µl buffer + pyruvate to make up to 100µl. The thermal stability of all DHDPS purified were measured with no pyruvate, 0.4 mM pyruvate and 0.8 mM pyruvate on May 1st. It was measured with no pyruvate, 0.08 mM pyruvate and 2 mM pyruvate on November 10th.

For DHDPR, each group contains 10µl purified enzyme solution, 20µl diluted sypro-orange dye, and 70µl buffer + NADPH/NADH to make up to 100µl. The thermal stability of CRE, OLU and SMO DHDPR are measured with 1.5 mM NADH and NADPH, the two cofactors used by DHDPR in the catalyzed reaction.

Size Exclusion Chromatography

A Malvern P3000 column is used to carry out gel filtration at 28°C [2]. 100µl enzyme is loaded onto the column and eluted with 20 mM Tris-HCl, 150 mM NaCl, pH 8.0 buffer at 0.4 ml/min [2]. A Viscotek TDA unit is used to measure the refractive index, right angle and low angle light scattering [2]. 5 mg/ml BSA is used as a standard protein for calibration [2].

The concentrations of DHDPS and DHDPR used to run the SEC experiments are shown below:

	concentration (mg/ml)
CRE DHDPS	6.9
CME DHDPS	5.1
OTA DHDPS	3.0

SMO DHDPS	0.4
CRE DHDPR	1.2
SMO DHDPR	8.3
OLU DHDPR	0.2

Table 14 Concentration of the filtered DHDPS and DHDPR used to run SEC

Enzyme freezing and store

Add 5% volume of glycerol into the enzyme solution, mix well, transfer 700μl of the mixture solution into each eppendorf tube, and put the tubes into liquid nitrogen. After the enzymes are frozen, put the tubes into the -80°C freezer.

Result and Discussion

Enzyme expression and purification

The *E. coli* cells transformed by the predicted genes of DHDPS and DHDPR from CRE, CME, OTA and SMO are cultured and the enzymes are purified. No UV signal of CME and OTA DHDPR is observed. The predicted DHDPR gene of OLU, which is from the same genus of OTA, is then used to transform the *E. coli* cells and the enzyme is successfully purified.

The CRE DHDPR solution turned cloudy in the 20 mM Tris 150 mM NaCl pH 8.0 buffer, but stayed clear in the SEC buffer B. The CRE DHDPR is tried to be dialysed in 20 mM Na_2HPO_4 500 mM NaCl pH 8.0 buffer, and the solution did not turn cloudy again during dialysis. Thus CRE DHDPR prefers high salt concentration environment. The CRE DHDPR used to carry out all the experiments is dialysed in the high salt buffer.

The SDS-PAGE photo of purified DHDPS and DHDPR are shown in Figure 14-17 below"

CRE DHDPS + CME DHDPS

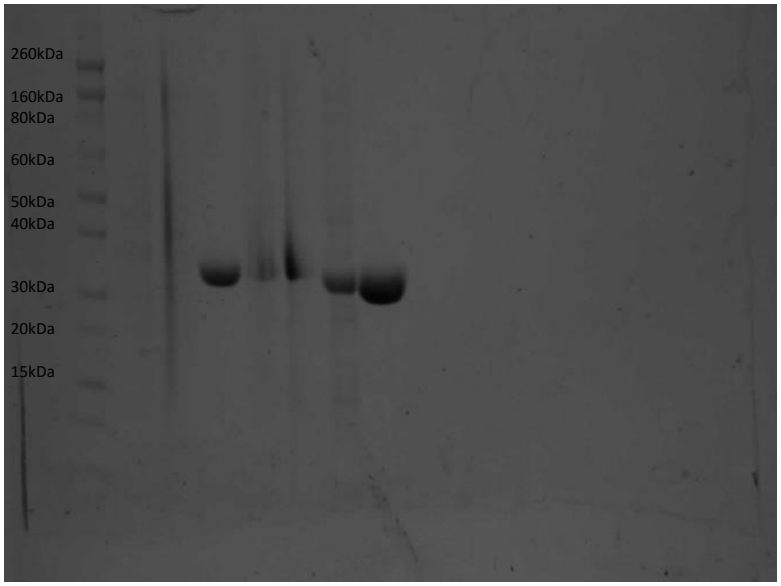

Figure 14 SDS-PAGE photo of CRE DHDPS and CME DHDPS. The columns from left to right are SDS marker, CRE DHDPS resuspend solution, CRE DHDPS post sonication

solution, purified CRE DHDPS, CME DHDPS resuspend solution, CME DHDPS post sonication solution, CME DHDPS affinity chromatography flow through solution, and purified CME DHDPS. The affinity chromatography flow through solution of CRE DHDPS was accidently not collected.

OTA DHDPS+SMO DHDPS

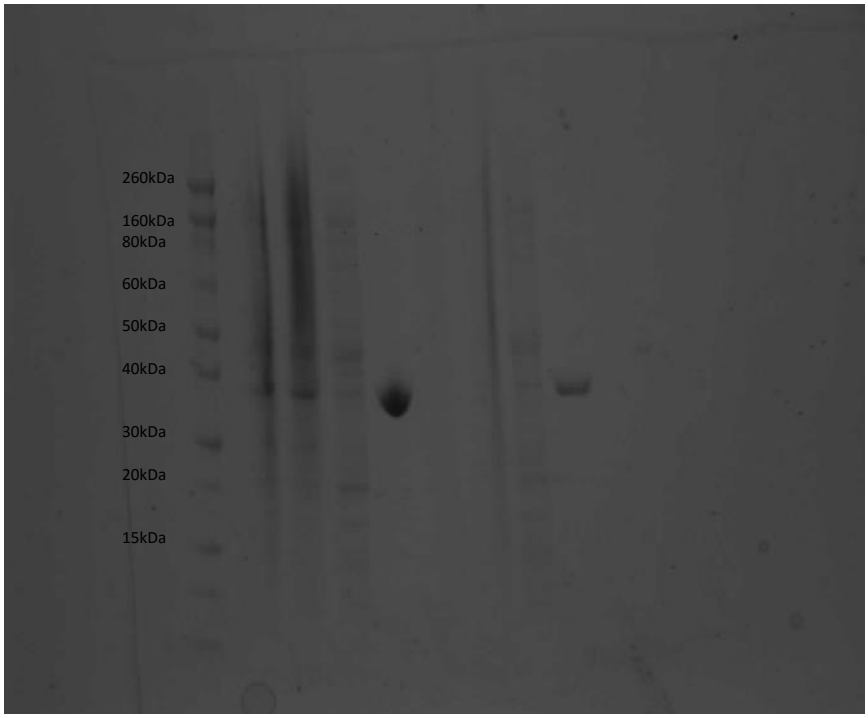

Figure 15 SDS-PAGE photo of OTA DHDPS and SMO DHDPS. The columns from left to right are SDS marker, OTA DHDPS resuspend solution, OTA DHDPS post sonication solution, OTA DHDPS affinity chromatography flow through solution, purified OTA DHDPS, SMO DHDPS resuspend solution, SMO DHDPS post sonication solution, SMO DHDPS affinity chromatography flow through solution and purified SMO DHDPS.

CRE DHDPR+SMO DHDPR

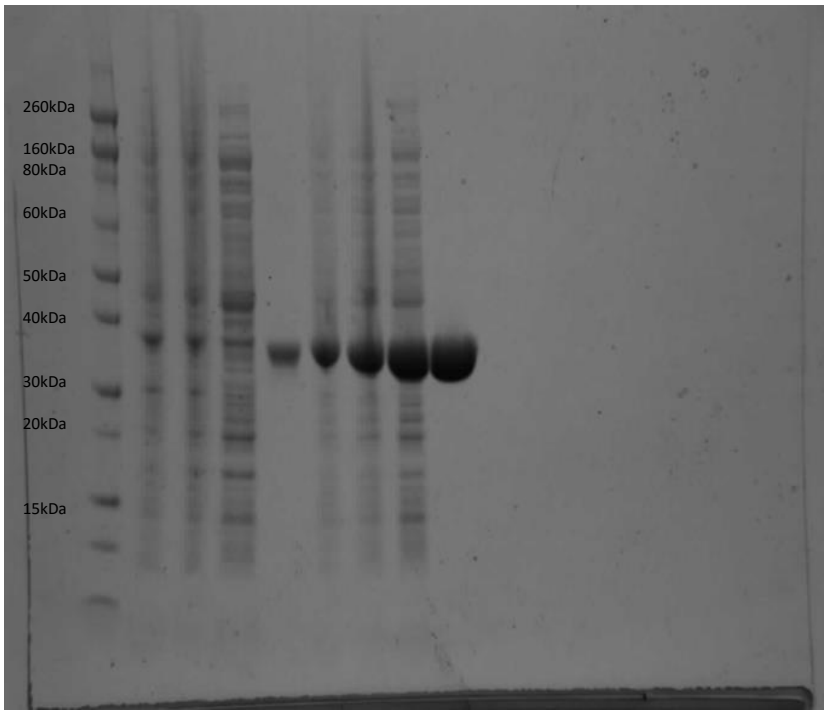

Figure 16 SDS-PAGE photo of CRE DHDPR+SMO DHDPR. The columns from left to right are SDS marker, CRE DHDPR resuspend solution, CRE DHDPR post sonication solution, CRE DHDPR affinity chromatography flow through solution, purified CRE DHDPR, SMO DHDPR resuspend solution, SMO DHDPR post sonication solution, SMO DHDPR affinity chromatography flow through solution and purified SMO DHDPR.

OLU DHDPR

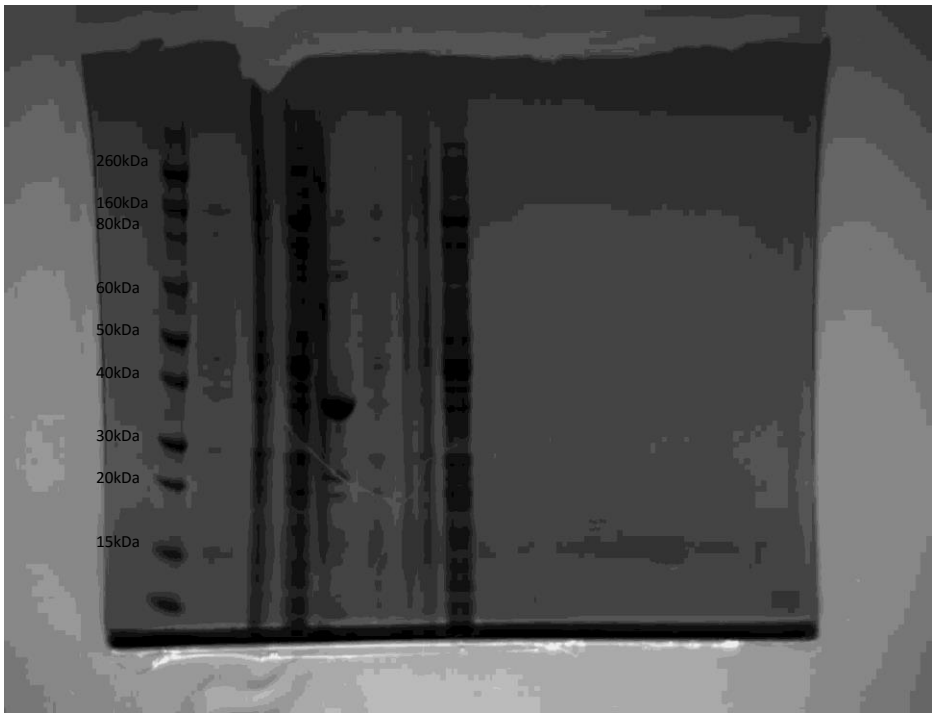

Figure 17 SDS-PAGE photo of OLU DHDPR. The columns from left to right are SDS marker, OLU DHDPR resuspend solution, OLU DHDPR post sonication solution, OLU DHDPR affinity chromatography flow through solution, purified OLU DHDPR, and the resuspend solution, post sonication solution and the affinity chromatography flow through solution of DHDPR from another species which was not expressed.

In the resuspend solution column, the E coli cells were intact and not many proteins could be found in the solution so there were only a few bands shown in the SDS-PAGE photos. In the post sonication solution columns and the affinity chromatography flow through columns, the E coli cells were broken and all the macromolecules inside were released, so bands representing different sized molecules could be seen all the way from top to bottom of the columns. And in the last column of each enzyme purified, only a single band could be seen representing the enzymes purified.

The monomer molecular weight of the DHDPS and DHDPR calculated by the ExPASy ProtParam website from the enzyme genes chosen after cleaving their chloroplast transient sequences are shown in Table 15 below:

	DHDPS	DHDPR
CRE	35176.2 Da	33429.1 Da
CME	33153.0 Da	36276.4 Da
OTA	33904.5 Da	29942.0 Da
SMO	36379.8 Da	25365.1 Da
OLU		30961.9 Da

Table 15 Monomer molecular weight of the DHDPS and DHDPR calculated by ExPASy ProtParam website [60].

The single bands representing the purified enzymes in the SDS photos are all in between the 30 kDa band and the 40 kDa band in the marker, which is consistent with the monomer molecular weight shown above.

Differential Scanning Fluorimetry

The RFU (relative fluorescence unit) vs Temperature and -(RFU)/dT (change in fluorescence with respect to time) data is exported and plotted in Excel. An example of the plotted curves of CRE DHDPS with 0.4mM pyruvate is shown below in Figure 18 and 19:

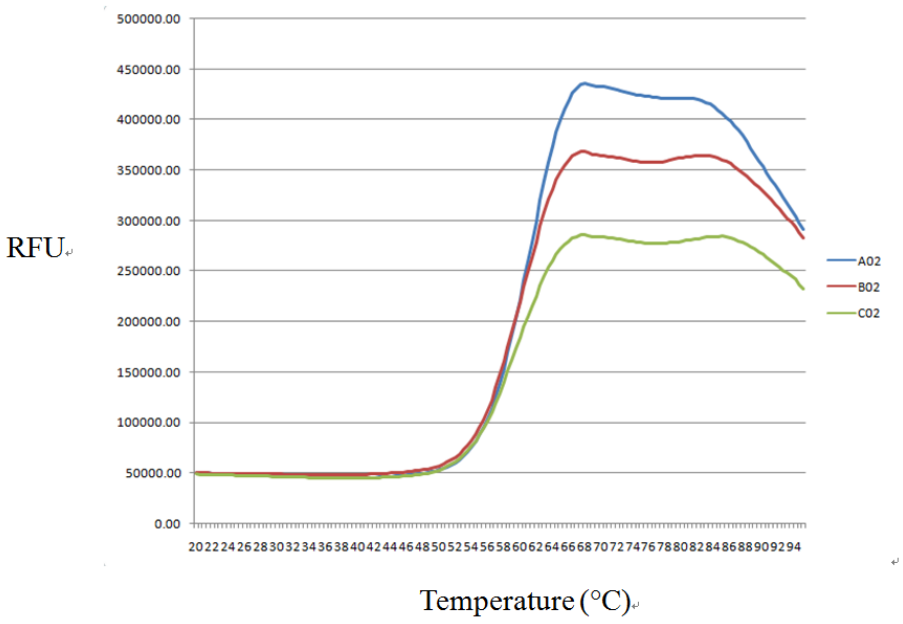

Figure 18 RFU vs Temperature plot of triplicate sample of CRE DHDPS with 0.4 mM pyruvate.

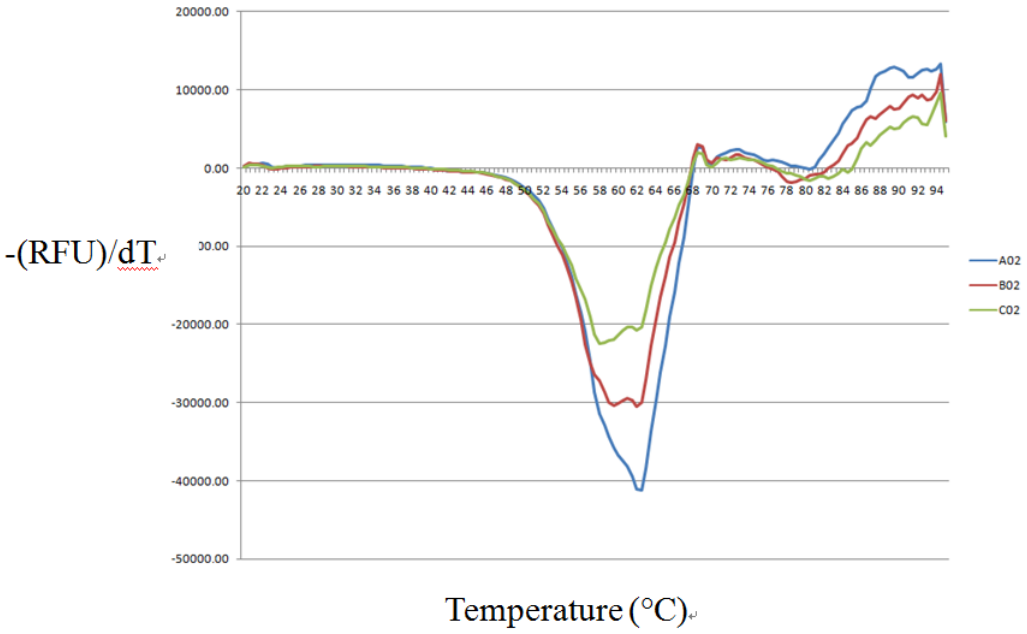

Figure 19 -(RFU)/dT vs Temperature plot of triplicate sample of CRE DHDPS with 0.4 mM pyruvate.

Figure 18 shows the change of fluorescence detected at different temperatures, when the fluorescence starts increasing, the protein is denatured and unfold to expose the dye bound to its hydrophobic part. Figure 19 shows the slope of the curve in Figure 18. The peak shown in Figure 19 represents the rapid increase of fluorescence detected. The peak temperatures of the 3 duplicates in Figure 19 are slightly different, the mean value is recorded as the melting temperature of this enzyme at this condition.

DHDPS DSF result:

The melting points of all four DHDPS in different pyruvate concentrations are summarized in Table 16 below:

May 1st	CRE DHDPS	CME DHDPS	OTA DHDPS	SMO DHDPS
No pyruvate	57°C	66°C	45°C	47°C
0.4 mM pyruvate	62°C	72°C	47°C	48°C
0.8 mM pyruvate	62°C	74°C	48°C	48°C
November 10th	CRE DHDPS	CME DHDPS	OTA DHDPS	SMO DHDPS
No pyruvate	60°C	68°C	47°C	50°C
0.08 mM pyruvate	62°C	68°C	48°C	51°C
2 mM pyruvate	70°C	77°C	53°C	54°C

Table 16 Melting points of DHDPS from CRE, CME, OTA and SMO. The 0.4 mM and 0.8 mM pyruvate groups are done on May 1st and the 0.08 mM and 2 mM pyruvate groups are done on November 10th.

The two sets of experiments were done on different dates with enzymes purified in different trials, the time between purification and the DSF experiment was also different. So the activity and concentration of DHDPS from the same species may be different while the DSF experiment is carried out. This explains why the melting points of control group DHDPS with no pyruvate of the November 10th set are slightly higher than that of the May 1st set. The effect of different concentrations of pyruvate is summarized in Table 17 below:

	CRE DHDPS	CME DHDPS	OTA DHDPS	SMO DHDPS
0.08 mM pyruvate	2°C	0°C	1°C	1°C
0.4 mM pyruvate	5°C	6°C	2°C	1°C
0.8 mM pyruvate	5°C	8°C	3°C	1°C
2 mM pyruvate	10°C	9°C	6°C	4°C

Table 17 The change in melting temperature caused by different concentrations of pyruvate compared to the control groups.

From Table 17 we can see that CRE, CME and OTA DHDPS are significantly stabilized by gradually increased concentrations of pyruvate while SMO DHDPS is not very sensitive to low concentration pyruvate, and significant change in the melting temperature of SMO DHDPS is only observed when the pyruvate concentration is raised to 2 mM. Among all the four DHDPS purified, CME DHDPS has the highest melting temperature of 68°C, because CME is a red alga found living in acidic hot springs with high sulfur [52].

Comparing Table 17 and Table 3 we can see the CRE and CME have similar melting temperatures to most of the previously characterized bacteria DHDPS, while OTA and SMO DHDPS have lower melting temperatures like the plant DHDPS. OTA is found in the ocean [53] and SMO is a moss, their living environment temperatures are not as high as CME or *T. maritima*, and that explains why their melting temperatures are lower than others.

DHDPR DSF result:

The CRE and SMO DHDPR reacted with the sypro orange dye, but the OLU DHDPR did not react well with the dye and the fluorescence was very high at 20°C, so the OLU DHDPR result is not discussed here. The result of CRE and SMO DHDPR is shown in Table 18 below:

	CRE DHDPR	SMO DHDPR
no NADPH or NADH	69°C	42°C
1.5 mM NADPH	76°C	47°C
1.5 mM NADH	76°C	52°C

Table 18 Melting temperatures of CRE and SMO DHDPR with different cofactors added.

From the Table 18 we can see the CRE DHDPR is much more stable than SMO DHDPR, with a melting point 27°C higher with no NADPH or NADH. The CRE DHDPR was stabilized by both NADPH and NADH and the melting temperature raised by both cofactors were the same. The SMO DHDPR was also stabilized by both cofactors, 1.5 mM NADPH raised its melting temperature by 5°C, and 1.5 mM NADH raised its melting temperature by 10°C. Thus CRE DHDPR is stabilized by NADPH and NADH by the same degree while SMO DHDPR is more stabilized by NADH than NADPH.

Comparing Table 18 and Table 6, we can find that CRE DHDPR behaves like the previously characterized bacteria DHDPR which have relatively high melting temperatures while SMO DHDPR behaves like plant DHDPR with lower melting temperatures.

Size Exclusion Chromatography

The size exclusion chromatography was done on the seven purified enzymes: CRE DHDPS, CME DHDPS, OTA DHDPS, SMO DHDPS, CRE DHDPR, SMO DHDPR and OLU DHDPR. The well studied bovine serum albumin (BSA) was used as the standard protein to calculate the molecular parameters of the DHDPS and DHDPR samples.

The first set of SEC experiments were done on the CRE, CME, and OTA DHDPS. The result of their elution peaks are shown below:

The standard BSA was eluted at around 13 ml and 15 ml as shown by the two major peaks of the refractive index (red) curve in Figure 20 below, representing the different polymerization state of BSA.

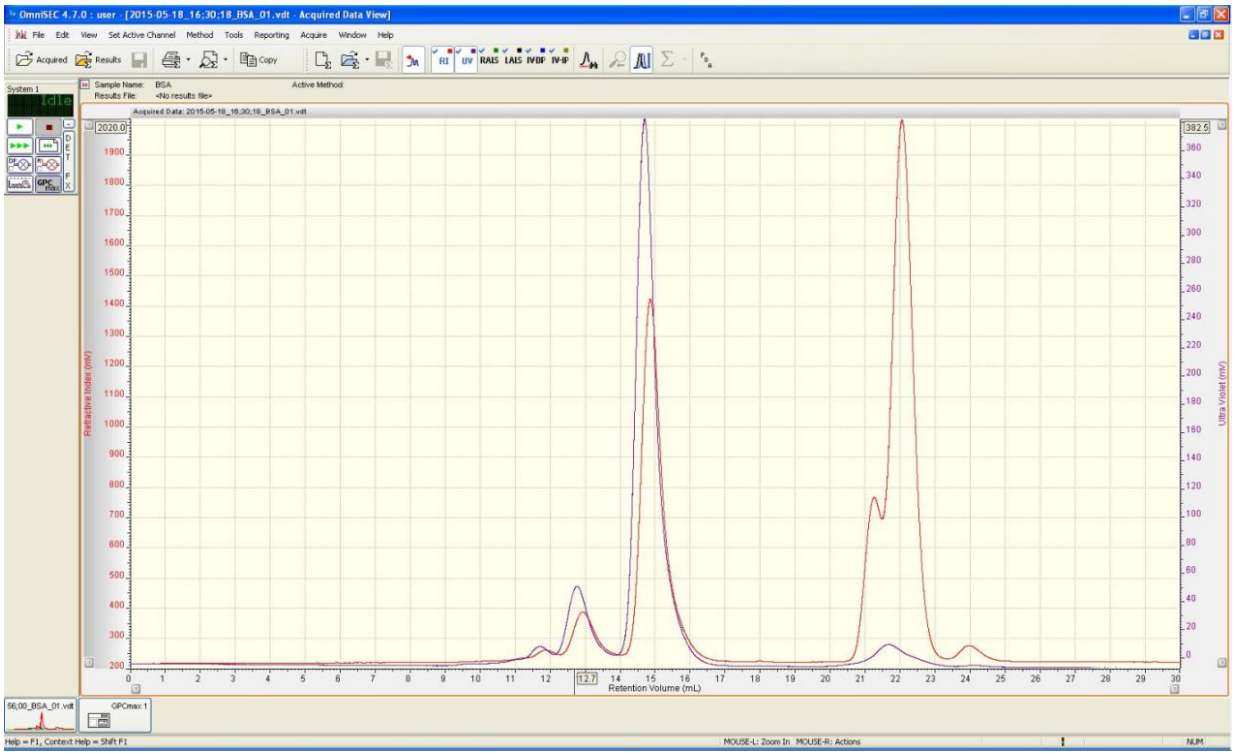

Figure 20 SEC curve of the standard BSA. The refractive index curve is shown in red and the UV curve is shown in purple.

The calculated molecular weight of the 14.837 ml peak is exactly 67 kDa which is very close to the characterized molecular weight of BSA monomer [54], and the 12.912 ml peak molecular weight is 136 kDa which is twice as much as the 14.837 peak, thus the 14.837 ml peak represents the BSA monomer and the 12.912 ml peak represents the BSA dimer.

Figure 21 below is the CRE DHDPS SEC result:

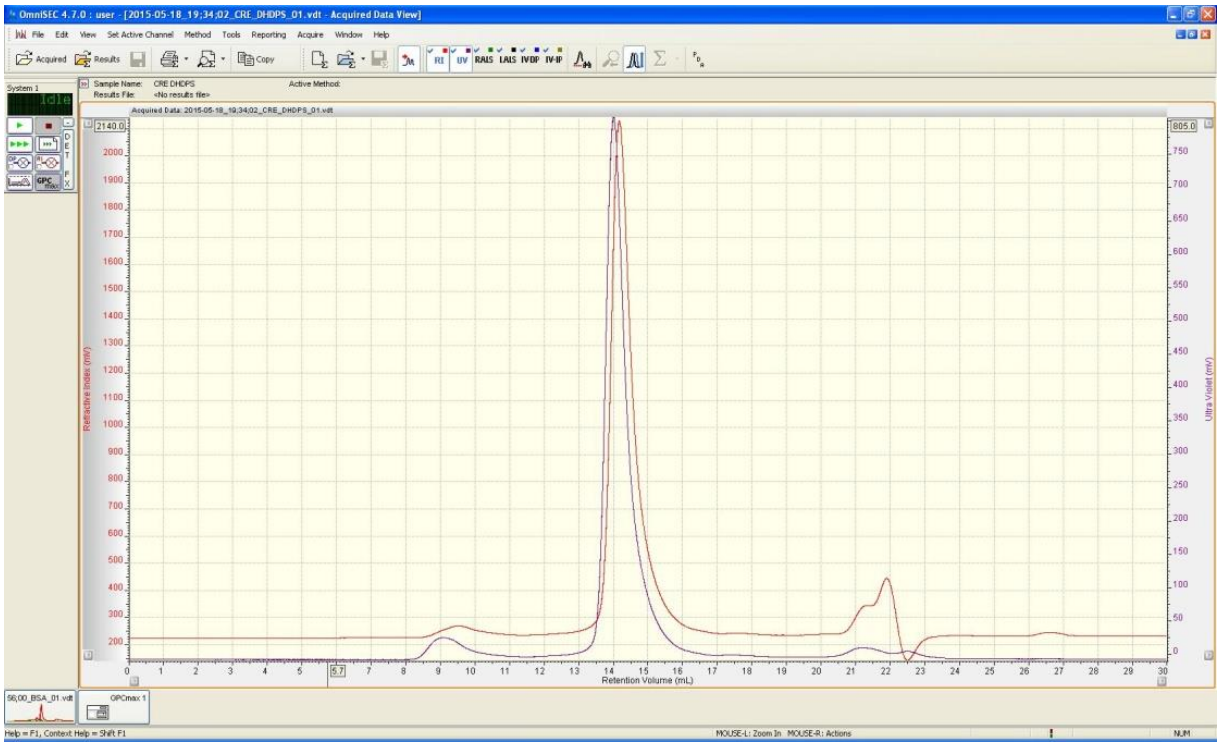

Figure 21 SEC curve of CRE DHDPS. The refractive index curve is shown in red and the UV curve is shown in purple.

The major peak shown in the graph representing CRE DHDPS is eluted at 14.148 ml and its molecular weight is calculated to be 135.7 kDa. The monomer molecular weight calculated from the CRE DHDPS gene used after cleaving the chloroplast transit peptide sequence is 35.2 kDa, so the enzyme exists as a tetramer in solution.

Figure 22 below is the CME DHDPS SEC result:

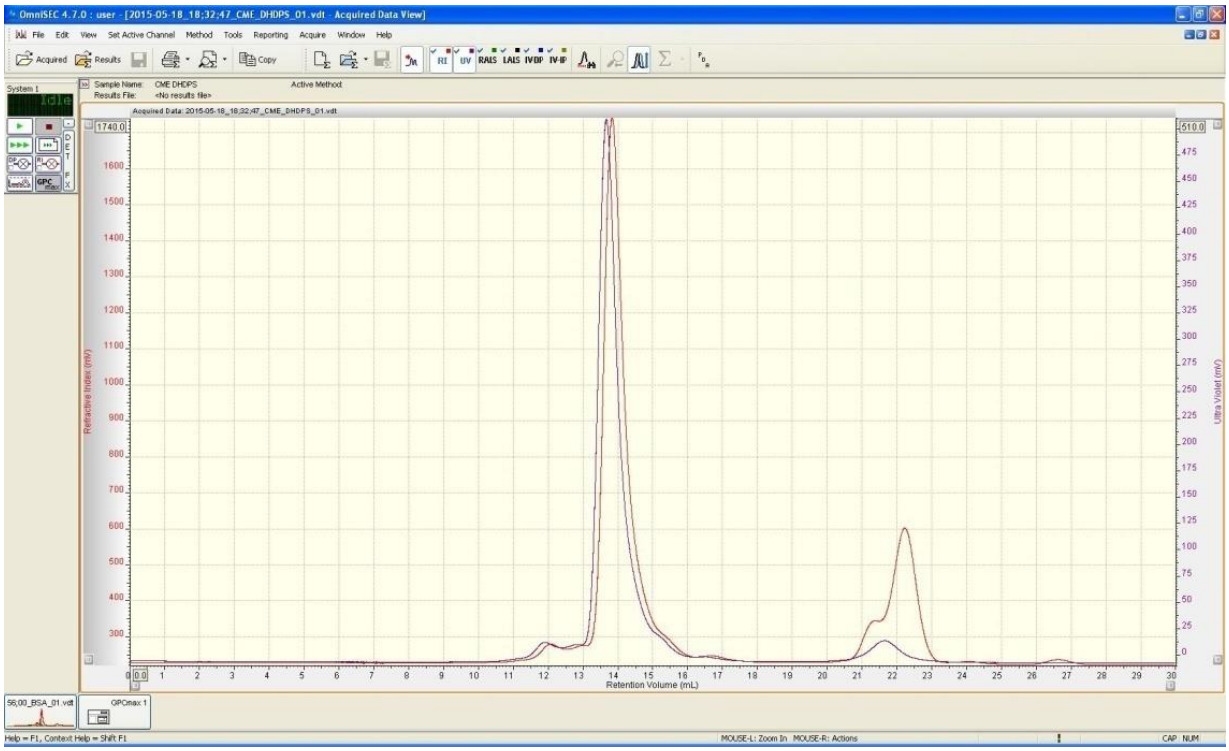

Figure 22 SEC curve of CME DHDPS. The refractive index curve is shown in red and the UV curve is shown in purple.

The CME DHDPS represented by the largest peak in Figure 20 is eluted at 13.8 ml, and its molecular weight is calculated to be 129.7 kDa. The monomer molecular weight calculated from the CME DHDPS gene used after cleaving the chloroplast transit peptide sequence is 33.2 kDa, so the enzyme exists as a tetramer in solution.

Figure 23 below is the OTA DHDPS SEC result:

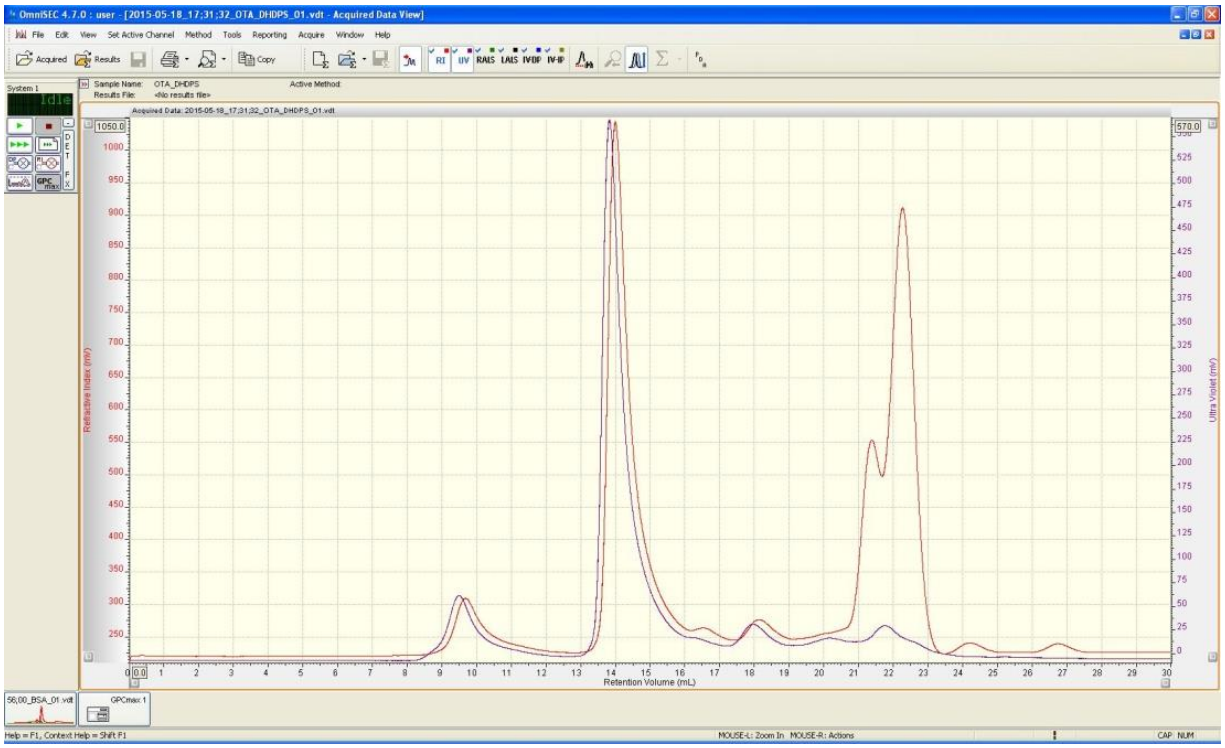

Figure 23 SEC curve of OTA DHDPS. The refractive index curve is shown in red and the UV curve is shown in purple.

The OTA DHDPS represented by the largest peak in Figure 21 was eluted at 13.97 ml and its molecular weight was calculated to be 118.8kDa. The monomer molecular weight calculated from the OTA DHDPS gene used after cleaving the chloroplast transient peptide sequence was 33.9 kDa, the calculated polymer molecular weight of OTA DHDPS is in between the molecular weight of a trimer and a tetramer in solution, but more close to a tetramer. In addition, there is no trimer DHDPS characterized before, we can conclude that OTA DHDPS exists as a tetramer in solution.

The next set of SEC experiment was done on the CRE and SMO DHDPR.
BSA was used as the standard proteinagain, its SEC result will not be discussed again here.

The CRE DHDPR result is shown in Figure 24 below:

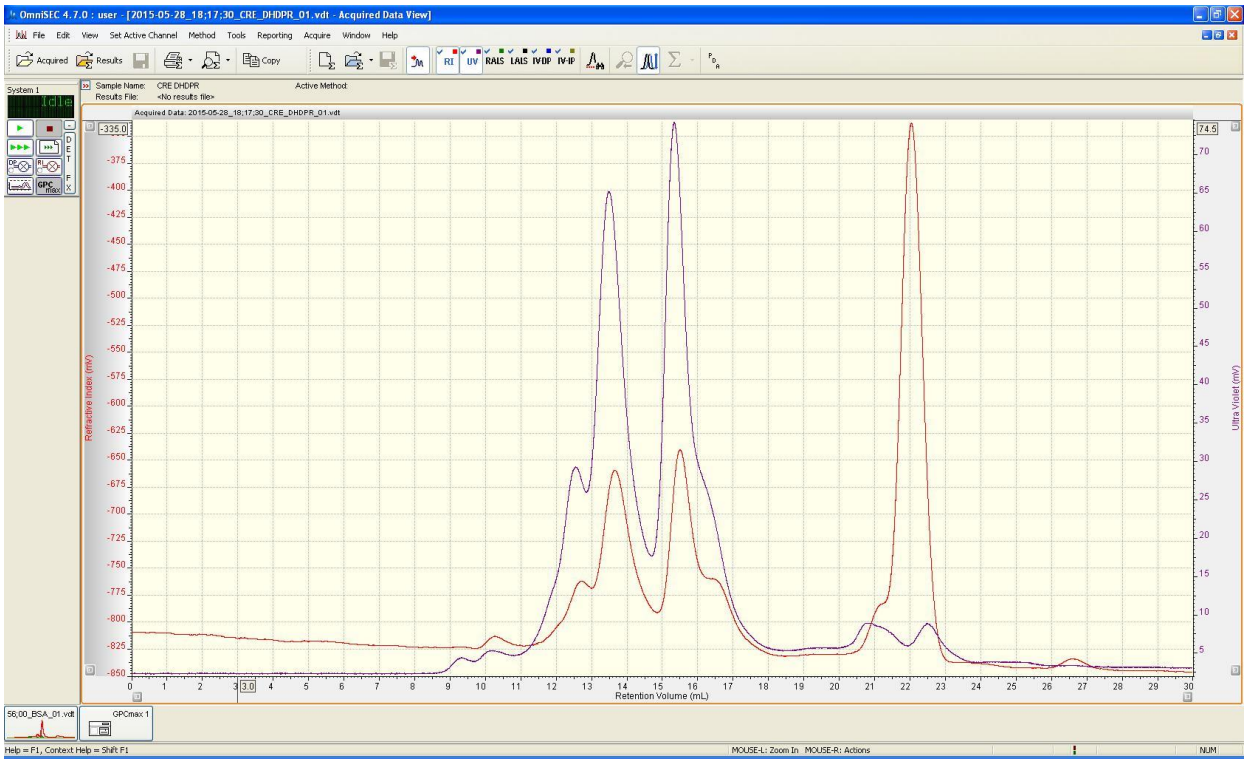

Figure 24 SEC curve of CRE DHDPR. The refractive index curve is shown in red and the UV curve is shown in purple.

There are two major peaks with the same size. The molecular weight of the 13.6 ml peak is 154 kDa, and the 15.5 ml peak is 80 kDa. The monomer molecular weight calculated from the CRE DHDPR gene used after cleaving the chloroplast transient peptide sequence is 33.4 kDa. Because the size of these two peaks are the same, CRE DHDPR may exist as an equilibrium of tetramer and dimer in solution.

The SMO DHDPR result is shown in Figure 25 below:

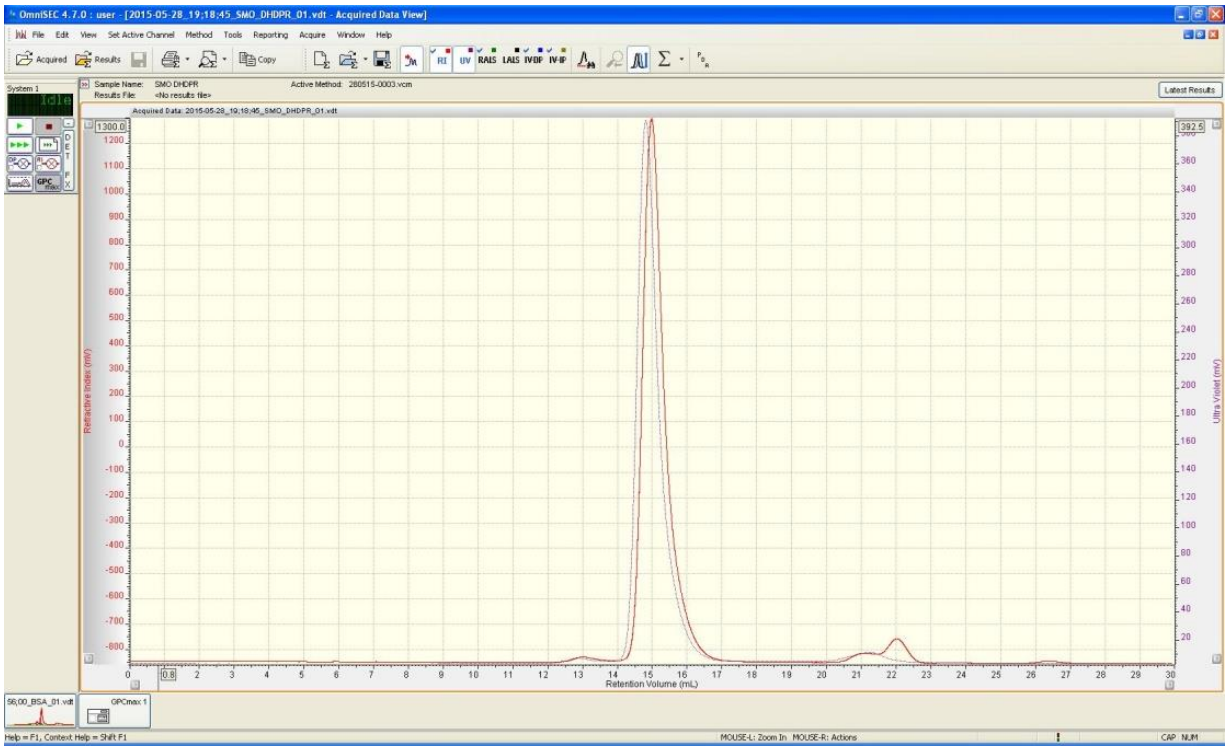

Figure 25 SEC curve of SMO DHDPR. The refractive index curve is shown in red and the UV curve is shown in purple.

The molecular weight of enzyme eluted at 15 ml is calculated to be 64.4 kDa. The monomer molecular weight calculated from the SMO DHDPR gene used after cleaving the chloroplast transient peptide sequence is 25.4 kDa, so SMO DHDPR exists as a dimer in solution.

The third set of SEC experiment was done on the OLU DHDPR and the SMO DHDPS on Again the BSA standard protein result is not discussed here.

Figure 26 below shows the OLU DHDPR result:

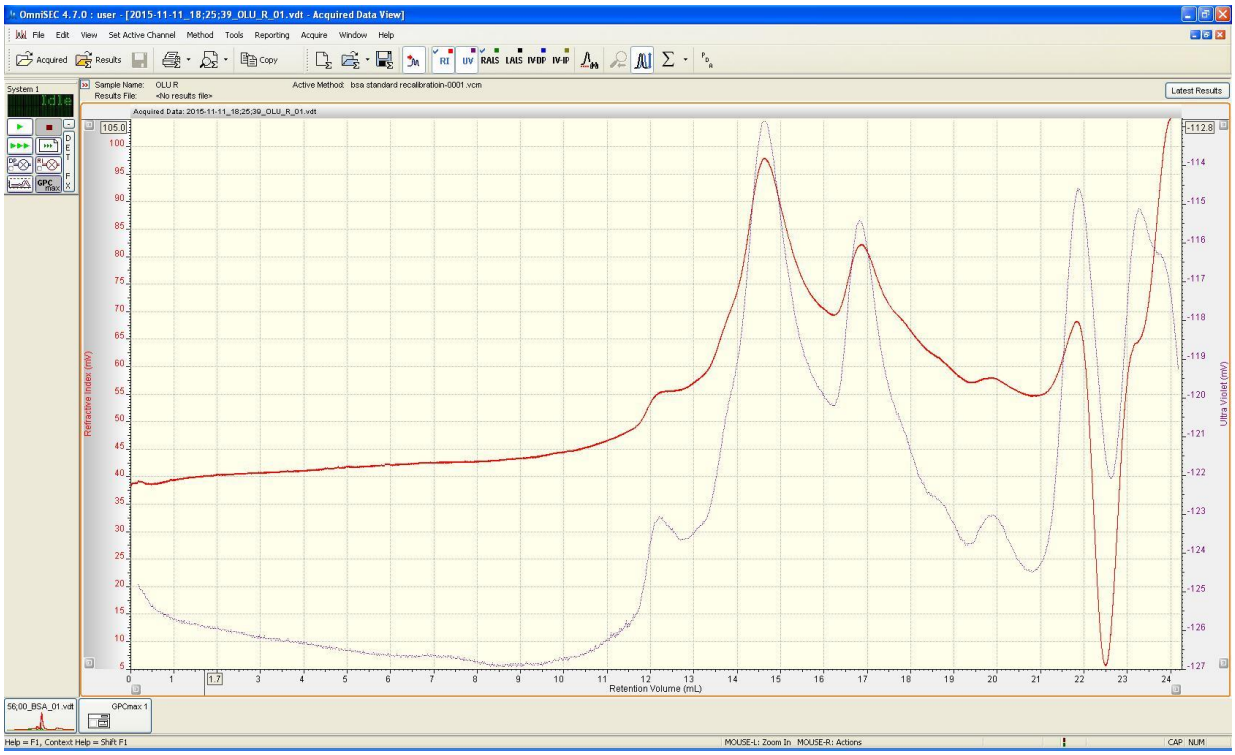

Figure 26 SEC curve of OLU DHDPR. The refractive index curve is shown in red and the UV curve is shown in purple.

The enzyme is eluted at 14.6 ml, represented by the largest peak in Figure 24. The OLU DHDPR had a molecular weight of 128 kDa. The monomer molecular weight calculated from the OLU DHDPR gene used after cleaving the chloroplast transient peptide sequence is 31 kDa, thus OLU DHDPR exists as a tetramer in solution.

Figure 27 below shows the SEC result of SMO DHDPS:

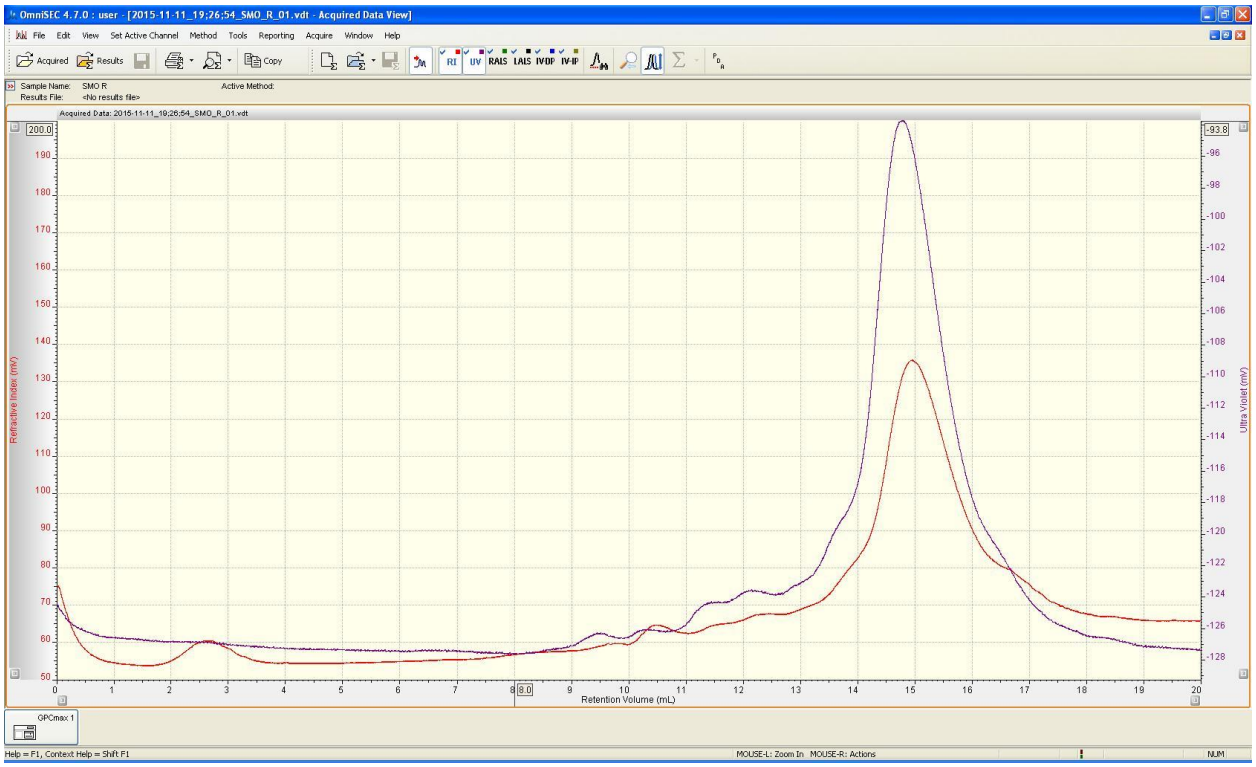

Figure 27 SEC curve of SMO DHDPS. The refractive index curve is shown in red and the UV curve is shown in purple.

The enzyme eluted at the 15 ml peak has a molecular weight of 102 kDa. The monomer molecular weight calculated from the SMO DHDPS gene used after cleaving the chloroplast transient peptide sequence is 36.4 kDa. The data shows SMO DHDPS is more close to a trimer than tetramer in solution.

However, the calculated molecular weight of SMO DHDPS along the peak is not a constant value like the other enzymes. Figure 28 shows the calculated molecular weight of CRE DHDPS along its peak and Figure 29 shows the calculated molecular weight of SMO DHDPS along its peak:

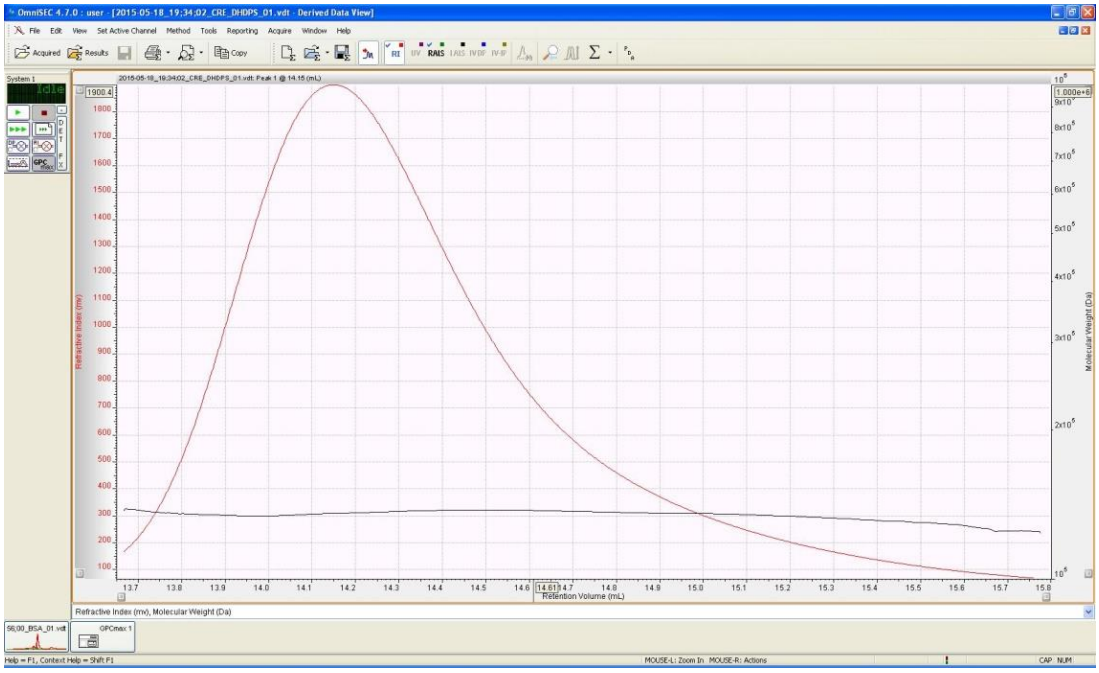

Figure 28 Calculated CRE DHDPS molecular weight. The horizontal black line represents the molecular weight calculated along the range of the peak.

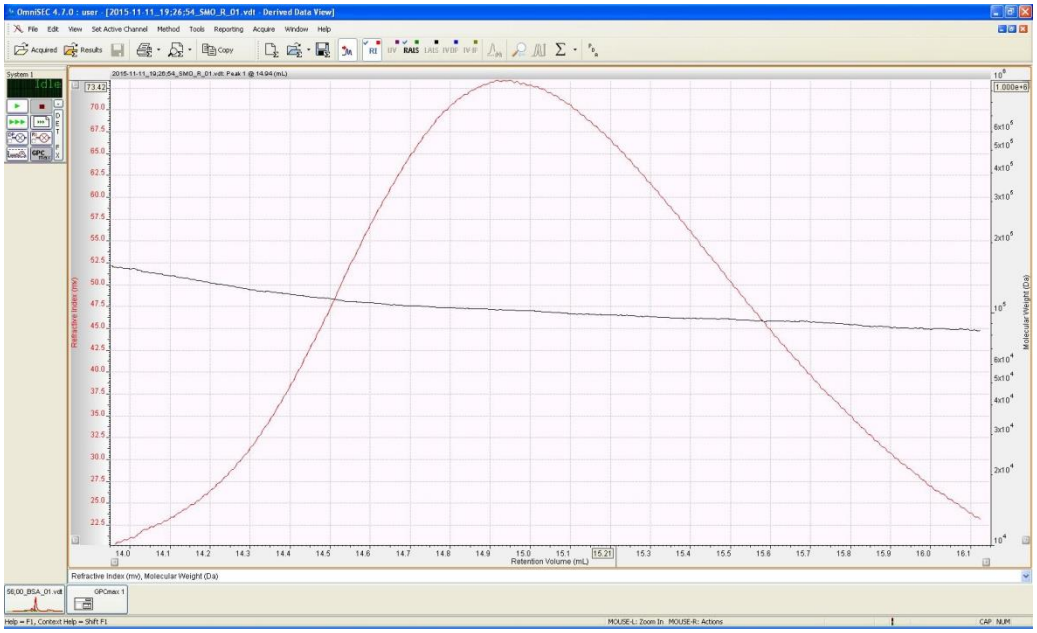

Figure 29 Calculated SMO DHDPS molecular weight. The horizontal black line represents the molecular weight calculated along the range of the peak.

The black line in Figure 29 is not horizontal as the line in Figure 28. This means the molecular weight of SMO DHDPS calculated from the refractive index varies along the peak. Together with the experimental data of previously characterized DHDPS, no trimer was reported, this SMO DHDPS trimer result is very questionable and needs further structural study.

Table 19 summarizes the SEC results described above:

Enzyme	Polymer molecular weight (kDa)	Monomer molecular weight (kDa)	Degree of polymerization
CRE DHDPS	135.7	35.2	4
CME DHDPS	129.7	33.2	4
OTA DHDPS	118.8	33.9	4
SMO DHDPS	101.8	36.4	3
CRE DHDPR	154 and 80	33.4	2 and 4
SMO DHDPR	64.4	25.4	2
OLU DHDPR	127.8	31	4

Table 19 Polymer molecular weight, monomer molecular weight and degree of polymerization of the characterized DHDPS and DHDPR enzymes.

The CRE DHDPR had a dimer peak and a tetramer peak of the same size, which means half of the enzyme exist as dimer and half as tetramer in solution. This leads to a hypothesis that the CRE DHDPR's dimer-dimer interface can bind and unbind freely and this process reaches an equilibrium in solution. In addition, the behavior of CRE DHDPR in purification and dialysis is not as good as other enzymes. It turned cloudy in the Tris buffer and stayed stable in the high salt buffer later. There might still be some environmental factor in the CRE DHDPR solution that could disrupt the interactions between the CRE DHDPR dimer-dimer interface and break down the tetramer enzyme into two dimers. Further structural study is needed to test this hypothesis.

The OLU DHDPR exists as a tetramer in solution, which is consistent with the characterized DHDPR from bacteria species like *S. aureus* [4], *M. tuberculosis* [17] and *E. coli* [3]. The SMO DHDPR exists as a dimer in solution, and this is consistent with the characterized DHDPR from plants like maize [41] and *A. thaliana* [2]. So SMO DHDPR is more closely related to plant DHDPR and OLU DHDPR is more close to bacteria ones.

The CRE and CME DHDPS exist as tetramers in solution. However the characterized plant and bacteria DHDPS are all tetramers in solution, so we cannot tell whether the CRE and CME DHDPS are more closely related to bacteria or plant DHDPS. Their crystal structures are needed to find out the arrangement pattern of the "dimer of the dimer" and then tell their relationship to plant or bacteria DHDPS.

Kinetics

Plotted DHDPS Kinetic Curves

CRE DHDPS vs pyruvate:

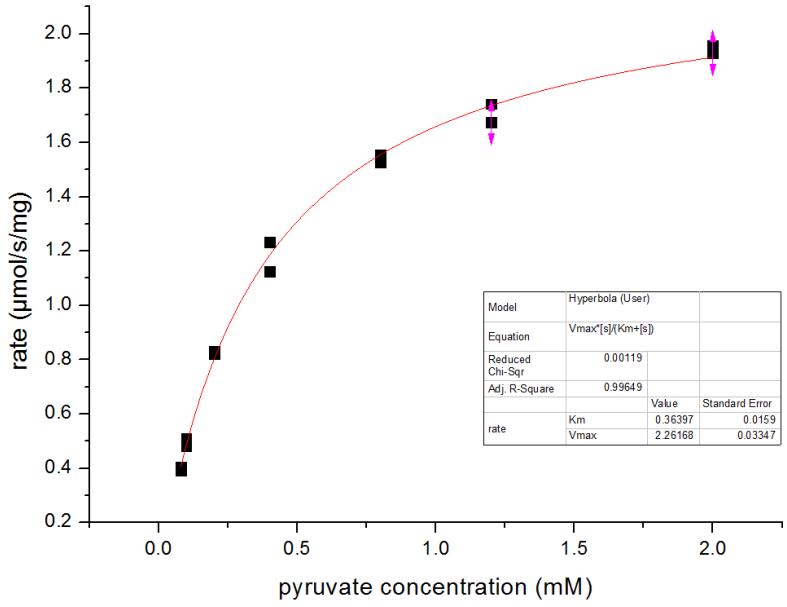

Figure 30 Plotted CRE DHDPS rate with different pyruvate concentrations.

CRE DHDPS vs ASA:

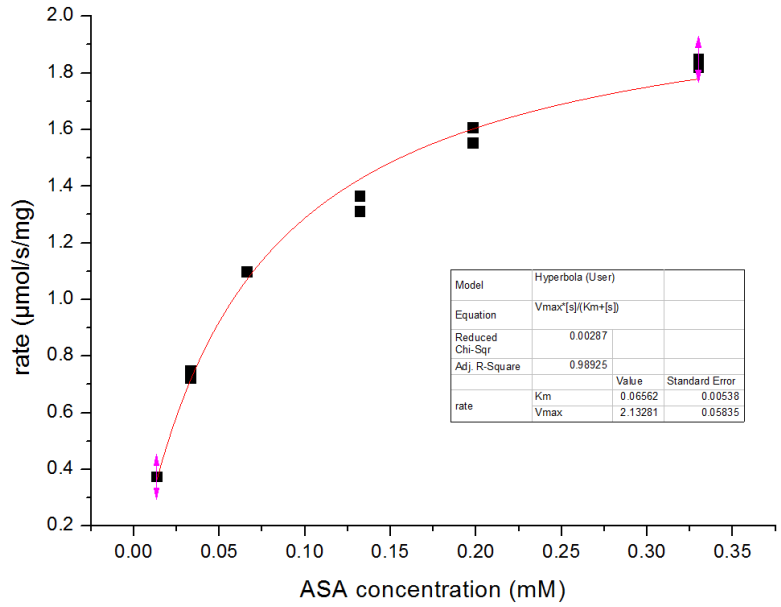

Figure 31 Plotted CRE DHDPS rate with different ASA concentrations.

CME DHDPS vs pyruvate:

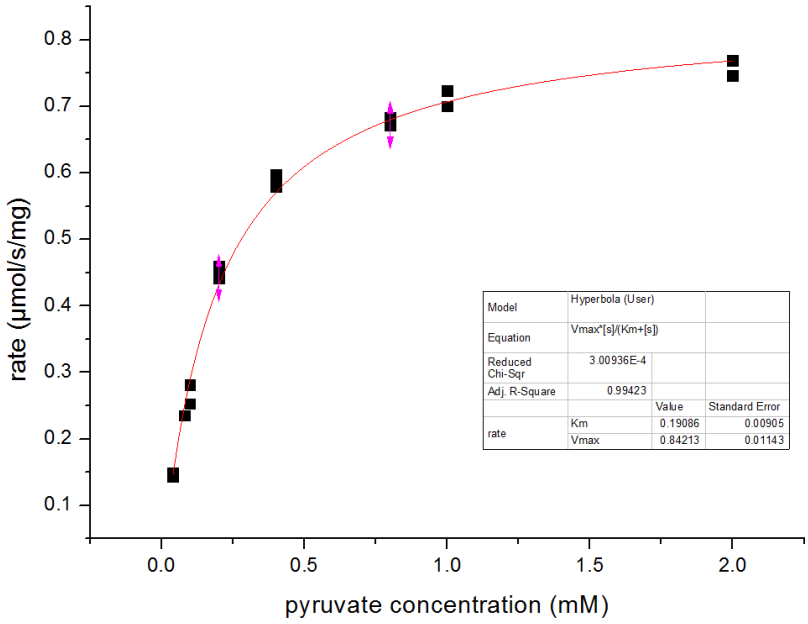

Figure 32 Plotted CME DHDPS rate with different pyruvate concentrations.

CME DHDPS vs ASA:

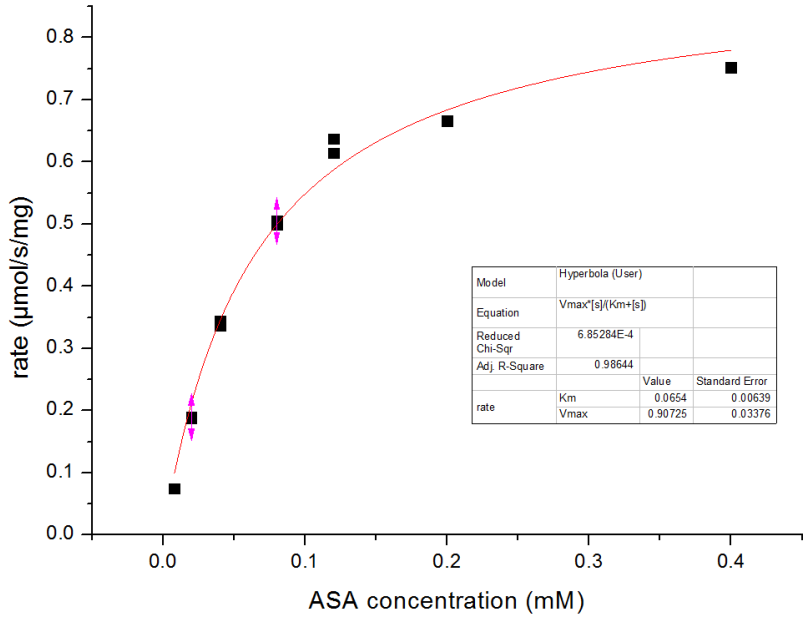

Figure 33 Plotted CME DHDPS rate with different ASA concentrations.

OTA DHDPS vs pyruvate:

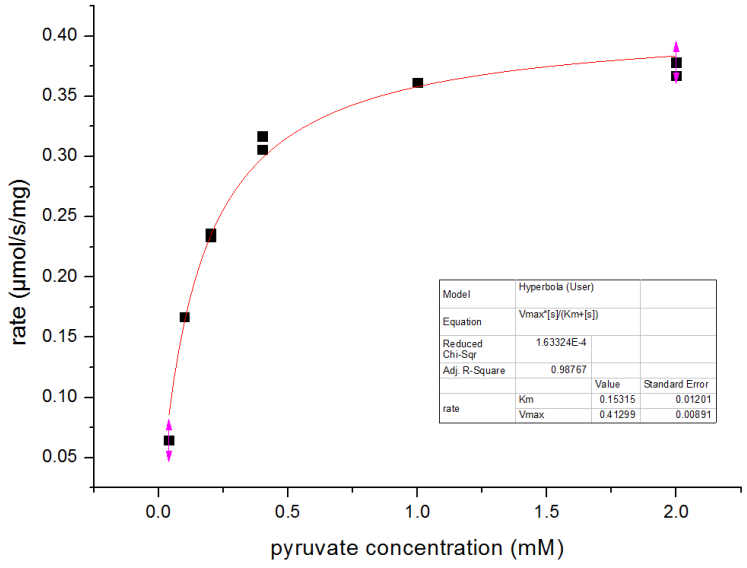

Figure 34 Plotted OTA DHDPS rate with different pyruvate concentrations.

OTA DHDPS vs ASA:

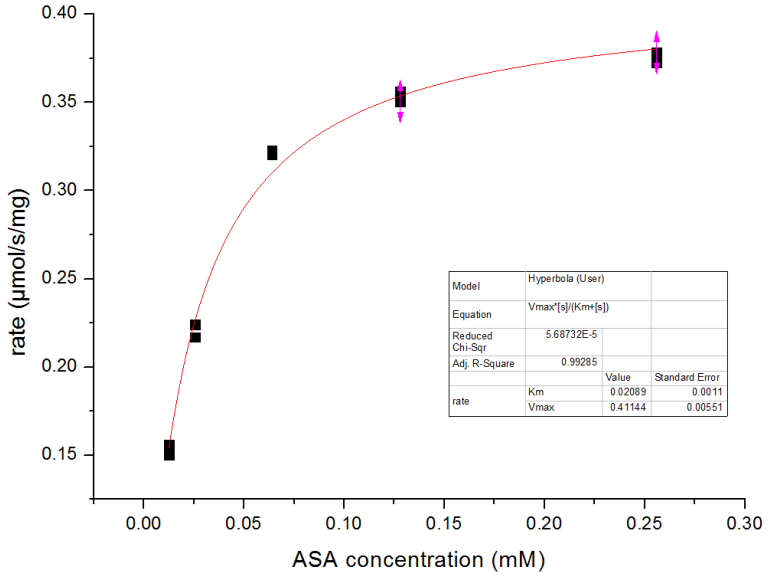

Figure 35 Plotted OTA DHDPS rate with different ASA concentrations.

SMO DHDPS vs pyruvate

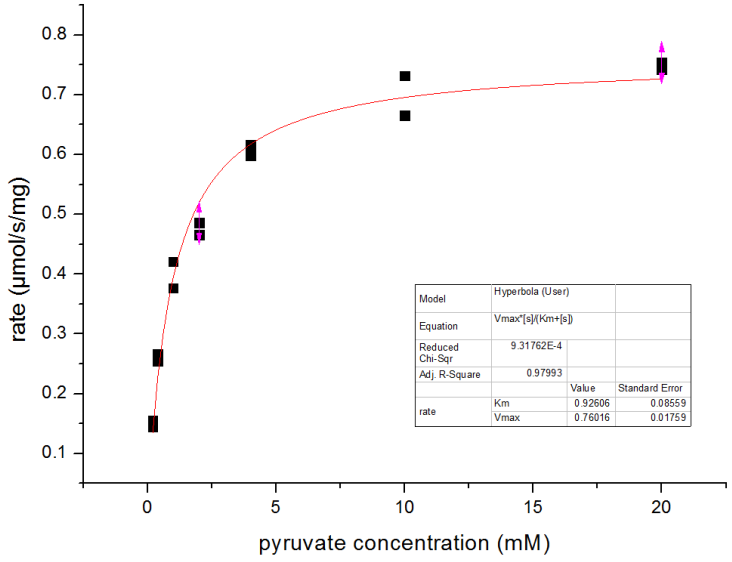

Figure 36 Plotted SMO DHDPS rate with different pyruvate concentrations.

SMO DHDPS vs ASA

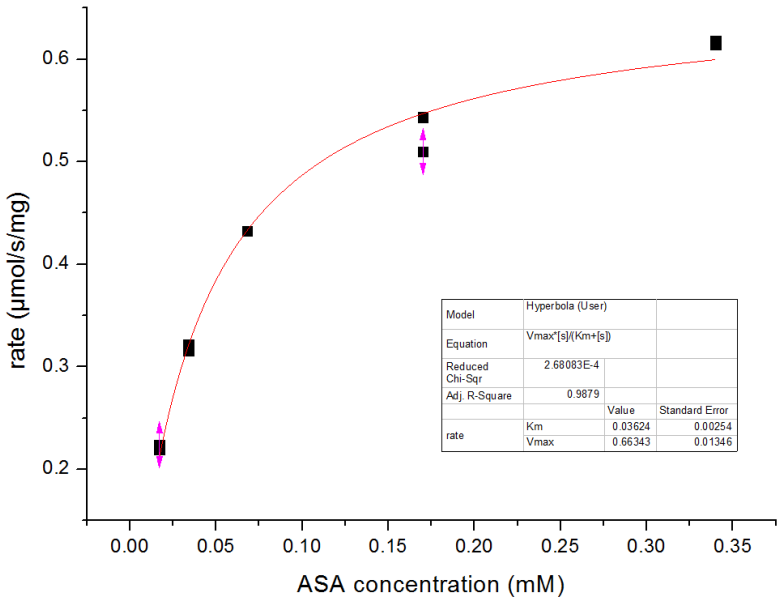

Figure 37 Plotted SMO DHDPS rate with different ASA concentrations.

DHDPS kinetics summary:

Table 20 summarizes the kinetic parameters of CRE, CME, OTA and SMO DHDPS:

DHDPS	K_m pyruvate (mM)	K_m ASA (mM)	K_{cat} pyruvate (s^{-1})	K_{cat} ASA (s^{-1})
CRE	0.36±0.016	0.07±0.005	77±1	74±1.8
CME	0.19±0.010	0.05±0.006	28±0.3	30±1
OTA	0.15±0.012	0.02±0.001	14±0.3	14±0.2
SMO	0.93±0.086	0.04±0.003	26±0.6	23±0.3

Table 20 K_m and K_{cat} values of DHDPS from CRE, CME, OTA, SMO

When comparing Table 20, Table 1 and Table 2, CRE, CME and OTA have similar K_m pyruvate values to bacteria DHDPS and SMO DHDPS K_m pyruvate is much higher than the other three and more close to plant DHDPS K_m pyruvate values. Thus in terms of kinetics, CRE CME and

OTA DHDPS behave more like bacteria DHDPS and SMO DHDPS behaves more like plant DHDPS.

The CRE, CME, OTA and SMO DHDPS all have similar K_m ASA values, but their K_m ASA are about 10 fold smaller than the previously characterized plant and bacteria DHDPS described in Table 1 and Table 2. However, as K_m ASA cannot be used to distinguish between plant and bacteria DHDPS, it will not be further discussed here.

Plotted Lysine inhibition kinetic curves

CRE DHDPS Lysine Inhibition

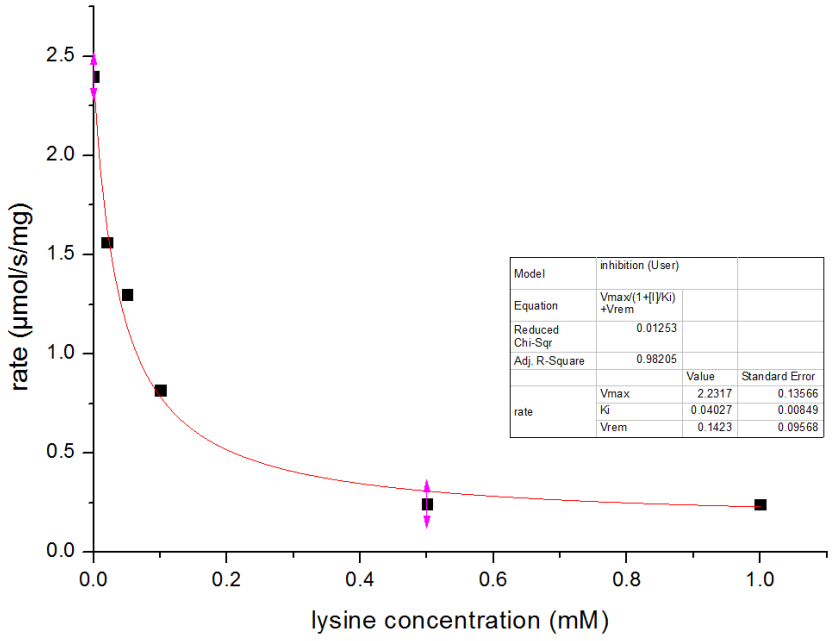

Figure 38 Plotted CRE DHDPS rate vs the inhibitor lysine concentration

CME DHDPS Lysine Inhibition

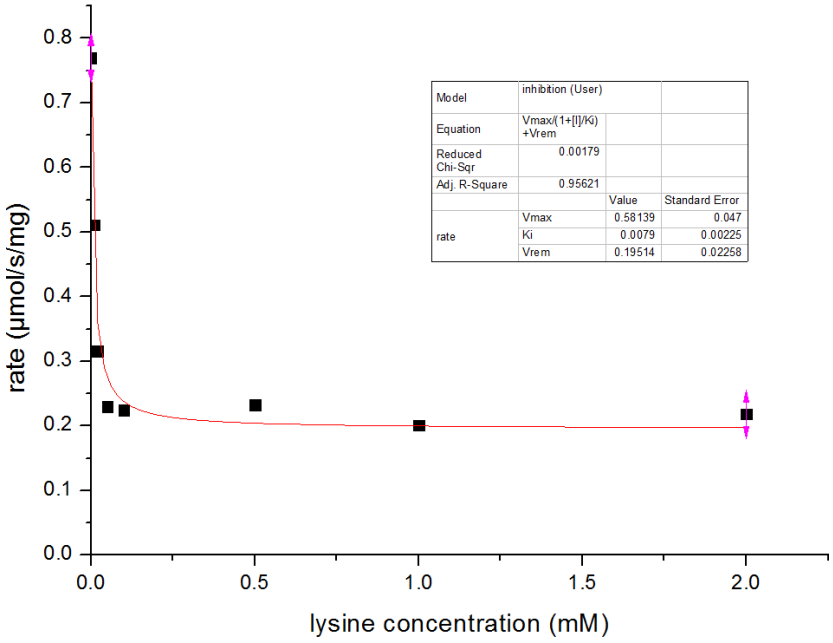

Figure 39 Plotted CME DHDPS rate vs the inhibitor lysine concentration

OTA DHDPS lysine inhibition

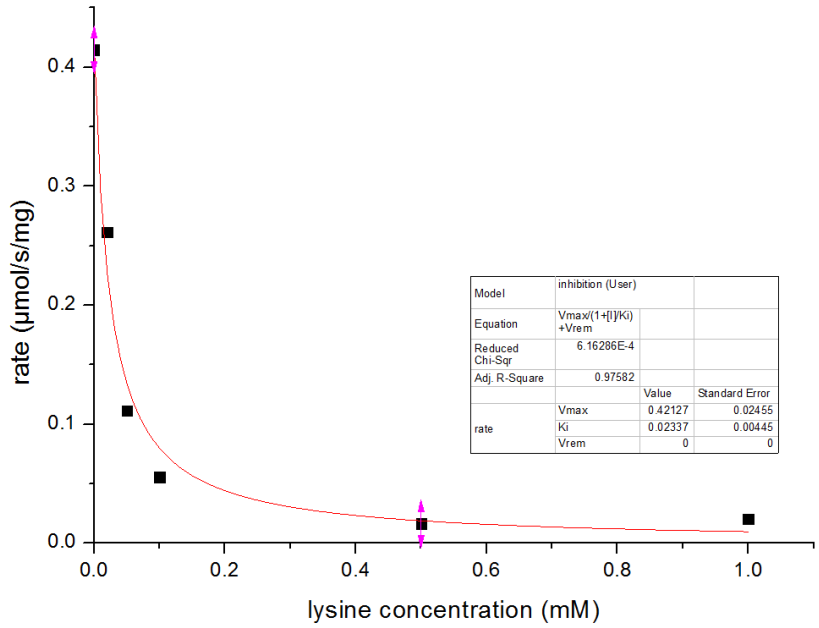

Figure 40 Plotted OTA DHDPS rate vs the inhibitor lysine concentration

SMO DHDPS lysine inhibition

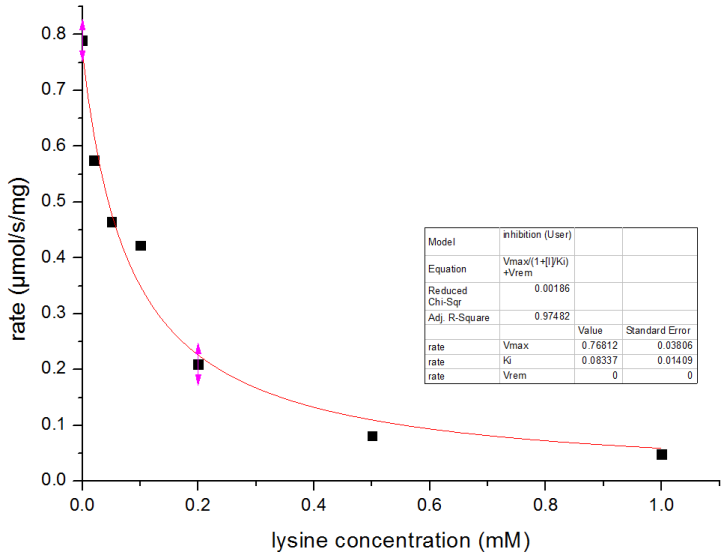

Figure 41 Plotted SMO DHDPS rate vs the inhibitor lysine concentration

Lysine inhibition summary:

Table 21 summarizes the K_i lysine values of the CRE, CME, OTA and SMO DHDPS and some previously characterized DHDPS:

DHDPS from	K_i lysine (mM)
CRE	0.06±0.008
CME	0.015±0.002
OTA	0.03±0.004
SMO	0.15±0.014
E. coli [13]	0.4
N. meningitidis [15]	0.058
V. vinifera [9]	0.049
A. thaliana [2]	0.023

Table 21 K_i lysine values of CRE, CME, OTA, SMO and some previously characterized plant and bacteria DHDPS.

From Table 21 we can see that SMO and *E. coli* DHDPS have a K_i lysine value about 10 fold higher than other DHDPS. The relationship between lysine sensitivity and lysine binding site residues of DHDPS is studied on *B. anthracis*, *C. glutamicum*, *E. coli*, *H. chejuensis*, *N. tabacum* and *Z. mays* [55]. Eight residues in *E. coli* DHDPS are responsible for lysine binding: S48, A49, L51, H53, H56, N80, E84 and Y106 [55]. And among the DHDPS from those 5 species, only the N80 and Y106 are strictly conserved [55]. Here we compare the DHDPS from Table 17 together with another completely lysine insensitive DHDPS from *B. anthracis* [16]:

```
SMO                 MPEIRTQECRALASSALCGTLGRAPRSAARCGSRRACLQIRAAVMQSTPLPMRSNELKNS
V.vinifera          ----------------------MGSSHHHHHSSGLVPRGSHMAVIPNFHLPMRSFEVKNR
A.thaliana          MSALKNYGLISIDSA-LH--FPRSNQLQSYKRRNAKWVSPIAAVVPNFHLPMRSLEDKNR
CRE                 --------------------MSLFSRTRAPTCPGARRARPSAVRVQATLLPLPA--SETR
OTA                 ----------------------MFSKHKPFDAAS--LTTPRSIV--SAAGDWGC--PEQG
CME                 ---------MAFLSSCPGGSCLTRDHHKHRLAIRSRLQRSLCCTTARTEQQV----QAQE
B.anthracis         ------------------------------------------------------------
E.coli              ------------------------------------------------------------
N.meningitidis      ------------------------------------------------------------

SMO                 TPVEEMKKLRLISAIKTPYLPDGR-FDLEAYDSLVRTQVDHGVEGLIVGGTTGEGHLMNW
V.vinifera          TSVDDIKSLRLITAIKTPYLPDGR-FDLEAYDALVNMQIVDGAEGVIVGGTTGEGQLMSW
A.thaliana          TNTDDIRSLRVITAIKTPYLPDGR-FDLQAYDDLVNTQIENGAEGVIVGGTTGEGQLMSW
CRE                 STVDRLKKLRLITAIKTPYLANGK-FDLPAYDALVSHQIENGVEGLIVGGTTGEGHLMSW
OTA                 CPVDVLRTKRLITAIKTPYLTSGK-VDLYAYDALVEAQIEGGVEGLIVGGTTGEGQLMSW
CME                 VERPKHFFGRVITALVTPFKLTGVEVDYGVAESLAAHLAENGSDAIIVAGTTGESATLTW
B.anthracis         ----MIDFGTIATAMVTPFDINGN-IDFAKTTKLVNYLIDNGTTAIVVGGTTGESPTLTS
E.coli              ------MFTGSIVAIVTPMDEKGN-VCRASLKKLIDYHVASGTSAIVSVGTTGESATLNH
N.meningitidis      ------MLQGSLVALITPMNQDGS-IHYEQLRDLIDWHIENGTDGIVAVGTTGESATLSV
                                *: **    *  .       *       *  .::  *****.  :.

SMO                 DEHIMLIAHTVNCFG-DKIKVIGNTGSNSTREAIHATEQGFAAGMHAALHINPYYGKTSM
V.vinifera          DEHIMLIGHTVNCFG-GSIKVIGNTGSNSTREAIHATEQGFAVGMHAALHINPYYGKTSL
A.thaliana          DEHIMLIGHTVNCFG-GRIKVIGNTGSNSTREAIHATEQGFAMGMHGALHINPYYGKTSI
CRE                 DEHVMLIAHTVNAFG-DKTAVIGNTGSNSTREALHATEQGFAVGMHASLQINPYYGKTSK
OTA                 DEHVMLIAHTAQKYG-DRVLVIGNTGSNSTREAVHATSQGFAVGMDASLQINPYYGKTSR
CME                 SEEYELFRVVKSAVAGTKCRVIAGAGSNSTEEAIEATKKSAKLGLDGTLQVVPYYNKPPQ
B.anthracis         EEKVALYRHVVSVVD-KRVPVIAGTGSNNTHASIDLTKKATEVGVDAVMLVAPYYNKPSQ
E.coli              DEHADVVMMTLDLAD-GRIPVIAGTGANATAEAISLTQRFNDSGIVGCLTVTPYYNRPSQ
N.meningitidis      EEHTAVIEAVVKHVA-KRVPVIAGTGANNTVEAIALSQAAEKAGADYTLSVVPYYNKPSQ
                    .*.  :   . .        **. :*:* *  ::  :.     *    : : *** :

SMO                 DGLLLHFKSVLAM---GPTVIYNVPGRTGQDIPPSVIEKIASS-PNFLGVKECMGN----
V.vinifera          EGLVSHFESVLPM---GPTVIYNVPSRTGQDIPPGVIHTVAQS-ANLAGVXECVGN----
A.thaliana          EGMNAHFQTVLHM---GPTIIYNVPGRTCQDIPPQVIFKLSQN-PNMAGVKECVGN----
CRE                 AGLLNHFNAVLNE---GPAVVYNVPGRTGQDIPDDVVMEICQH-SNFLGMKECTGN----
OTA                 RGLIEHFGAVMDL---GPAIVYNVPARTSQDIAPEVMFELAKH-KNFAGVKECEGN----
CME                 QGIMAHFRAIANAAPDLPMMLYNIPGRTGINMTAETSIKLAEMCPNIVALKEASGNLEQF
B.anthracis         EGMYQHFKAIAES-TPLPVMLYNVPGRSIVQISVDTVVRLSEI-ENIVAIKDAGGDVLTM
E.coli              EGLYQHFKAIAEH-TDLPQILYNVPSRTGCDLLPETVGRLAKV-KNIIGIKEATGNLTRV
N.meningitidis      EGMYRHFKAVAEA-AAIPMILYNVPGRTVVSMNNETILRLTEI-PNIVGVKEASGNIGSN
                     *:  ** ::       * ::**:*.*:  .:   .   : .   *: .: :. *:

SMO                 ERVKHYTEQGIAVWSGNDDQCHDSRWDFGARGVISVVSNLVPKLMHELMFS-------GK
```

```
V.vinifera          DRIKQYTDNRIVVWSGNDDQCHDAKWDYGATGVISVTSNLIPGLMRQLLFK-------GK
A.thaliana          NRVEEYTEKGIVVWSGNDDQCHDSRWDHGATGVISVTSNLVPGLMRKLMFE-------GR
CRE                 SRIKNYTSKGVNCWSGNDDESHDARHSNGAVGVISVTSNVIPGLMHKLMHG-------SP
OTA                 VRIKGYTDKGVTCWTGNDDEVHEARYEAGAVGVISVTSNLVPELMRELLFD-------GP
CME                 ARIRRATSPDFALYSGDDALTLP-LLSLGGNGVVSVASHFIGPEIQRMIEHFVDLGNPEE
B.anthracis         TEIIEKTADDFAVYSGDDGLTLP-AMAVGAKGIVSVASHVIGNEMQEMIAAFQA-GEFKK
E.coli              NQIKELVSDDFVLLSGDDASALD-FMQLGGHGVISVTANVAARDMAQMCKLAAE-GHFAE
N.meningitidis      IELINRAPEGFVVLSGDDHTALP-FMLCGGHGVITVAANAAPKLFADMCRAALQ-VDIAL
                     .:   .   .   :*:*          *. *:::*.:.     :  :

SMO                 NQERNEKLMPLINWLFVEPNPIGLNTALSQLGLIR-PVFRLPYAPLNVEKRQEFVKIVEG
V.vinifera          NPSLNAKIMPLVNWLFEEPNPIGLNTALAQLGVVR-PVFRLPYVPLPLAKRVEFVNIVKE
A.thaliana          NSALNAKLLPLMDWLFQEPNPIGVNTALAQLGVAR-PVFRLPYVPLPLSKRIEFVKLVKE
CRE                 DPQLNADLKELMAWMFCEPNPISLNTALAMCGLAR-PVFRLPYVPLSRAQREKGAVLLNK
OTA                 NPELRDRLLPLMGWLFREPNPIGVNTATAMLGVAK-PVFRLPYVPYAADLRAEGAALLRD
CME                 AFRIHCRYMDLFEALFVMANPIPAKAALRLLGWPV-GPTRLPLTDITASAEQQLRQAMIA
B.anthracis         AQKLHQLLVRVTDSLFMAPSPTPVKTALQMVGLDV-GSVRLPLLPLTEEERVTLQSVMQS
E.coli              ARVINQRLMPLHNKLFVEPNPIPVKWACKELGLVATDTLRLPMTPITDSGRETVRAALKH
N.meningitidis      ARELNNRLIPIYDTMFCEPSPAAPKWAVSALGRCE-PHVRLPLVPLTEGGQAKVRAALKA
                        .     :   :*   .*   : *    *       ***        .      :

SMO                 IGRENFPGCTEVRLLKDDDFLLVERY
V.vinifera          IGRENFVGEKDVKVLDDDDFILVGRY
A.thaliana          IGREHFVGDRDVQVLDDDDFILIGRY
CRE                 VQ-EHIPGCKSVRVMEDHEFILVGRH
OTA                 VG-V-----ANAQPLADDDFTLLREW
CME                 AGLLSNGSG-----------------
B.anthracis         IPR-----------------------
E.coli              AGLL----------------------
N.meningitidis      SGQL----------------------
```

S48 and L51are responsible for stabilizing the amino group on lysine side chain with their backbone oxygen [55], and they are partly conserved with residues which have similar chemical properties shown in yellow above. A49 has the same role as S48 and L51 [55], but is only conserved in 3 species shown in blue above. H53 works as a cap to help orient the inhibitor lysine [55], but it is not found in *B. anthracis* and *N. meningitidis*. The other 6 enzymes aligned have a tryptophan at that position (shown in yellow), which also has a ring structure like histidine and can act as a cap. H56 is hydrogen bonded to the lysine side chain [55]and it is partly conserved shown in yellow above. N80 and Y106 hydrogen bonds to the carboxyl group of lysine [55] and they are strictly conserved in all the DHDPS sequence aligned, shown in blue above. E84 interacts with the amino group of lysine by its side chain [55], and it is conserved in all DHDPS aligned except *B. anthracis*.

From the plotted lysine inhibition curves in Figure 38-41 we can see the CRE, OTA and SMO DHDPS are almost completely inactivated by 1mM lysine, however the CME DHDPS is still partial active when the lysine concentration was raised to 2 mM. Thus the CRE, OTA and SMO

DHDPS exhibits non-competitive inhibition by lysine and the CME DHDPS exhibits partial-mixed inhibition by lysine.

Plotted DHDPR kinetic curves

CRE DHDPR vs NADPH

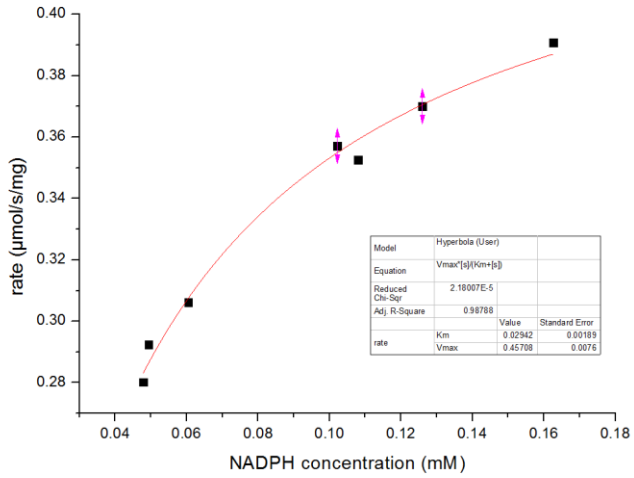

Figure 42 Plotted CRE DHDPR rate vs NADPH concentration

CRE DHDPR vs NADH

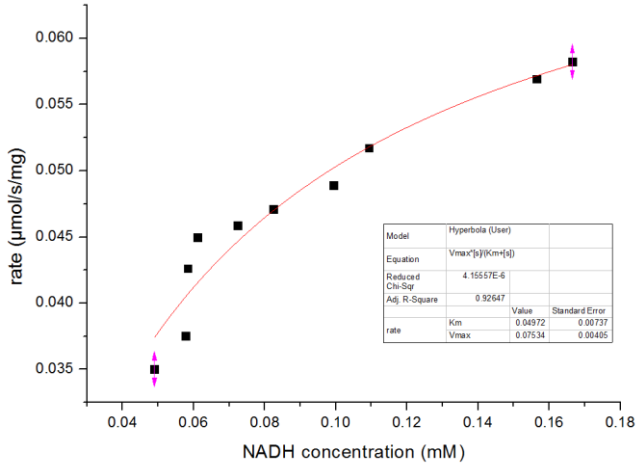

Figure 43 Plotted CRE DHDPR rate vs NADH concentration

CRE DHDPR vs HPTA (NADPH)

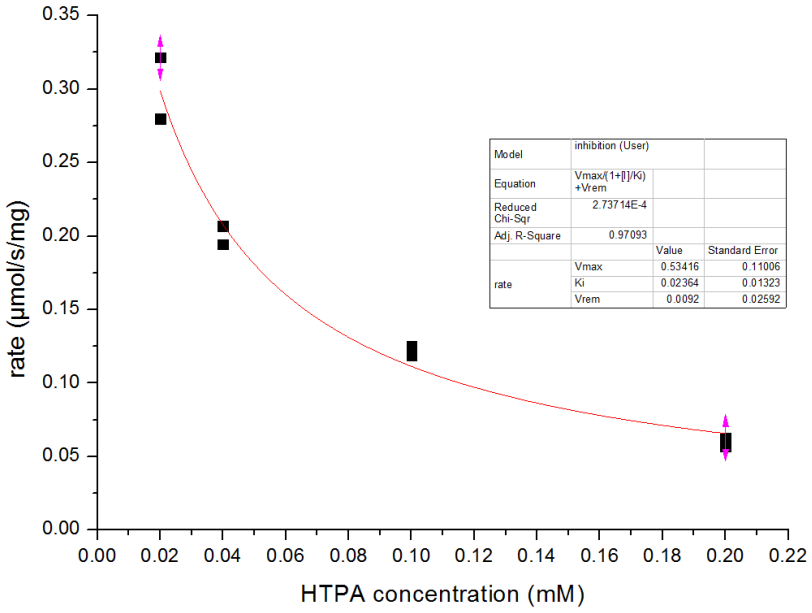

Figure 44 Plotted CRE DHDPR rate vs HTPA concentration (NADPH used as cofactor)

CRE DHDPR vs HPTA (NADH)

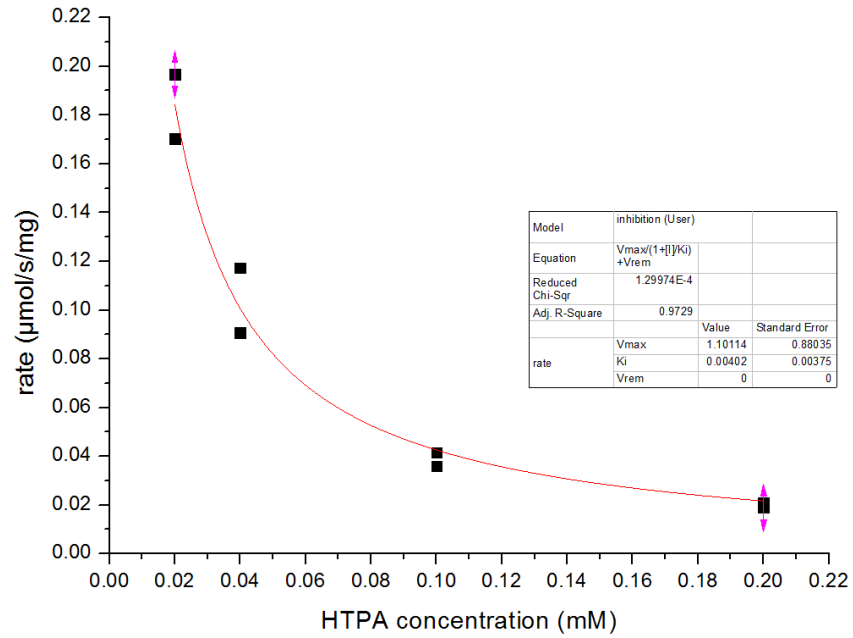

Figure 45 Plotted CRE DHDPR rate vs HTPA concentration (NADH used as cofactor)

SMO DHDPR vs NADPH

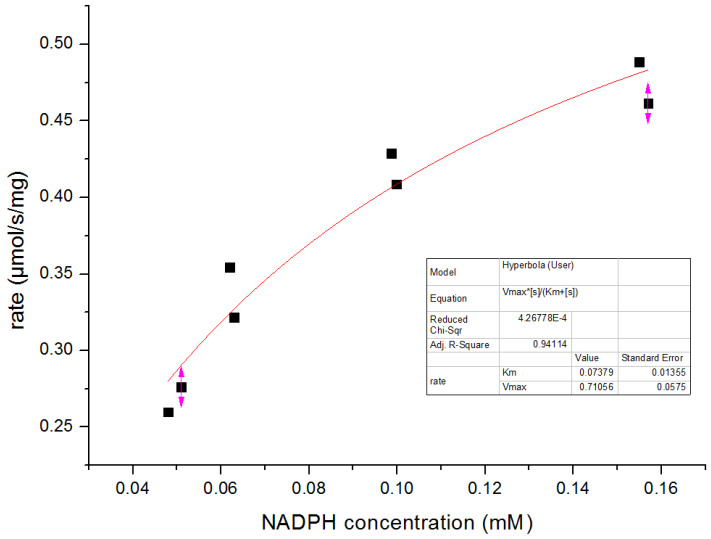

Figure 46 Plotted SMO DHDPR rate vs NADPH concentration

SMO DHDPR vs NADH

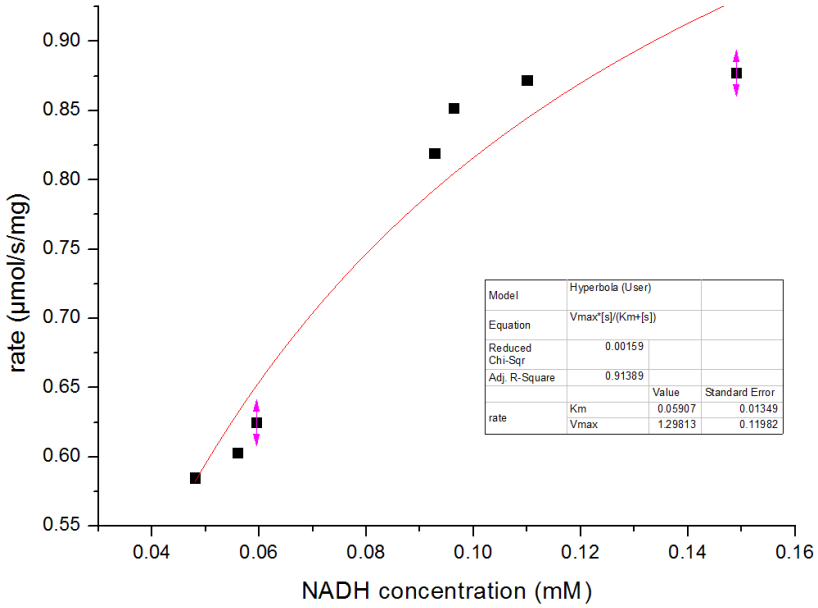

Figure 47 Plotted SMO DHDPR rate vs NADH concentration

SMO DHDPR vs HTPA (NADPH)

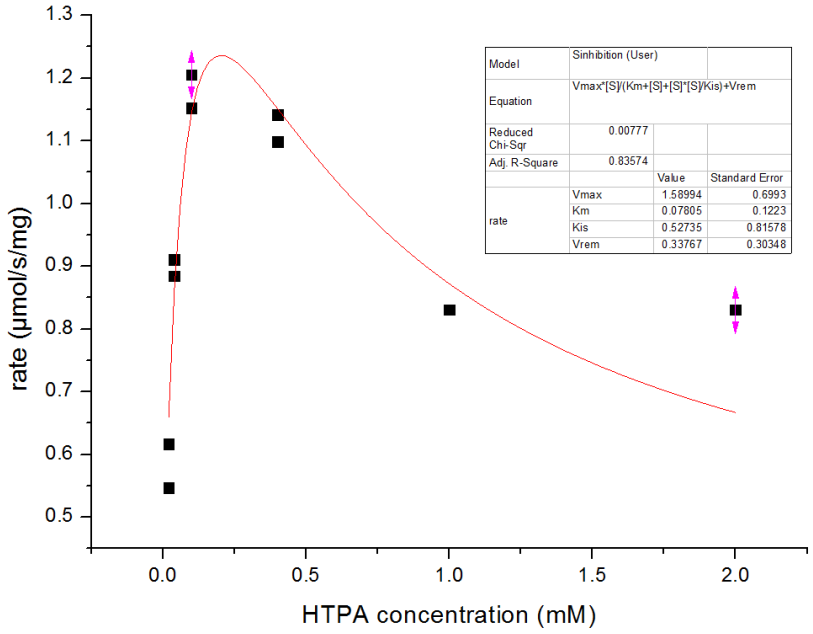

Figure 48 Plotted SMO DHDPR rate vs HTPA concentration (NADPH used as cofactor)

SMO DHDPR vs HTPA (NADH)

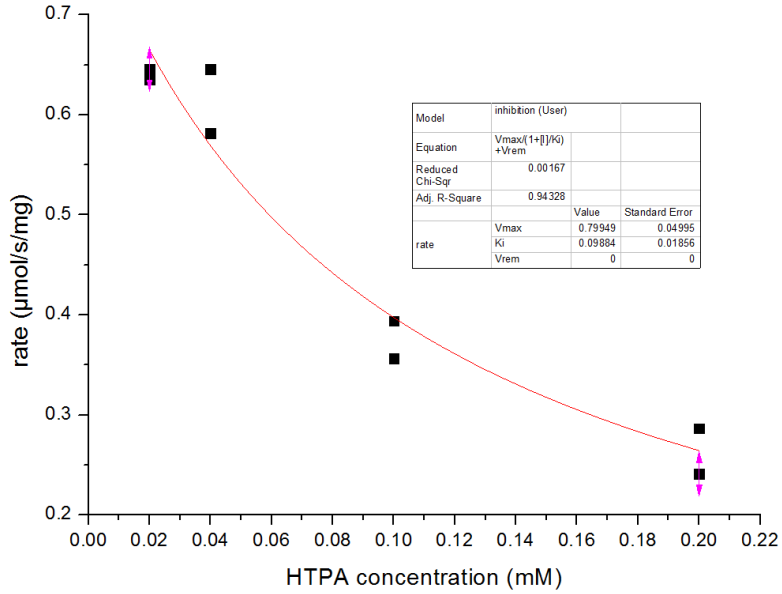

Figure 49 Plotted SMO DHDPR rate vs HTPA concentration (NADH used as cofactor)

OLU DHDPR vs NADPH

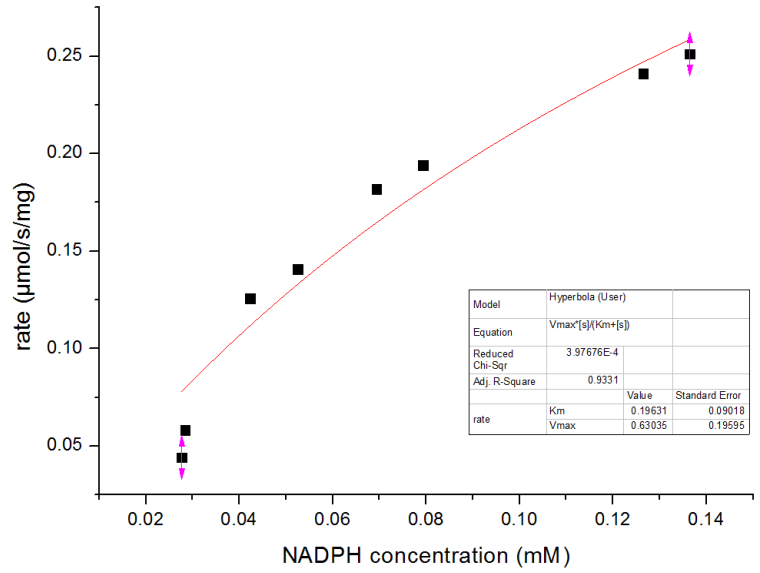

Figure 50 Plotted OLU DHDPR vs NADPH concentration

OLU DUDPR vs NADH

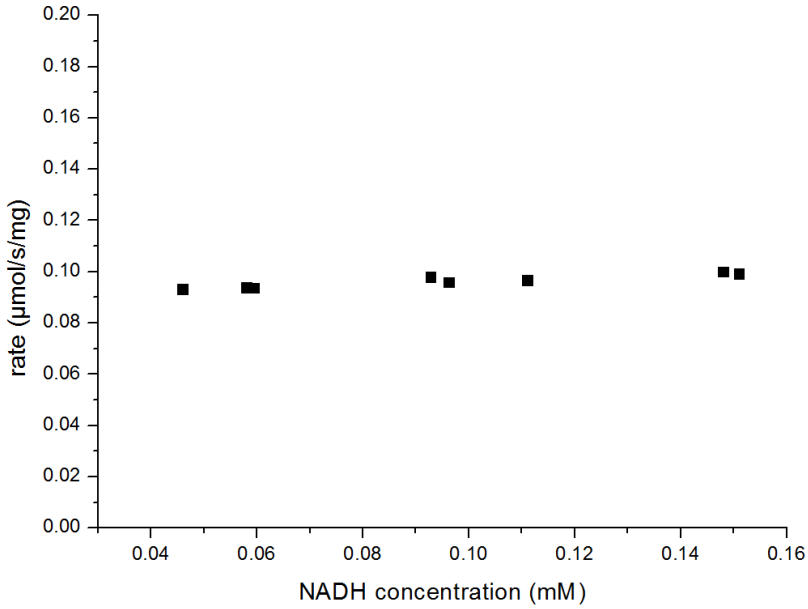

Figure 51 Plotted OLU DHDPR vs NADH concentration

OLU DHDPR vs HTPA (NADPH)

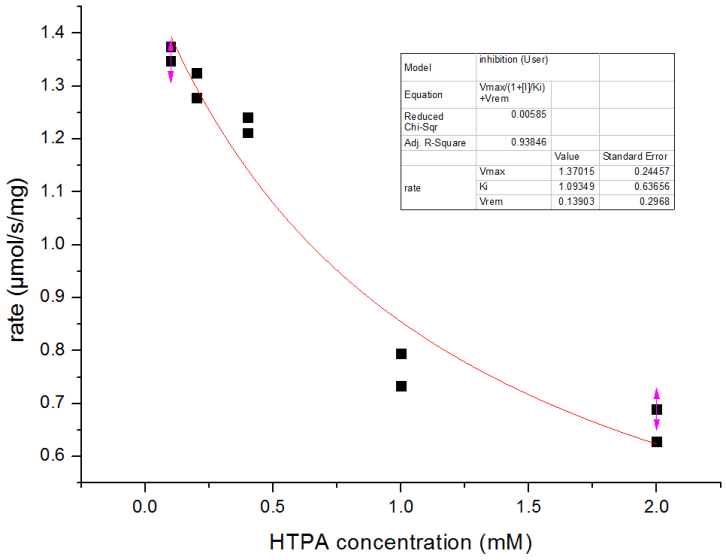

Figure 52 Plotted OLU DHDPR vs HTPA concentration (NADPH used as cofactor)

OLU DHDPR vs HTPA (NADH used as cofactor)

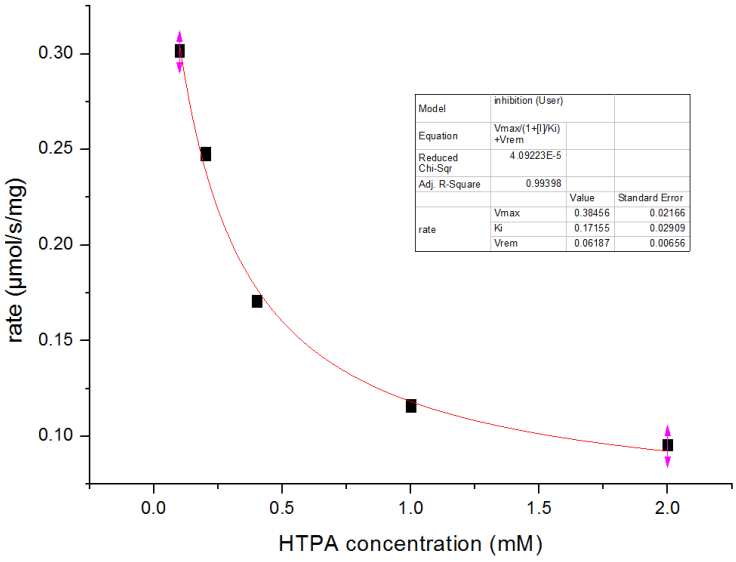

Figure 53 Plotted OLU DHDPR vs HTPA concentration (NADH used as cofactor)

DHDPR kinetics summary:

While doing DHDPR kinetics, it is difficult to measure the rate with NADPH or NADH concentration lower than 0.04 mM because of the other material used in the assay have some background absorbance. With NAD(P)H concentration lower than 0.04 mM, the absorbance of the nucleotide is lower than the background value, and no decrease of absorbance can be observed after initializing the assay.

Due to the background absorbance, the NAD(P)H concentration in each assay is back calculated by the amount of absorbance decreased.

The OLU DHDPR K_m NADH was too low to measure. As the plotted graph shows, the reaction rate stayed at V_{max} even though the NADH concentration was very close to zero.

While altering the HTPA concentration, most of the plotted graphs show only a decrease in reaction rate when HTPA concentration is increased. Only for the SMO DHDPR-NADPH combination, a very quick increase can be seen at very low HTPA concentration. The SMO DHDPR K_m HTPA is about 0.02 mM, while the other K_m HTPA are too low to be measured.

Table 22 below summarizes the K_m and K_{cat} values of CRE, OLU, SMO DHDPR:

Species	K_m NADPH (mM)	K_m NADH (mM)	K_m HTPA (mM)	K_{cat} NADPH (s^{-1})	K_{cat} NADH (s^{-1})	K_{cat} HTPA (s^{-1})
CRE	0.03±0.002	0.05±0.007		15.4±0.26	2.51±0.13	
OLU	0.1±0.09			11.5±0.9	3.1	
SMO	0.07±0.014	0.06±0.013		18±1.4	33±3.1	30.4±11.5

Table 22 K_m and K_{cat} values of CRE, OLU, SMO DHDPR

Looking at Table 22 alone, CRE and SMO DHDPR have similar K_m NADH and K_m NADPH values, while the OLU DHDPR has higher K_m NADPH than K_m NADH. CRE and OLU DHDPR also have higher K_{cat} values when NADPH is used as the cofactor while SMO DHDPR has higher K_{cat} when NADH is used.

When comparing Table 22 and Table 4, the CRE, OLU and SMO DHDPR have similar K_m and K_{cat} values to the previously characterized ones.

In order to compare the cofactor preference of CRE and SMO DHDPR with previously characterized DHDPR, and find its relationship to the residues that are important for cofactor binding, the sequences of CRE, SMO, OLU,*E. coli*, *M. tuberculosis* and *S. aureus* DHDPR have been aligned, the result is shown below:

```
CRE                 ------------------------------------------------------MVNSCTGK
OLU                 ---------MRARGRA----------------------IVATRASADGATTRVMVNGVSGK
SMO                 MVCCSLGLEWKARPGVLISASTAQGAKSSSSNIKVGSFHFPFSLVSRFLAQVIVSGACKD
M.tuberculosis      ------------------------------------------------MRVGVLGAKGK
E.coli              ---------------------------------------------MHDANIRVAIAGAGGR
S.aureus            ------------------------------------------------MKILLIGYGAM
                                                                       : .

CRE                 MGHAAAEALV-DAGVKLVPHTFTGMSAGVAVKNIGV---RGVATQLVGAEKRQAALD---
OLU                 MGHATACGVVKRAGFELVPYALTKRATAATTDVLGT----EVRGVDVGEEDAGETLE---
SMO                 IGKAAIAAISKSRGMEVAGA----------ID---TIRVGEDVGEVAGLEALEVPVSNNL
M.tuberculosis      VGTTMVRAVAAADDLTLSAE----------L-------------------DAGDPL----
E.coli              MGRQLIQAALALEGVQLGAA----------LEREGSSLLGSDAGELAGAGKTGVTV----
S.aureus            NQ-------------RVARL----------AEEKGHGIVGVIE----NTPKATTPYQ---
                                   :

CRE                 -----LIKAEYPGMMIVDYTLAHCVEDHVRLYADNGLPFVMGTMGGDRDRMRAYVE---E
OLU                 -----RAKREYPGFIVVDYTQPDSVNSNAALYVKHGVPFVMGTTGGDRERMLREVK---E
SMO                 VTVLGSLSQSRPTGVVVDFSEASEVLENVRQATAFGMRSVVAVPGVDLDVVSQLITFC-E
M.tuberculosis      -----SLLTDGNTEVVIDFTHPDVVMGNLEFLIDNGIHAVVGTTGFTAERFQQVESWLVA
E.coli              --QSSLDAIKDDFDVFIDFTRPEGTLNHLAFCRQHGKGMVIGTTGFDEAGKQAIRD---A
S.aureus            --QYQHIADVKDADVAIDFSNPNLLFPLL--DEEFHLPLVVATTGEKEKLLNKLDE---L
                                 : :*::                  *:.. *

CRE                 KGVYAV-LPSAAGEQAMNLFALLTSLGAPLPPHFDTYTWETVGRGDALALDLLNPQDAGE
OLU                 SGNYAV-IAPQMGKQVVAFQAAMKLMAEQFPGAFEGYTLTVTESHQSSKKDT--SGTAKA
SMO                 KASMGCVIAPTLSIGAV---LLQEAAIAAS---FHYSHVDIVESQQSAKNVYP-SSEALR
M.tuberculosis      KPNTSVLIAPNFAIGAV---LSMHFAKQAARFF---DSAEVIELHHPHKADAP-SGTAAR
E.coli              AADIAIVFAANFSVGVN---VMLKLLEKAAKVMGDYTDIEIIEAHHRHKVDAP-SGTALA
S.aureus            SQNMPVFFSANMSYGVH---ALTKILAAAVPLLDD-FDIELTEAHHNKKVDAP-SGTLEK
                           :    .  .                              .

CRE                 IVATLRAMGIQADDGQI--YRMRASLQSRVGLNLERE--PQ-GALHALQGRGSSRTCRIT
OLU                 IVASFNDLGCGFDLNDIELVRDVESQTGKMGVPEEHL--LG-HA---------FHTYRLT
SMO                 VAKSMTGMGRV--YN--------DSDF-SKEHPARGELVDDGIRIHSMVSPGFISSLAVS
M.tuberculosis      TAKLIAEARKG--LPP-------NPDATSTSLPGARGADVDGIPVHAVRLAGLVAHQEVL
E.coli              MGEAIAHALDK-DLKD-------CAVYSREGHTGER--VPGTIGFATVRAGDIVGEHTAM
```

```
S.aureus            LYDVIVSL----KENV-------TPVYDRHELNEKR--QPQDIGIHSIRGGTIVGEHEVL
                        :

CRE                 APGAVPRLFLRHYGLSRAAFAAGAVEALRFLAARVAEGADQRVYDMVDVLRAYQG-EQDK
OLU                 SADGTVSFEFQHNVCGRSIYAEGTVDAVGFLKRKVDAKDPKTLYDMIDVLKEGAMGEWVK
SMO                 LSGPGEVFSLRHDITDVKALMPGLLVAIRRVIRL-----QSLVYGLEKIL----------
M.tuberculosis      FGTEGETLTIRHDSLDRTSFVPGVLLAVRRIAER-----PGLTVGLEPLLDLH-------
E.coli              FADIGERLEITHKASSRMTFANGAVRSALWLSGK-----ENGLFDMRDVLDLNNL-----
S.aureus            FAGTDETIQITHRAQSKDIFANGAIQAAERLVNK-----PNGFYTFDNL-----------
                           : : *          * : :   :              :  :

CRE                 LHAVRASQQFSSNVVVAGSSVTATAATSA
OLU                 ------------------------------
SMO                 ------------------------------
M.tuberculosis      ------------------------------
E.coli              ------------------------------
S.aureus            ------------------------------
```

The conserved ^{12}GXXGXXG^{18} dinucleotide binding motif [36] mentioned before is shown in red. The Gly12 is missing in CRE DHDPR, Gly15 is missing in SMO DHDPR, and Gly18 is missing in *S. aureus* DHDPR. The Arg39 from E. coli and Lys35 from S. aureus which are important for NADPH binding [39] are shown in blue. This residue is not found in SMO DHDPR or OLU DHDPR but Lys39 is found in CRE DHDPR, also shown in blue.

From the alignment data alone SMO DHDPR appears to have a higher affinity for NADPH than NADH while CRE and OLU DHDPR prefer NADH than NADPH. This is consistent with the OLU DHDPR having a much lower K_m NADH than K_m NADPH, but the CRE and SMO DHDPR have similar K_m NADH and K_m NADPH values. The thermal stability data in Table 19 shows that SMO DHDPR is more stabilized by NADH than NADPH, and the SMO DHDPR has a higher K_{cat} value when NADH is used as a cofactor than NADPH, which is not consistent with the sequence alignment data. The reason might be that some residues which are far away from the conserved nucleotide binding residues in the peptide sequence are placed at the same position due to the spatial arrangement or folding of the actual enzyme structure, like the Lys9 of *M. tuberculosis* DHDPR being positioned near the Arg39 of *E. coli* DHDPR [37]. Detailed structural study is needed to further study the cofactor preference of CRE, SMO and OLU DHDPR.

Conclusion

In all the DHDPS and DHDPR purified and characterized, the SMO DHDPS has a K_m pyruvate value similar more close to the plant K_m pyruvate values than bacteria. This is consistent with the phylogenetic tree diagram shown in Figure 12 in which the SMO DHDPS is more close to the maize DHDPS than the other bacteria DHDPS. The SMO DHDPR is proved to be a dimer in solution by SEC, which behaves like a plant DHDPR, which is not consistent with the information of SMO DHDPR being more close to the bacteria DHDPR while OLU and CRE DHDPR being more close to plant ones shown in Figure 13. In terms of thermal stability, both SMO DHDPS and DHDPR have lower melting temperatures than the other enzymes characterized, which is also similar to the plant DHDPS and DHDPR. Thus it can be concluded that the DHDPS and DHDPR from SMO evolved in the same direction as plant DHDPS and DHDPR, while the other green algae and red algae DHDPS and DHDPR all behaved like the bacteria ones in terms of both structure and activity. The detailed crystal structure of these DHDPS is needed to further study their substrate binding site residues, inhibitor binding site residues and their quaternary structure arrangement to compare them to enzymes from plant and bacteria species.

References:

1. Coulter, C. V., Gerrard, J. A., Kraunsoe, J. A. E., & Pratt, A. J. (1999). Escherichia coli dihydrodipicolinatesynthase and dihydrodipicolinatereductase: kinetic and inhibition studies of two putative herbicide targets. *Pesticide Science, 55*(9), 887-895.doi: 10.1002/(sici)1096-9063(199909)55:9<887::aid-ps36>3.3.co;2-2

2. Griffin, M. D. W., Billakanti, J. M., Wason, A., Keller, S., Mertens, H. D. T., Atkinson, S. C., . . . Pearce, F. G. (2012). Characterisation of the First Enzymes Committed to Lysine Biosynthesis in Arabidopsis thaliana.*Plos One, 7*(7), 12.doi: 10.1371/journal.pone.0040318

3. Mirwaldt, C., Korndorfer, I., & Huber, R. (1995). THE CRYSTAL-STRUCTURE OF DIHYDRODIPICOLINATE SYNTHASE FROM ESCHERICHIA-COLI AT 2.5-ANGSTROM RESOLUTION*Journal of Molecular Biology, 246*(1), 227-239.doi: 10.1006/jmbi.1994.0078

4. Girish, T. S., Sharma, E., & Gopal, B. (2008). Structural and functional characterization of Staphylococcus aureus dihydrodipicolinate synthase.*Febs Letters, 582*(19), 2923-2930. doi:10.1016/j.febslet.2008.07.035

5. Kaur, N., Gautam, A., Kumar, S., Singh, A., Singh, N., Sharma, S., . . . Singh, T. P. (2011). Biochemical studies and crystal structure determination of dihydrodipicolinate synthase from Pseudomonas aeruginosa. *International Journal of Biological Macromolecules, 48*(5), 779-787. doi:10.1016/j.ijbiomac.2011.03.002

6. Mank, N., Arnette, A., Klapper, V., Offermann, L., &Chruszcz, M. (2015). Structure of dihydrodipicolinate synthase from the commensal bacterium Bacteroidesthetaiotaomicron at 2.1 angstrom resolution.*ActaCrystallographica Section F-Structural Biology Communications, 71*, 449-454. doi:10.1107/s2053230x15004628

7. Blickling, S., Beisel, H. G., Bozic, D., Knablein, J., Laber, B., & Huber, R. (1997). Structure of dihydrodipicolinate synthase of Nicotianasylvestris reveals novel quaternary structure. *Journal of Molecular Biology, 274*(4), 608-621. doi:10.1006/jmbi.1997.1393

8. Atkinson, S. C., Dogovski, C., Downton, M. T., Pearce, F. G., Reboul, C. F., Buckle, A. M., . . .Perugini, M. A. (2012). Crystal, Solution and Insilico Structural Studies of Dihydrodipicolinate Synthase from the Common Grapevine. *Plos One, 7*(6), 9. doi:10.1371/journal.pone.0038318

9. Atkinson, S. C., Dogovski, C., Downton, M. T., Czabotar, P. E., Dobson, R. C. J., Gerrard, J. A., . . . Perugini, M. A. (2013). Structural, kinetic and computational investigation of Vitisvinifera DHDPS reveals new insight into the

mechanism of lysine-mediated allosteric inhibition. *Plant Molecular Biology, 81*(4-5), 431-446. doi:10.1007/s11103-013-0014-7

10. Blickling, S., Renner, C., Laber, B., Pohlenz, H. D., Holak, T. A., & Huber, R. (1997). Reaction mechanism of Escherichia coli dihydrodipicolinate synthase investigated by X-ray crystallography and NMR spectroscopy.*Biochemistry, 36*(1), 24-33. doi:10.1021/bi962272d

11. Muscroft-Taylor, A. C., da Costa, T. P. S., & Gerrard, J. A. (2010). New insights into the mechanism of dihydrodipicolinate synthase using isothermal titration calorimetry.*Biochimie, 92*(3), 254-262. doi:10.1016/j.biochi.2009.12.004

12. Dobson, R. C. J., Valegard, K., & Gerrard, J. A. (2004). The crystal structure of three site-directed mutants of Escherichia coli dihydrodipicolinate synthase: Further evidence for a catalytic triad. *Journal of Molecular Biology, 338*(2), 329-339. doi:10.1016/j.jmb.2004.02.060

13. Dobson, R. C. J., Griffin, M. D. W., Jameson, G. B., & Gerrard, J. A. (2005). The crystal structures of native and (S)-lysine-bound dihydrodipicolinate synthase from Escherichia coli with improved resolution show new features of biological significance. *ActaCrystallographica Section D-Biological Crystallography, 61*, 1116-1124. doi:10.1107/s0907444905016318

14. Conly, C. J. T., Skovpen, Y. V., Li, S., Palmer, D. R. J., & Sanders, D. A. R. (2014). Tyrosine 110 Plays a Critical Role in Regulating the Allosteric Inhibition of Campylobacter jejuniDihydrodipicolinate Synthase by Lysine. *Biochemistry, 53*(47), 7396-7406. doi:10.1021/bi5012157

15. Devenish, S. R. A., Huisman, F. H. A., Parker, E. J., Hadfield, A. T., & Gerrard, J. A. (2009). Cloning and characterisation of dihydrodipicolinate synthase from the pathogen Neisseria meningitidis.*BiochimicaEtBiophysicaActa-Proteins and Proteomics, 1794*(8), 1168-1174. doi:10.1016/j.bbapap.2009.02.003

16. Domigan, L. J., Scally, S. W., Fogg, M. J., Hutton, C. A., Perugini, M. A., Dobson, R. C. J., . . . Devenish, S. R. A. (2009). Characterisation of dihydrodipicolinate synthase (DHDPS) from Bacillus anthracis.*BiochimicaEtBiophysicaActa-Proteins and Proteomics, 1794*(10), 1510-1516. doi:10.1016/j.bbapap.2009.06.020

17. Dobson, R. C. J., Gerrard, J. A., & Pearce, F. G. (2004). Dihydrodipicolinate synthase is not inhibited by its substrate,(S)-aspartate beta-semialdehyde. *Biochemical Journal, 377*, 757-762. Retrieved from <Go to

ISI>://WOS:000188927900024

18. Burgess, B. R., Dobson, R. C. J., Bailey, M. F., Atkinson, S. C., Griffin, M. D. W., Jameson, G. B., . . . Perugini, M. A. (2008). Structure and evolution of a novel dimeric enzyme from a clinically important bacterial pathogen*Journal of Biological Chemistry, 283*(41), 27598-27603. doi:10.1074/jbc.M804231200

19. Griffin, M. D. W., Dobson, R. C. J., Gerrard, J. A., &Perugini, M. A. (2010). Exploring the dihydrodipicolinate synthase tetramer: How resilient is the dimer-dimer interface? *Archives of Biochemistry and Biophysics, 494*(1), 58-63. doi:10.1016/j.abb.2009.11.014

20. Pearce, F. G., Dobson, R. C. J., Weber, A., Lane, L. A., McCammon, M. G., Squire, M. A., . . . Gerrard, J. A. (2008). Mutating the Tight-Dimer Interface of Dihydrodipicolinate Synthase Disrupts the Enzyme Quaternary Structure: Toward a Monomeric Enzyme. *Biochemistry, 47*(46), 12108-12117. doi:10.1021/bi801094t

21. Evans, G., Schuldt, L., Griffin, M. D. W., Devenish, S. R. A., Pearce, F. G., Perugini, M. A., . . . Gerrard, J. A. (2011). A tetrameric structure is not essential for activity in dihydrodipicolinate synthase (DHDPS) from Mycobacterium tuberculosis. *Archives of Biochemistry and Biophysics, 512*(2), 154-159. doi:10.1016/j.abb.2011.05.014

22. Rice, E. A., Bannon, G. A., Glenn, K. C., Jeong, S. S., Sturman, E. J., &Rydel, T. J. (2008). Characterization and crystal structure of lysine insensitive Corynebacteriumglutamicumdihydrodipicolinate synthase (cDHDPS) protein. *Archives of Biochemistry and Biophysics, 480*(2), 111-121. doi:10.1016/j.abb.2008.09.018

23. Dereppe, C., Bold, G., Ghisalba, O., Ebert, E., &Schar, H. P. (1992). PURIFICATION AND CHARACTERIZATION OF DIHYDRODIPICOLINATE SYNTHASE FROM PEA.*Plant Physiology, 98*(3), 813-821. doi:10.1104/pp.98.3.813

24. Kumpaisal, R., Hashimoto, T., & Yamada, Y. (1987). PURIFICATION AND CHARACTERIZATION OF DIHYDRODIPICOLINATE SYNTHASE FROM WHEAT SUSPENSION-CULTURES.*Plant Physiology, 85*(1), 145-151. doi:10.1104/pp.85.1.145

25. Frisch, D. A., Gengenbach, B. G., Tommey, A. M., Sellner, J. M., Somers, D. A., & Myers, D. E. (1991). ISOLATION AND CHARACTERIZATION OF DIHYDRODIPICOLINATE SYNTHASE FROM MAIZE.*Plant Physiology, 96*(2), 444-452. doi:10.1104/pp.96.2.444

26. Voss, J. E., Scally, S. W., Taylor, N. L., Atkinson, S. C., Griffin, M. D. W., Hutton, C. A., . . . Perugini, M. A. (2010). Substrate-mediated Stabilization of a Tetrameric Drug Target Reveals Achilles Heel in Anthrax.*Journal of Biological Chemistry, 285*(8), 5188-5195. doi:10.1074/jbc.M109.038166

27. Webster, F. H., &Lechowic.Rv. (1970). PARTIAL PURIFICATION AND CHARACTERIZATION OF DIHYDRODIPICOLINIC ACID SYNTHETASE FROM SPORULATING BACILLUS-MEGATERIUM.*Journal of Bacteriology, 101*(1), 118-&. Retrieved from <Go to ISI>://WOS:A1970F126500015

28. Halling, S. M., &Stahly, D. P. (1976). DIHYDRODIPICOLINIC ACID SYNTHASE OF BACILLUS-LICHENIFORMIS - QUATERNARY STRUCTURE, KINETICS, AND STABILITY IN PRESENCE OF SODIUM-CHLORIDE AND SUBSTRATES.*BiochimicaEtBiophysicaActa, 452*(2), 580-596. doi:10.1016/0005-2744(76)90209-6

29. Pearce, F. G., Perugini, M. A., McKerchar, H. J., & Gerrard, J. A. (2006). Dihydrodipicolinate synthase from Thermotogamaritima.*Biochemical Journal, 400*, 359-366. doi:10.1042/bj20060771

30. Wolterink-van Loo, S., Levisson, M., Cabrieres, M. C., Franssen, M. C. R., & van der Oost, J. (2008). Characterization of a thermostabledihydrodipicolinate synthase from Thermoanaerobactertengcongensis.*Extremophiles, 12*(3), 461-469. doi:10.1007/s00792-008-0152-z

31. Sridharan, U., Ebihara, A., Kuramitsu, S., Yokoyama, S., Kumarevel, T., &Ponnuraj, K. (2014). Crystal structure and in silico studies of dihydrodipicolinate synthase (DHDPS) from Aquifexaeolicus.*Extremophiles, 18*(6), 973-985. doi:10.1007/s00792-014-0667-4

32. Muscroft-Taylor, A. C., Catchpole, R. J., Dobson, R. C. J., Pearce, F. G., Perugini, M. A., & Gerrard, J. A. (2010). Disruption of quaternary structure in Escherichia coli dihydrodipicolinate synthase (DHDPS) generates a functional monomer that is no longer inhibited by lysine. *Archives of Biochemistry and Biophysics, 503*(2), 202-206. doi:10.1016/j.abb.2010.08.009

33. Pollard, A. J., &Frasch, C. (2001). Development of natural immunity to Neisseria meningitidis.*Vaccine, 19*(11-12), 1327-1346. doi:10.1016/s0264-410x(00)00333-9

34. Achenbachrichter, L., Gupta, R., Stetter, K. O., &Woese, C. R. (1987). WERE THE ORIGINAL EUBACTERIA THERMOPHILES.*Systematic and Applied Microbiology, 9*(1-2), 34-39. Retrieved from <Go to ISI>://WOS:A1987G879400008

35. Scapin, G., Blanchard, J. S., &Sacchettini, J. C. (1995). 3-DIMENSIONAL STRUCTURE OF ESCHERICHIA-COLI DIHYDRODIPICOLINATE REDUCTASE.*Biochemistry, 34*(11), 3502-3512. doi:10.1021/bi00011a003

36. Scapin, G., Reddy, S. G., Zheng, R., & Blanchard, J. S. (1997). Three-dimensional structure of Escherichia coli

dihydrodipicolinate reductase in complex with NADH and the inhibitor 2,6-pyridinedicarboxylate. *Biochemistry, 36*(49), 15081-15088. doi:10.1021/bi9719915

37. Cirilli, M., Zheng, R. J., Scapin, G., & Blanchard, J. S. (2003). The three-dimensional structures of the mycobacterium tuberculosis dihydrodipicolinate reductase-NADH-2,6-PDC and -NADPH-2,6-PDC complexes. Structural and mutagenic analysis of relaxed nucleotide specificity.*Biochemistry, 42*(36), 10644-10650. doi:10.1021/bi030044v

38. Janowski, R., Kefala, G., & Weiss, M. S. (2010). The structure of dihydrodipicolinate reductase (DapB) from Mycobacterium tuberculosis in three crystal forms.*ActaCrystallographica Section D-Biological Crystallography, 66*, 61-72. doi:10.1107/s0907444909043960

39. Girish, T. S., Navratna, V., & Gopal, B. (2011). Structure and nucleotide specificity of Staphylococcus aureus dihydrodipicolinate reductase (DapB).*Febs Letters, 585*(16), 2561-2567. doi:10.1016/j.febslet.2011.07.021

40. Baugh, L., Gallagher, L. A., Patrapuvich, R., Clifton, M. C., Gardberg, A. S., Edwards, T. E., . . . Van Voorhis, W. C. (2013). Combining Functional and Structural Genomics to Sample the Essential BurkholderiaStructome.*Plos One, 8*(1), 10. doi:10.1371/journal.pone.0053851

41.Tyagi, V. V. S., Henke, R. R., &Farkas, W. R. (1983). PARTIAL-PURIFICATION AND CHARACTERIZATION OF DIHYDRODIPICOLINIC ACID REDUCTASE FROM MAIZE.*Plant Physiology, 73*(3), 687-691. doi:10.1104/pp.73.3.687

42. Dommaraju, S. R., Dogovski, C., Czabotar, P. E., Hor, L., Smith, B. J., &Perugini, M. A. (2011). Catalytic mechanism and cofactor preference of dihydrodipicolinate reductase from methicillin-resistant Staphylococcus aureus.*Archives of Biochemistry and Biophysics, 512*(2), 167-174. doi:10.1016/j.abb.2011.06.006

43. Reddy, S. G., Sacchettini, J. C., & Blanchard, J. S. (1995). EXPRESSION, PURIFICATION, AND CHARACTERIZATION OF ESCHERICHIA-COLI DIHYDRODIPICOLINATE REDUCTASE.*Biochemistry, 34*(11), 3492-3501. doi:10.1021/bi00011a002

44. Kimura, K., &Goto, T. (1977). DIHYDRODIPICOLINATE REDUCTASES FROM BACILLUS-CEREUS AND BACILLUS-MEGATERIUM.*Journal of Biochemistry, 81*(5), 1367-1373. Retrieved from <Go to ISI>://WOS:A1977DG78900024

45. Pearce, F. G., Sprissler, C., & Gerrard, J. A. (2008). Characterization of dihydrodipicolinate reductase from

Thermotogamaritima reveals evolution of substrate binding kinetics. *Journal of Biochemistry, 143*(5), 617-623. doi:10.1093/jb/mvn012

46. Wang, F., Blanchard, J. S., & Tang, X. J. (1997). Hydrogen exchange electrospray ionization mass spectrometry studies of substrate and inhibitor binding and conformational changes of Escherichia coli dihydrodipicolinate reductase.*Biochemistry, 36*(13), 3755-3759. doi:10.1021/bi963065g

47. Dogovski, C., Dommaraju, S. R., Small, L. C., &Perugini, M. A. (2012). Comparative structure and function analyses of native and his-tagged forms of dihydrodipicolinate reductase from methicillin-resistant Staphylococcus aureus. *Protein Expression and Purification, 85*(1), 66-76. doi:10.1016/j.pep.2012.06.017

48. Farkas, W., &Gilvarg, C. (1965). REDUCTION STEP IN DIAMINOPIMELIC ACID BIOSYNTHESIS.*Journal of Biological Chemistry, 240*(12), 4717-&. Retrieved from <Go to ISI>://WOS:A19657097200023

49. Atkinson, S. C., Dogovski, C., Newman, J., Dobson, R. C. J., &Perugini, M. A. (2011). Cloning, expression, purification and crystallization of dihydrodipicolinate synthase from the grapevine Vitisvinifera.*ActaCrystallographica Section F-Structural Biology and Crystallization Communications, 67*, 1537-1541. doi:10.1107/s1744309111038395

50. Schagger, H. (2006). Tricine-SDS-PAGE.*Nature Protocols, 1*(1), 16-22. doi:10.1038/nprot.2006.4

51. Ericsson, U. B., Hallberg, B. M., DeTitta, G. T., Dekker, N., &Nordlund, P. (2006). Thermofluor-based high-throughput stability optimization of proteins for structural studies.*Analytical Biochemistry, 357*(2), 289-298. doi:10.1016/j.ab.2006.07.027

52. Matsuzaki, M., Misumi, O., Shin-I, T., Maruyama, S., Takahara, M., Miyagishima, S. Y., . . .Kuroiwa, T. (2004). Genome sequence of the ultrasmall unicellular red alga Cyanidioschyzonmerolae 10D. Nature, 428(6983), 653-657. doi:10.1038/nature02398

53. Courties, C., Vaquer, A., Troussellier, M., Lautier, J., Chretiennotdinet, M. J., Neveux, J., . . .Claustre, H. (1994). SMALLEST EUKARYOTIC ORGANISM.Nature, 370(6487), 255-255.doi:10.1038/370255a0

54. Wise SA, Watters RL (2010-06-30). "Bovine Serum Albumin (7 % Solution)". Certificate of Analysis.United States National Institute of Standards & Technology.Retrieved 2011-12-22.

55. Geng, F., Chen, Z., Zheng, P., Sun, J. B., & Zeng, A. P. (2013). Exploring the allosteric mechanism of

dihydrodipicolinate synthase by reverse engineering of the allosteric inhibitor binding sites and its application for lysine production.*Applied Microbiology and Biotechnology, 97*(5), 1963-1971. doi:10.1007/s00253-012-4062-8

56. Pearce, F. G., Dobson, R. C. J., Jameson, G. B., Perugini, M. A., & Gerrard, J. A. (2011). Characterization of monomeric dihydrodipicolinate synthase variant reveals the importance of substrate binding in optimizing oligomerization. *BiochimicaEtBiophysicaActa-Proteins and Proteomics, 1814*(12), 1900-1909. doi:10.1016/j.bbapap.2011.07.016

57. Kefala, G., Evans, G. L., Griffin, M. D. W., Devenish, S. R. A., Pearce, F. G., Perugini, M. A., . . . Dobson, R. C. J. (2008). Crystal structure and kinetic study of dihydrodipicolinate synthase from Mycobacterium tuberculosis. *Biochemical Journal, 411*, 351-360. doi:10.1042/bj20071360

58. http://www.cbs.dtu.dk/services/ChloroP/

59. http://www.ebi.ac.uk/Tools/msa/clustalo/

60. http://web.expasy.org/protparam/